Fall 2012

# Chelating compounds as potential flash rust inhibitors and melamine & aziridine cure of acrylic colloidal unimolecular polymers (CUPs)

Jigar K. Mistry



Department: Chemistry

# CHELATING COMPOUNDS AS POTENTIAL FLASH RUST INHIBITORS AND MELAMINE & AZIRIDINE CURE OF ACRYLIC COLLOIDAL UNIMOLECULAR POLYMERS (CUPs)

by

JIGAR KISHORKUMAR MISTRY

A DISSERTATION

Presented to the Faculty of the Graduate School of the

MISSOURI UNIVERSITY OF SCIENCE AND TECHNOLOGY

In Partial Fulfillment of the Requirements for the Degree

DOCTOR OF PHILOSOPHY

in

CHEMISTRY

2012

Approved by

Dr. Michael R. Van De Mark, Advisor
Dr. Chariklia Sotiriou-Leventis
Dr. Yinfa Ma
Dr. Manashi Nath
Dr. Eric Bohannan

## PUBLICATION DISSERTATION OPTION

This dissertation has been prepared in the form of four manuscripts for publication. Papers included are prepared as per the requirements of the journal in which they are published or are submitted. This dissertation contains the following four manuscripts for publication:

PAPER I

Pages 51-66 have been published in *European Coatings Journal* 2008, 12, 35-39.

PAPER II

Pages 67-101 have been accepted for publication in *Journal of Heterocyclic Chemistry*.

PAPER III

Pages 102-128 have been submitted to the *Journal of Coatings Technology: Research.*

PAPER IV

Pages 129-158 have been submitted to the *Journal of Applied Polymer Science*.

## ABSTRACT

Waterborne coatings on ferrous substrates usually show flash rusting which decreases the adhesion of the coating and the corrosion products can form a stain. Chelating compounds were investigated as potential flash rust inhibitors. Compounds being evaluated include amine alcohols, diamines and sulfur containing amines. A new corrosion inhibitor 2,5-bis(thioaceticacid)-1,3,4-thiadiazole (H2ADTZ) was synthesized and its performance characteristics were evaluated. It was noted that the observed structure of 1,3,4-thiadiazolidine-2,5-dithione (also known as 2,5-dimercapto-1,3,4-thiadiazole (DMTD or DMcT)) has been previously reported in three different tautomeric forms including –dithiol and –dithione. The relative stability of each form as well as the synthesis and characterization of the structures of mono- and dialkylated forms of 5-mercapto-1,3,4-thiadiazole-2(3H)-thione (MTT) were examined. The methods of X-ray crystallography, NMR spectroscopy and ab-initio electronic structure calculations were combined to understand the reactivity and structure of each compound.

Polymers were synthesized with a 1:7 or 1:8 ratio of acrylic acid to acrylate monomers to produce an acid rich resin. The polymers were reduced and solvent stripped to produce Colloidal Unimolecular Polymers (CUPs). These particles are typically 3-9 nanometers in diameter depending upon the molecular weight. They were then formulated into a clear coating with either a melamine (bake) or an aziridine (ambient cure) and then cured. The melamine system was solvent free, a near zero VOC and the aziridine system was very low to near zero VOC. The coatings were evaluated for their MEK resistance, adhesion, hardness, gloss, flexibility, wet adhesion, abrasion and impact resistance properties.

## ACKNOWLEDGEMENTS

First and foremost, I would like to thank my advisor, Dr. Michael R. Van De Mark for his continuous guidance and support during my pursuit of graduate studies at Missouri S&T. His technical, professional and personal guidance has helped me to not only be successful academically but also to be a better human being. I admire his compassion and discipline which taught me to be passionate and hard-working.

I want to thank my Advising Committee Members, Dr. Chariklia Sotiriou-Leventis, Dr. Yinfa Ma, Dr. Manashi Nath and Dr. Eric Bohannan for their support and guidance throughout the completion of my Ph.D. program. I thank the Department of Chemistry and the Missouri S&T Coatings Institute for financial support and other resources. I would like to thank Dr. Richard Dawes, Dr. Amitava Chowdhury, Dr. Gerald Rex, Dr. Wei Wycoff for their contribution towards my research. I acknowledge fellow researchers: Cynthia Riddles, Sagar Gade, Ameya Natu and Yousef Dawib for their help and support at various occasions.

I am grateful to my mentors: Dr. Vinod Malshe, Mr. Dilip Raghavan, Dr. Shashank Mhaske; my friends: Romit, Prashant, Mohit, Priyanka, Siddharth and Yongjie who believed in me and my endeavors. Sincere thanks to my late friend Ravi S. Shah whose memories lives with us.

Last but not the least, I am truly indebted to my Family: my parents: Mr. Kishorkumar Mistry and Mrs. Rita Mistry; my grandfather: Mr. Vasantlal Mistry; my sister: Dhara Mistry-Sarvaiya and my Brother-in-law Dr. Bhavik Sarvaiya as well as my cousins and familiars for their unconditional love and support.

# TABLE OF CONTENTS

# LIST OF ILLUSTRATIONS

# LIST OF TABLES

## ACRONYMS & ABBREVIATIONS

| | |
|---|---|
| DMTD | 5-mercapto-1,3,4-thiadiazole-2(3H)-thione |
| DMcT | 5-mercapto-1,3,4-thiadiazole-2(3H)-thione |
| MTT | 5-mercapto-1,3,4-thiadiazole-2(3H)-thione |
| $H_2$ADTZ | 2,5-bis(thioaceticacid)-1,3,4-thiadiazole; 2,5-(S-acetic acid)-dimercapto-1,3,4-thiadiazole |
| Me-MTT | mono-alkylated MTT; 5-(methylthio)-1,3,4-thidiazole-2(3H)-thione |
| Me-MTT-Me | di-alkylated MTT; 2,5-bis(methylthio)-1,3,4-thiadiazole |
| DMSO | dimethyl sulfoxide |
| MAA | methacrylic acid |
| EA | ethyl acrylate |
| EMA | ethyl methacrylate |
| BMA | butyl methacrylate |
| 2-EHMA | 2-ethylhexylmethacrylate |
| AIBN | 2,2′-azobis(2-methylpropionitrile) |
| THF | tetrahydrofuran |
| MEK | methyl ethyl ketone |
| NaOH | sodium hydroxide |
| KOH | Potassium hydroxide |
| TMS | Tetramethylsilane |
| Cr(acac) | Chromium acac; Chromium acetyl acetonate |
| CUP(s) | Colloidal Unimolecular Polymer(s) |
| VOC | Volatile Organic Compound(s) |

| | |
|---|---|
| $^{1}H/^{13}CNMR$ | Proton/Carbon-13 Nuclear Magnetic Resonance Spectroscopy |
| IR/FT-IR | Infrared (Fourier Transform) Spectroscopy |
| GC | Gas Chromatography |
| MS | Mass Spectroscopy |
| GPC | Gel Permeation Chromatography |
| DLS | Dynamic Light Scattering Spectroscopy |
| MS | Mass Spectroscopy |
| VT | Varied Temperature |
| Tg | Glass Transition Temperature |
| MFFT | Minimum Film Formation Temperature |
| ASTM | American Standards for Testing of Materials |
| m/z | mass to charge ratio |
| nm | nanometer(s) |
| min. | time in minutes |

# 1. INTRODUCTION

## 1.1 FLASH RUSTING

Flash rusting is an objectionable property of water thinned coatings which occurs due to the corrosion of a ferrous substrate caused by the presence of water and rapid diffusion of oxygen during the drying process of aqueous coatings. These corrosion products can migrate towards the surface and form a visible stain.

Flash rusting is a type of corrosion reaction which can only occur when the following conditions are met[1]:

1) an aqueous phase exists
2) oxygen is present
3) ions such as chloride, sodium, etc. are present
4) a conductive pathway exists between the anodic and the cathodic areas.

## 1.2 FLASH RUST INHIBITORS

Chemical agents that interact with the metal surface and reduce their corrosion tendencies are called corrosion inhibitors. Flash rust inhibitors are a class of corrosion inhibitors which stops or significantly reduces the formation and/or the migration of corrosion products in the coating film during the process of drying, thereby eliminating stain formation. In general, corrosion inhibitor types can be divided into[1]:

1) Those that form layers of considerable thickness on the substrate
2) Those that form films by reactions with the protected substrate
3) Those which function by surface adsorption with no significant reaction with the substrate.

It has been reported that certain inorganic salts or organic compounds eliminate flash rusting in water-borne coating systems.[2,3] In an extensive review, Riggs gives the structure of 207 organic compounds that are used as corrosion inhibitors.[4] All of these compounds are polar in nature and contain an active group capable of strong bonding to an iron surface. Typical groups include acetylenic bond, primary, secondary and tertiary amines, ether, thioether, aldehyde, carboxyl, nitrogen in a ring, sulfur in a ring, hydroxyl, thiol, sulfoxide and phosphonium.

Conventional flash rust inhibitors show system dependency and their effectiveness varies with the type of pigment, extender or the resin used and henceforth have to be used in excess. Nitrites, commonly used as flash rust inhibitors leach out over a period of time and can cause blistering.[5] If a chemical agent is designed such that it forms a tight chelated complex with the metal substrate and thereby prevent it from corroding, it would potentially be an effective flash rust inhibitor. Based on the principle of chelation, a new-generation additive: 2,5-bis(thioaceticacid)-1,3,4-thiadiazole was synthesized and its performance characteristics were evaluated in a water-borne coating system.

ASTM D-610 has been the most widely used method to date, to evaluate the extent of flash rusting, but this method is subjective and operator dependent as human

eyes are used to count the flash rust spots to estimate the rusted surface area as compared to the whole surface covered by the coating.[6] Photographs of different percentage of flash rust coverage are used as the standard for evaluation. It was pivotal to develop a quantitative method based on the use of a color spectrophotometer to avoid operator bias. A color computer can be employed to record the Hunter Whiteness Indices which can be deciphered to give the % flash rusting[1]. The extent of flash rusting can be obtained from the following equation:

$$\% \text{ Flash Rusting} = [(\text{Standard} - \text{Sample}) / (\text{Standard} - \text{Blank})] * 100 \qquad (1.2.a)$$

Here, standard, sample and the blank are the Hunter Whiteness Index values measured spectrophotometrically for the respective panels and are defined as follows:

*Sample* = a steel panel coated with the paint of specific thickness containing a flash rust inhibitor and exposed to conventional drying conditions of testing.

*Blank* = a steel panel coated with the paint of same thickness containing no inhibitor and exposed to the same drying condition.

*Standard* = an aluminum panel with the paint of same thickness containing no inhibitor and not exposed to the drying conditions of the test.

## 1.3 5-MERCAPTO-1,3,4-THIADIAZOLE-2(3H)-THIONE

During the research work of evaluating the flash rust inhibition performance of 2,5-bis(thioaceticacid)-1,3,4-thiadiazole for its use as a potential flash-rust inhibitor and a corrosion inhibitor in coatings,[7] the compound 5-mercapto-1,3,4-thiadiazole-2(3H)-thione (MTT) was used as a starting material. It is commonly known as DMTD or DMcT and has been shown to have three possible tautomeric structures,[8,9] *Figure 1.1*, with the dithiol form being the most commonly reported in the literature.

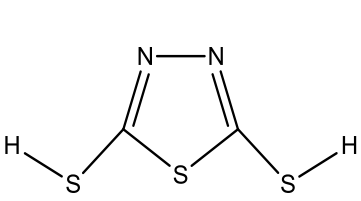


-dithiol form

**Structure 1**

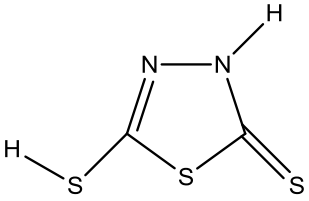


5-mercapto-1,3,4-thiadiazole-2(3H)-thione

**Structure 2**

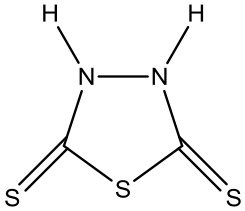


-dithione form

**Structure 3**

**Figure 1.1** The three tautomeric forms of MTT

The alkylated derivatives of MTT were to be evaluated as flash rust and corrosion inhibitors for waterborne coatings. Thus, it was important to know and understand the substitution mechanism of this compound and its various substitution products as well as to determine the structures and their stability by combining results of ab-initio electronic structure calculations, X-ray crystallography and nuclear magnetic resonance spectroscopy to validate and better understand the chemistry of MTT.

**1.3.1 Structure of MTT in DMSO Solution.** There have been several discrepancies in the literature for the reported structure of MTT as observed from the $^{1}H$ and/or $^{13}C$ NMR of MTT in DMSO-$d_6$. The structure of MTT has been widely reported in its dithiol form.[10,11,12] This can be attributed to the fact that both the substitutions on MTT occur on the sulfur. Several recent reports refer to the structure of MTT as that in the dithione form.[13,14,15]

If MTT existed either in the dithiol or the dithione form as reported often in the scientific literature, then both the hydrogens and the carbons of MTT would be identical and thus, only 1 peak should be observed in $^{1}H$ and $^{13}C$ NMR spectras. But the reality was strikingly different. No peaks for MTT were observed in many of the deuterated solvents during the NMR experiments, *Table 1*. The only solvents able to record $^{1}H$ NMR were DMSO-$d_6$ and 'Unisol' (sold by Norell; proprietary chemical; contains $CDCl_3$-d and DMSO-$d_6$ with TMS standard for calibration of chemical shifts). $^{13}C$ NMR for MTT in solution was only observed in ethanol-$d_6$ and Unisol.

**1.3.1.1 Experimental.** $^{1}H$-NMR and $^{13}C$-NMR liquid state NMR experiments were performed on a 400 MHz Varian FT/NMR spectrometer under the guidance of Dr. Gerald Rex (Dept. of Chemistry, MST). Solid state NMR was performed on a Bruker DRX-300 spectrometer with CP-MAS and 7mm diameter solid rotor by Dr. Wei Wycoff (Dept. of Chemistry, University of Missouri-Columbia), who also helped with some liquid state NMR experiments on a 500 MHz Bruker DRX-500 spectrometer equipped with a cryo-chilled TCI probe. X-ray crystallography was performed by Dr. Amitava Choudhury (Dept. of Chemistry, MST) on a Bruker Smart Apex diffractometer.

**Table 1.** NMR spectra of MTT in various solvents

| NMR Solvent | Solubility | Max. Conc. (mg/ml) | $^{1}$H | $^{13}$C |
|---|---|---|---|---|
| Benzene | No | - | - | - |
| Toluene | No | - | - | - |
| Acetonitrile | No | - | - | - |
| Cyclohexane | No | - | - | - |
| Chloroform | Sparing | 40 | Not Observed | |
| Dichloromethane | Sparing | 20 | Not Observed | |
| Methanol | Sparing | 30 | Not Observed | |
| Water | Sparing | 20 | Not Observed | |
| Acetone | Sparing | 20 | Not Observed | |
| Dioxane | Yes | 50 | Not Observed | |
| DMSO | Yes | 60 | 2 Peaks | Not Obs. |
| Ethanol | Yes | 50 | Not Obs. | 2 Peaks |
| Unisol | Yes | 50 | 2 Peaks | 2 Peaks |

Interestingly, the 2 peaks observed in the $^{1}$H NMR spectra were broad, indicating a possible H-transfer phenomenon due to the rapid transformation of one tautomeric form of MTT to another. To validate this hypothesis, varied temperature experiments (VT-NMR) were performed on a Varian 400 MHz FT/NMR spectrometer for MTT solution in DMSO-$d_6$ at a concentration of 50 mg/ml in a 5 mm outer diameter thin-walled glass tube at various temperatures of 25 $^{o}$C, 40 $^{o}$C, 60 $^{o}$C, 80 $^{o}$C, 100 $^{o}$C and 120 $^{o}$C, *Figure 1.2-1.7*. It was observed that as the temperature increased, the 2 broad peaks would move towards each other and merge at 60 $^{o}$C to give a broad peak across 3-15 ppm. At elevated temperatures, this peak would sharpen across 3-5 ppm at 120 $^{o}$C. After 30 sec., the top of the NMR blew off and on taking out the tube, a yellow precipitate was found.

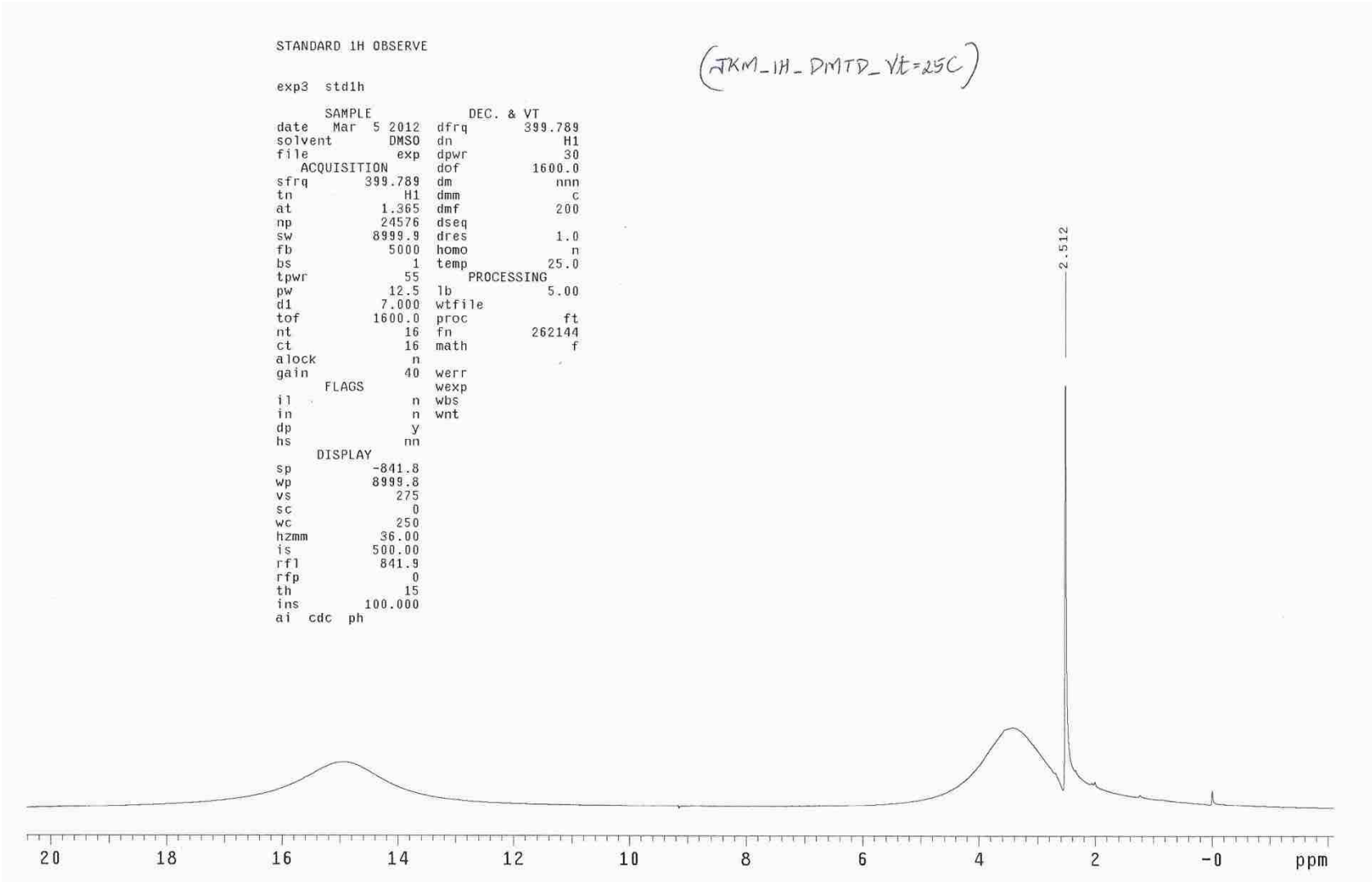


**Figure 1.2** Varied temperature 1H NMR of MTT in DMSO-d6 at 25 $^{o}$C

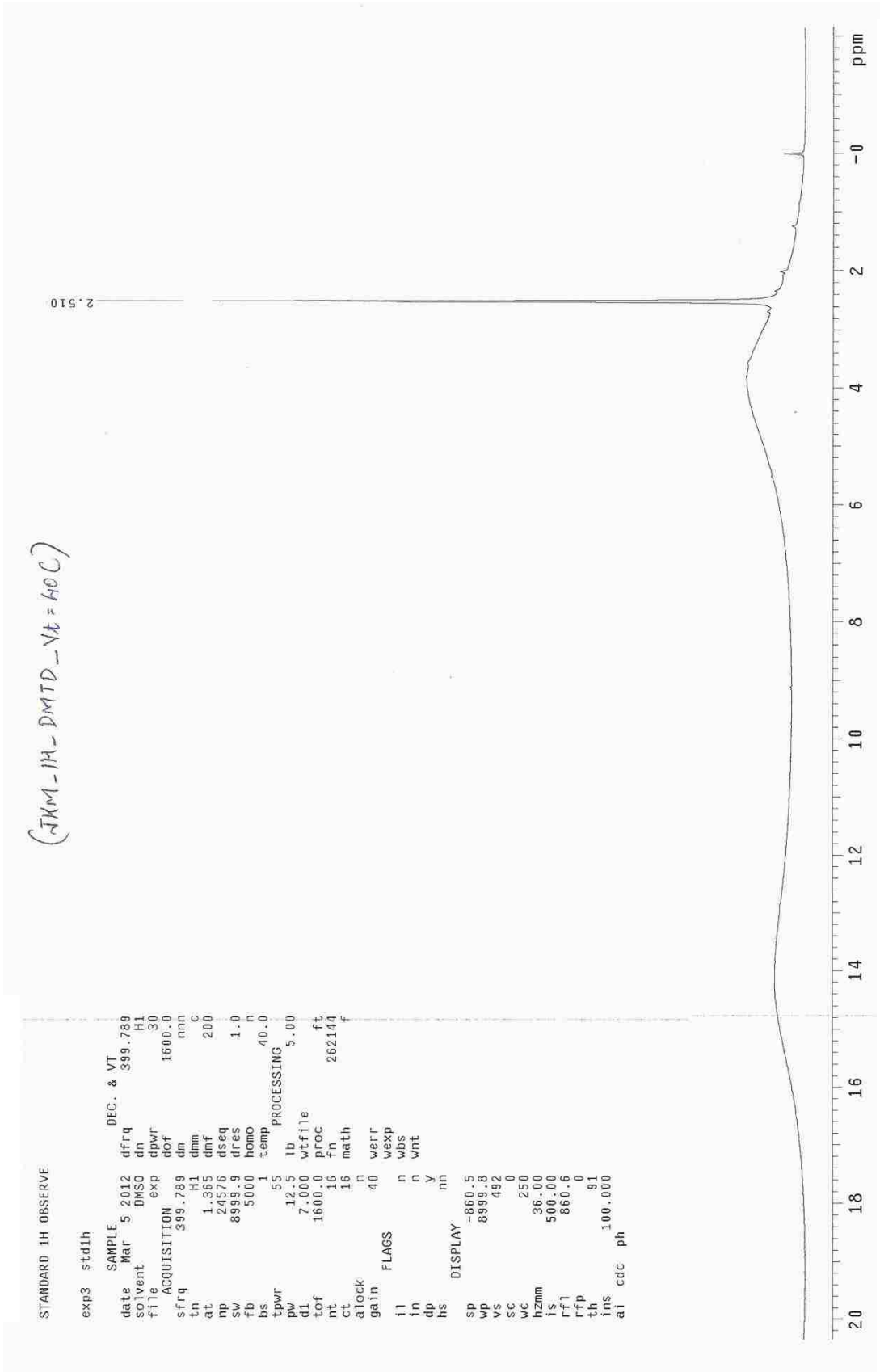


**Figure 1.3** Varied temperature 1H NMR of MTT in DMSO-d6 at 40 $^{o}$C

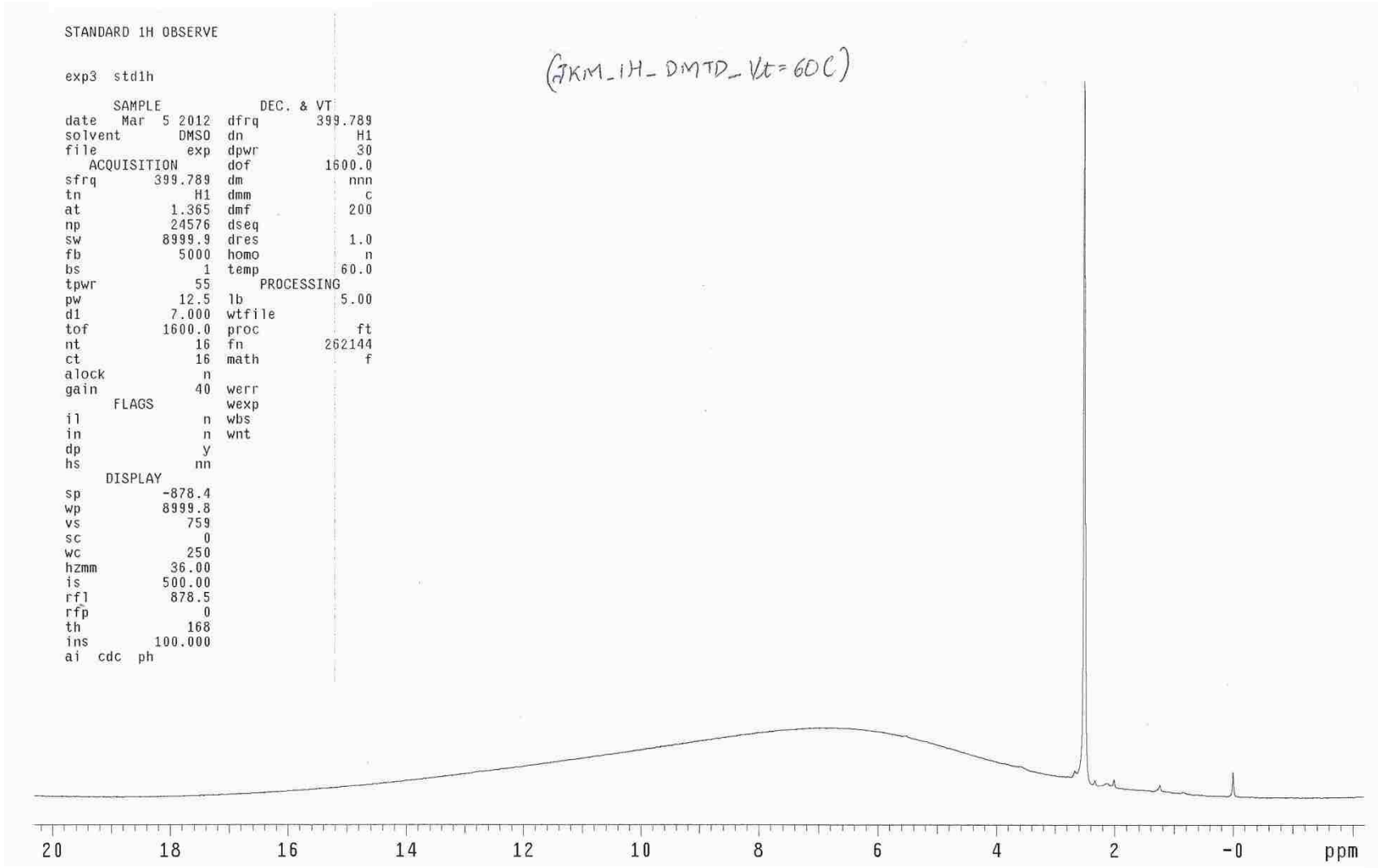


**Figure 1.4** Varied temperature $^{1}$H NMR of MTT in DMSO-$d_6$ at 60 $^{o}$C

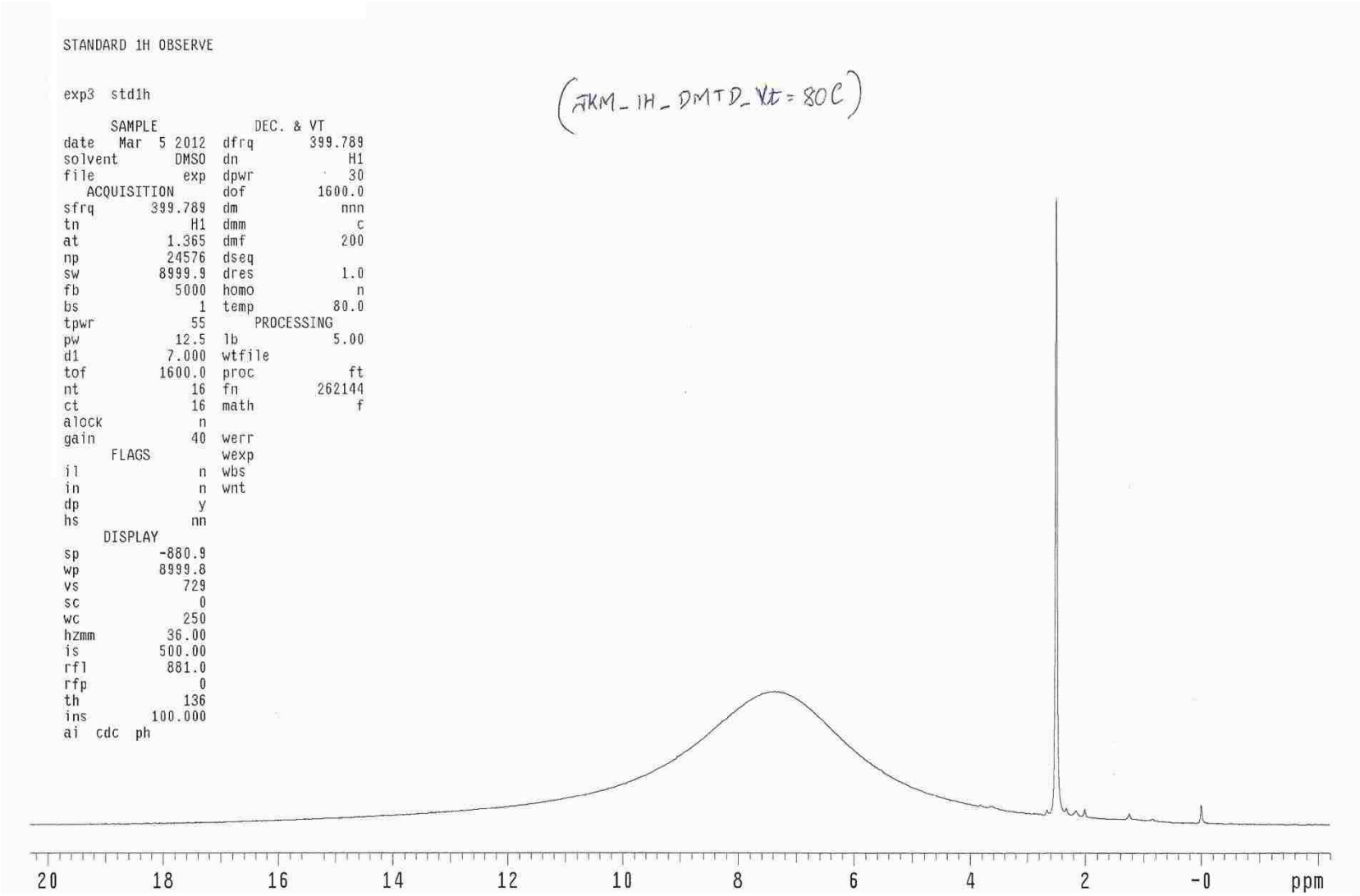


**Figure 1.5** Varied temperature $^{1}H$ NMR of MTT in DMSO-$d_6$ at 80 $^{o}C$

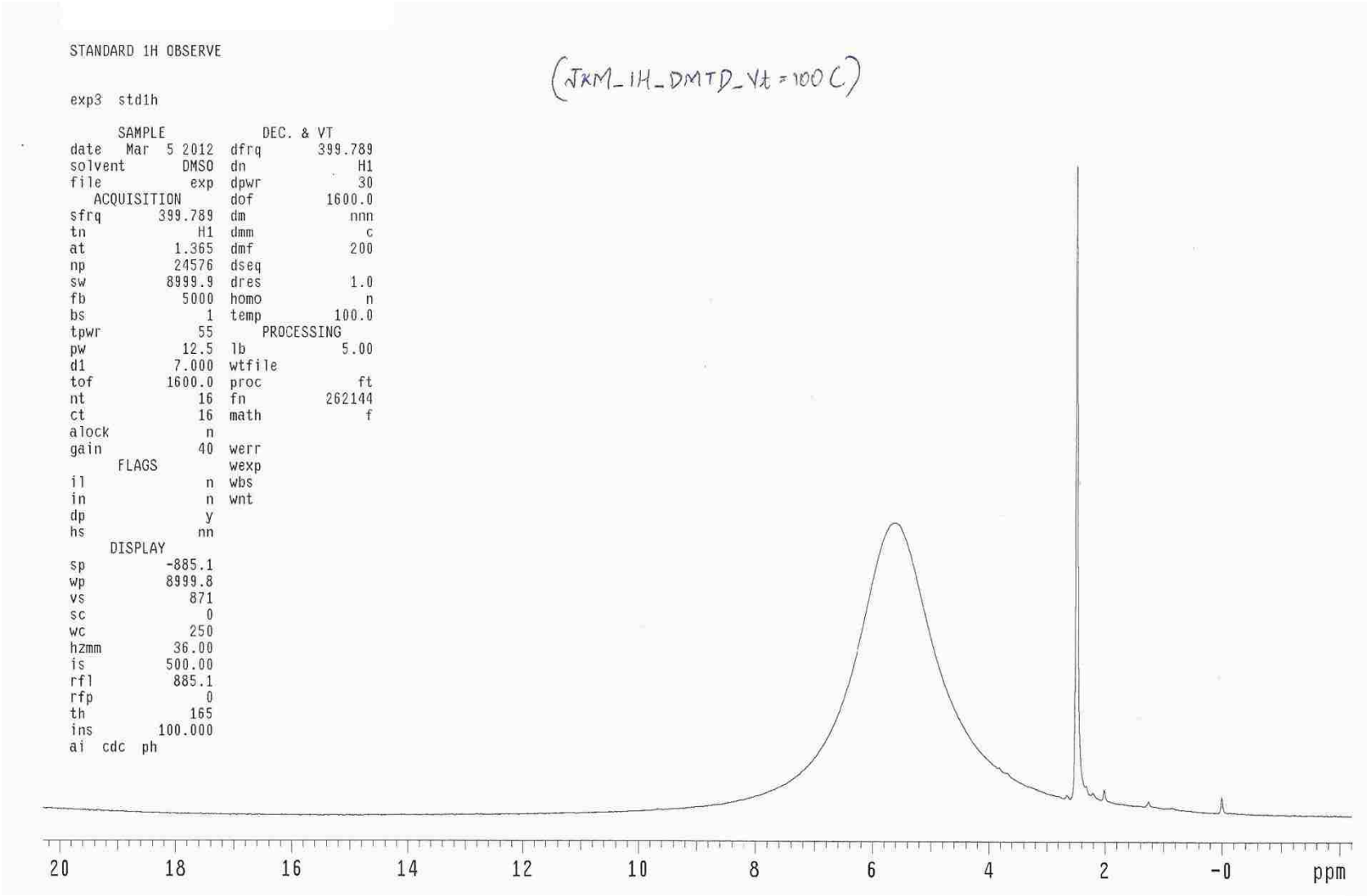


**Figure 1.6** Varied temperature $^{1}$H NMR of MTT in DMSO-$d_6$ at 100 $^{o}$C

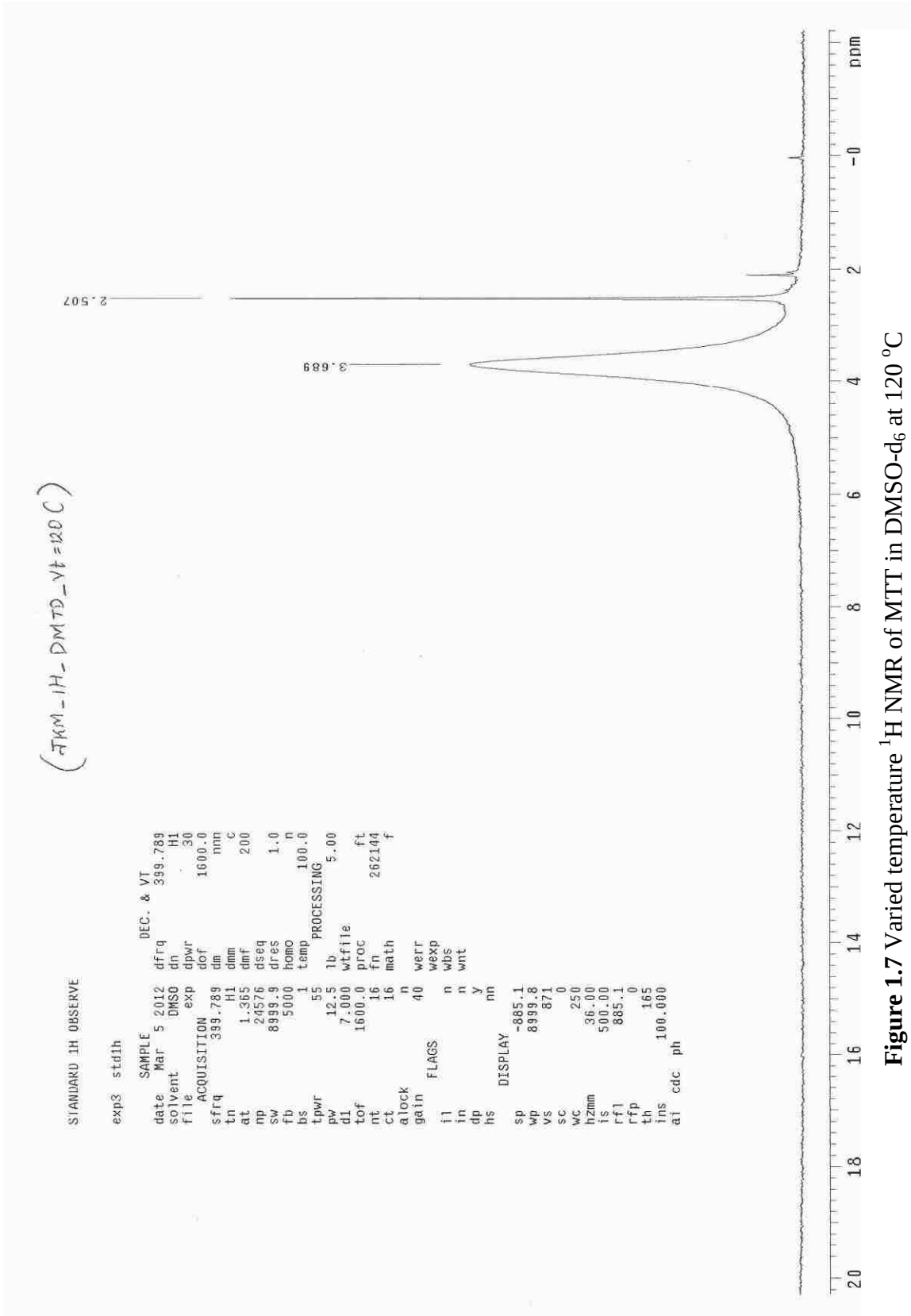


**Figure 1.7** Varied temperature $^{1}$H NMR of MTT in DMSO-$d_6$ at 120 $^{o}$C

The product formed in the NMR tube after the varied temperature experiments was insoluble in DMSO, THF, benzene, acetone, water, ethanol and chloroform. The melting point of this product was found to be 175-178 $^{o}$C which was identical to that of MTT.

To simulate the conditions of the VT-NMR experiment, 1.5 g of MTT was heated in 22.5 g of DMSO at 110 $^{o}$C for 1 hour in a micro-distillation assembly. The collection flask started getting hazy around 40 $^{o}$C after 10 min. and the distillation product started coming out around 80 $^{o}$C. The distillation product was separated into two components: one which had a boiling point of 38 $^{o}$C and another which had a boiling point of 100 $^{o}$C. The 1$^{st}$ component of the distillation product was identified as dimethyl sulfide ($Me_2S$) by means of a $^{1}$H NMR in DMSO (2.1 ppm) and the 2$^{nd}$ component was identified as water by means of a $^{1}$H NMR in DMSO (3.3 ppm) as well as refractive index (1.3325 at 20 $^{o}$C, by Abbe Refractometer). The precipitate formed at the end of the reaction in the reaction flask was washed with diethyl ether and weighed 1.47 g. This product had a M.P. of 175-178 $^{o}$C and was insoluble in DMSO, THF, benzene, acetone, water, ethanol and chloroform. This validates that the product was the same as that formed in the VT-NMR experiments. It was postulated that the product could possibly be either an extended H-bonded network of MTT molecules or a dimer/trimer of MTT. Since the product formed was insoluble in most common NMR solvents, it was not possible to record NMR spectra to determine its structure. In another set of experiments to determine the stability of MTT in DMSO, it was observed that the same product, as described earlier, was formed after different time intervals depending on the concentration of MTT in DMSO. For 0.5% concentration, traces of the product, as precipitate, were observed after 3 days while at a

higher concentration of 5%, traces of precipitate were observed after 1 day. This depicts the instability of MTT in DMSO and that the reaction of MTT with DMSO always gives $Me_2S + H_2O$ + an uncharacterized product.

To better understand the product formed as well as the reaction mechanism of MTT with DMSO, the reaction of MTT with benzyl mercaptan was studied. MTT (1.5g, 0.01m) was dissolved in benzene (30g) in a round bottom flask and benzyl mercaptan (2.48g, 0.02m) was added, after which the reaction mixture was stirred and refluxed for 24 hours to ensure the completion of reaction. The anticipated product was bis-benzylmercaptan-MTT, *Figure 1.8*:

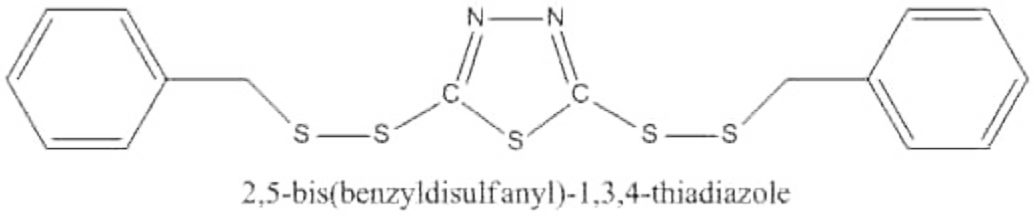


2,5-bis(benzyldisulfanyl)-1,3,4-thiadiazole

**Figure 1.8** Structure of the expected product bis-benzylmercaptan-MTT

After completion of the reaction, the product was filtered and air-dried. After filtration, the solvent used for the reaction, benzene, was found to be colorless indicating no presence of unreacted MTT. The product formed (2.36g) had a melting point of 153 $^{o}$C and was found to be soluble in acetonitrile, ethanol and 1,4-dioxane; sparingly soluble in water and insoluble in DMSO, benzene, chloroform and acetone. The product was recrystallized in 1,4-dioxane and by means of X-ray crystallography, its structure was found to be the mono-benzylmercaptan-MTT, *Figure 1.9*:

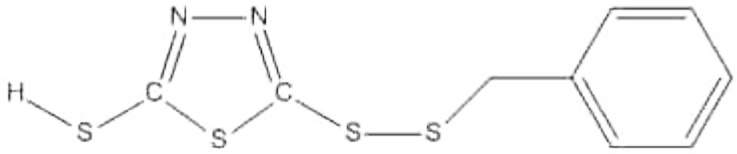

5-(benzyldisulfanyl)-1,3,4-thiadiazole-2-thiol

**Figure 1.9** Structure of the actual product mono-benzylmercaptan-MTT

The results of this reaction can be extrapolated to assume that the product formed from the reaction of MTT with DMSO might be bis-MTT, *Figure 1.10* with just one disulfide bond.

Dithiol form

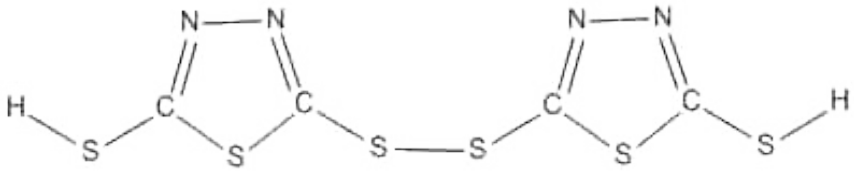

5,5′-disulfanediylbis(1,3,4-thiadiazole-2-thiol)

Dithione form

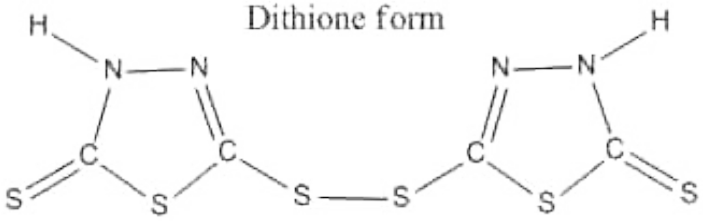

5,5′-disulfanediylbis(1,3,4-thiadiazole-2(3*H*)-thione)

Thiol-Thione form

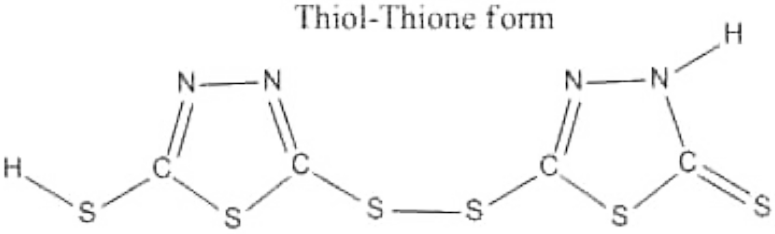

5-((5-mercapto-1,3,4-thiadiazol-2-yl)disulfanyl)-1,3,4-thiadiazole-2(3*H*)-thione

**Figure 1.10** The 3 possible structures of bis-MTT

By means of the solid-state NMR spectra, *Figure 1.11*, it was indicative that the product of MTT with DMSO may be an impure mixture of all of the 3 tautomeric forms described in *Figure 1.10* or a mixture of dimer along with MTT.

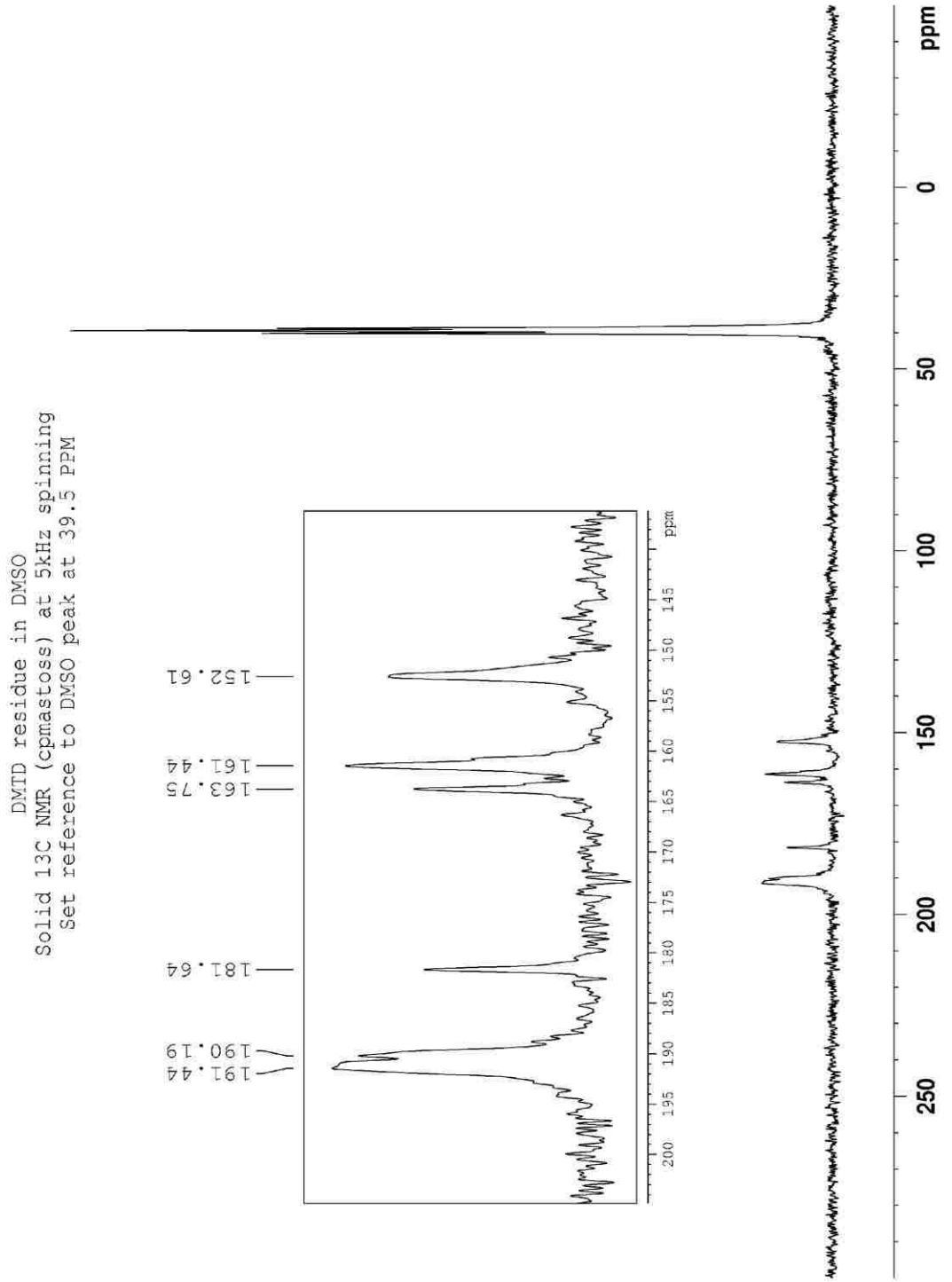


**Figure 1.11** $^{13}C$ solid state NMR of bis-MTT at 25 $^{o}C$

A part of the product of the MTT-DMSO reaction was recrystallized in 1,4-dioxane and a yield of 78% was reported for the pure product, based on the starting material MTT. By means of X-ray crystallography, *Figure 1.12*, this uncharacterized product was established as the dithione form of bis-MTT, which was consistent with the structure of bis-MTT reported in the literature.[16]

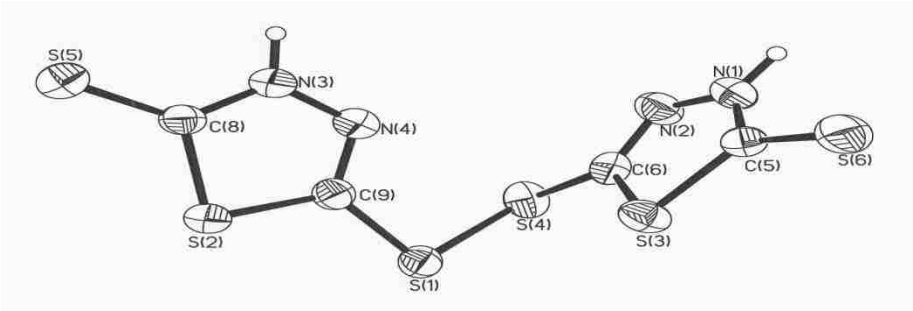


**Figure 1.12** X-ray crystal structure of bis-MTT

It was noted that the $^1$H NMR for MTT in acetone-$d_6$ was not observed at 400 MHz and 25 $^o$C. However, at higher magnetic field of 500 MHz at 25 $^o$C, the spectra showed 3 peaks, 2 of which are the same as that found in DMSO at 25 $^o$C and another one around 8-9 ppm which seems to be a median of the 2 peaks, *Figure 1.13*. This median broad peak indicates two labile hydrogen atoms which might be exchanging very rapidly. To study the effect of disulfide bond formation of MTT with DMSO, 1:1 mole amount of DMSO-$d_6$ (10.5 uL) was added to MTT (19 mg) in acetone-$d_6$ (1 ml) and the $^1$H NMR spectra now showed only 1 median peak around 8-9 ppm, *Figure 1.14-1.17*. To see the effect of increased MTT to the solution of 19 mg MTT in 1ml d6-acetone + 10.5ul DMSO-$d_6$, an additional 24 mg of MTT, and it appeared not soluble anymore. This agrees with the *Table 1* data, that MTT was only sparingly soluble in acetone, 20 mg/ml is about the maximum. Then 0.5ml DMSO-$d_6$ was added to the solution and the insoluble MTT immediately dissolved. The $^1$H NMR for the same showed two broad peaks, as seen earlier in the spectra of MTT in DMSO.

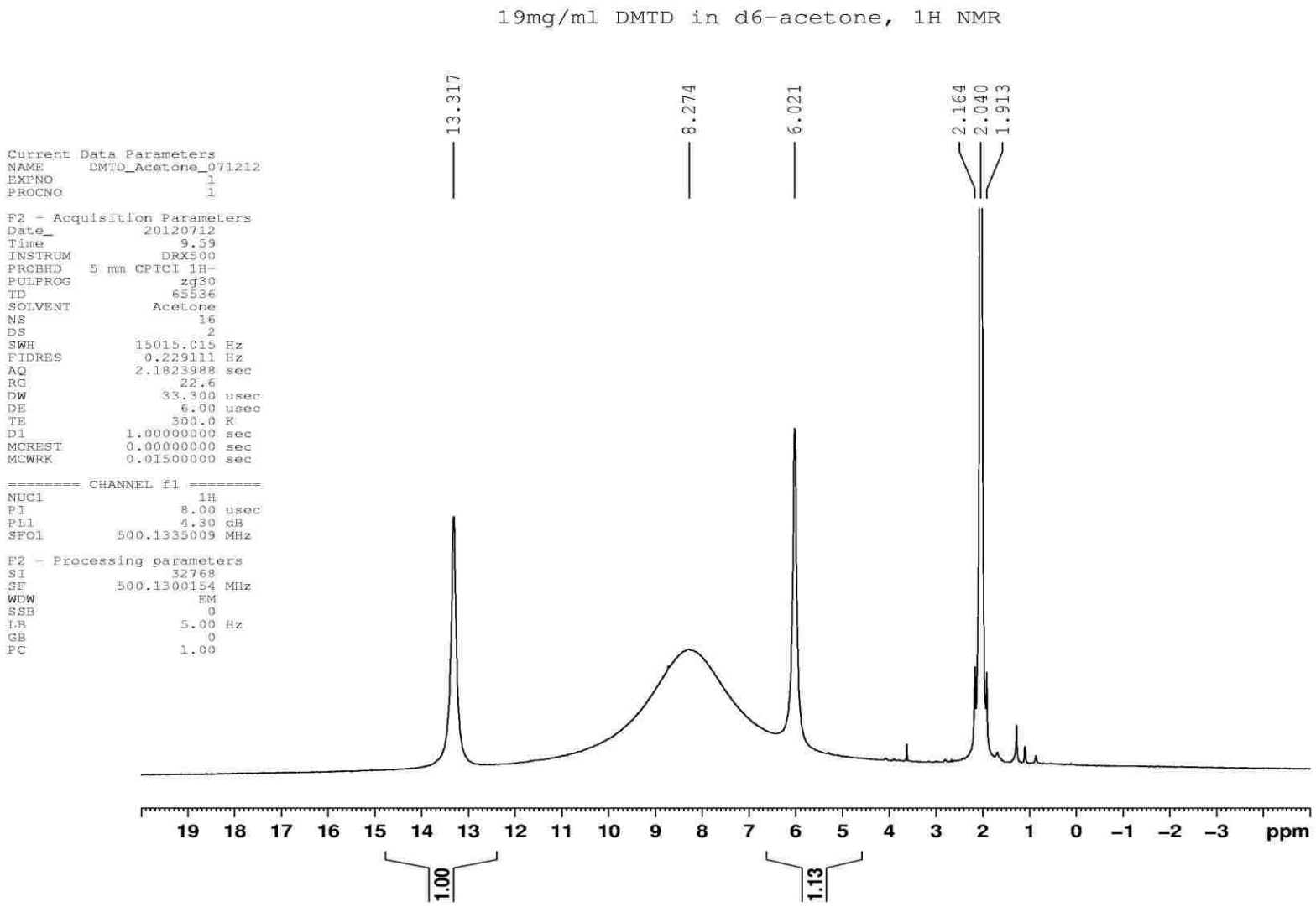


**Figure 1.13** $^{1}$H NMR of MTT in acetone-$d_6$ at 500 MHz

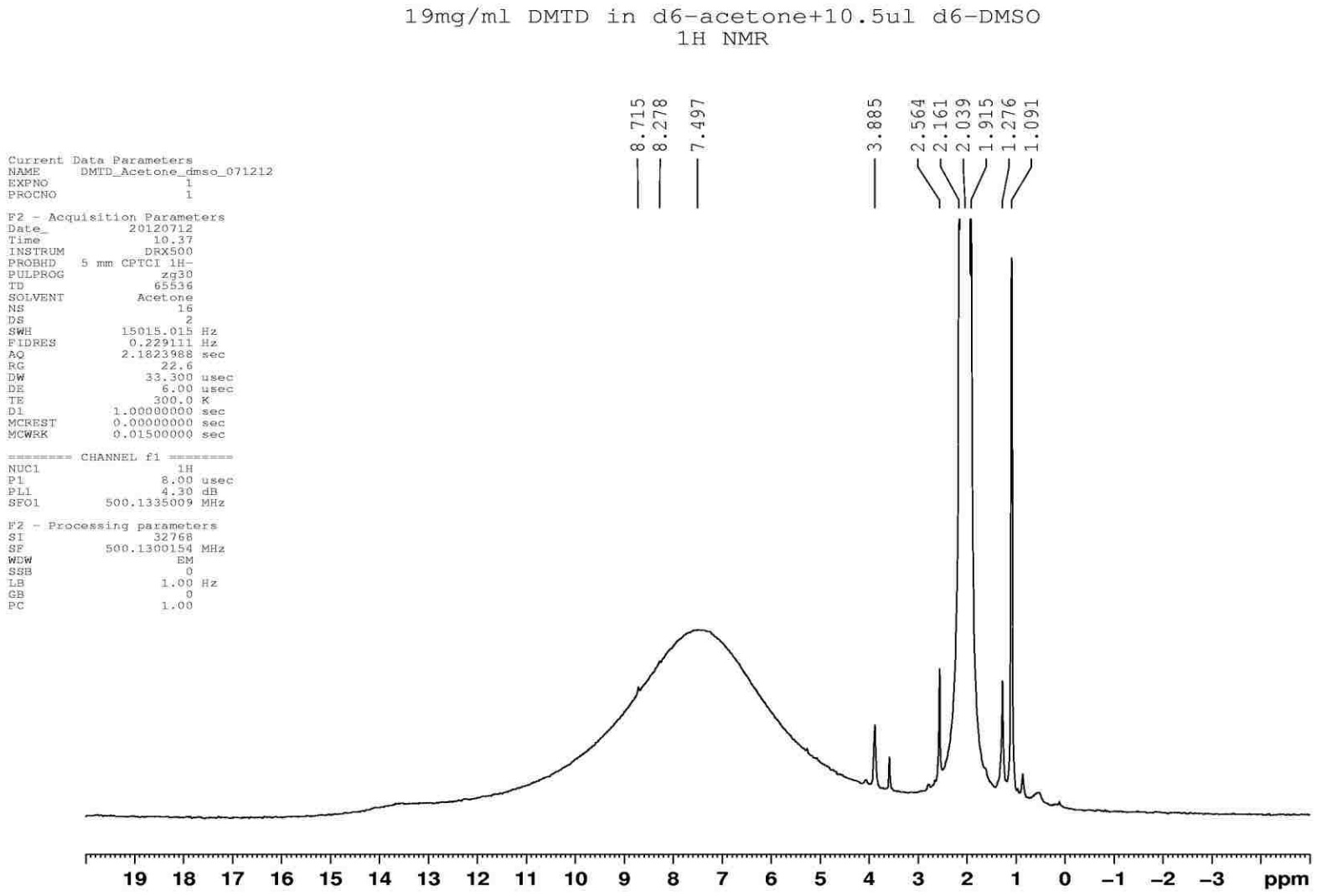


**Figure 1.14** Effect of DMSO on MTT as observed by $^{1}H$ NMR in acetone-$d_6$

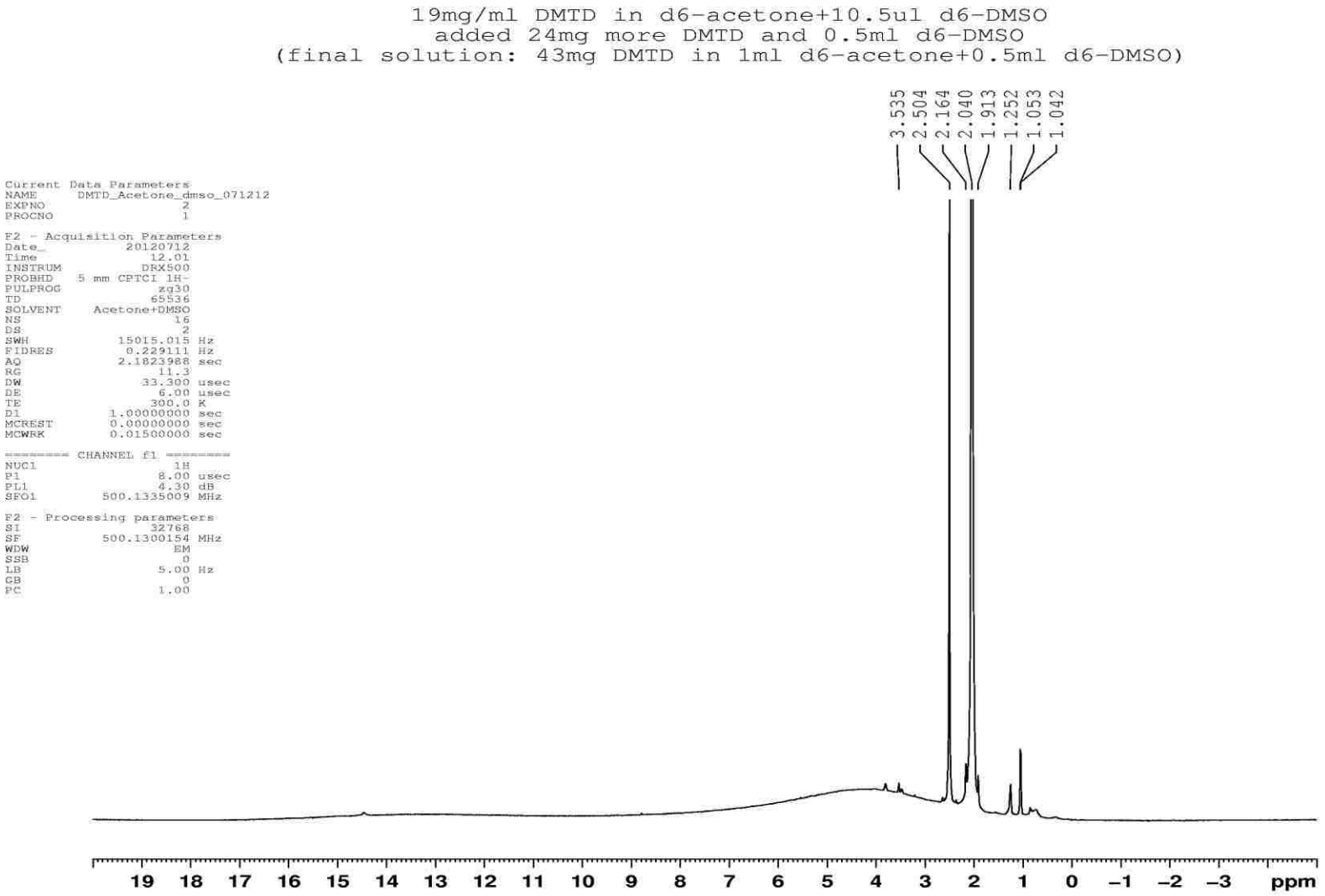


**Figure 1.15** Effect of extra DMSO on MTT as observed by $^{1}$H NMR in acetone-$d_6$

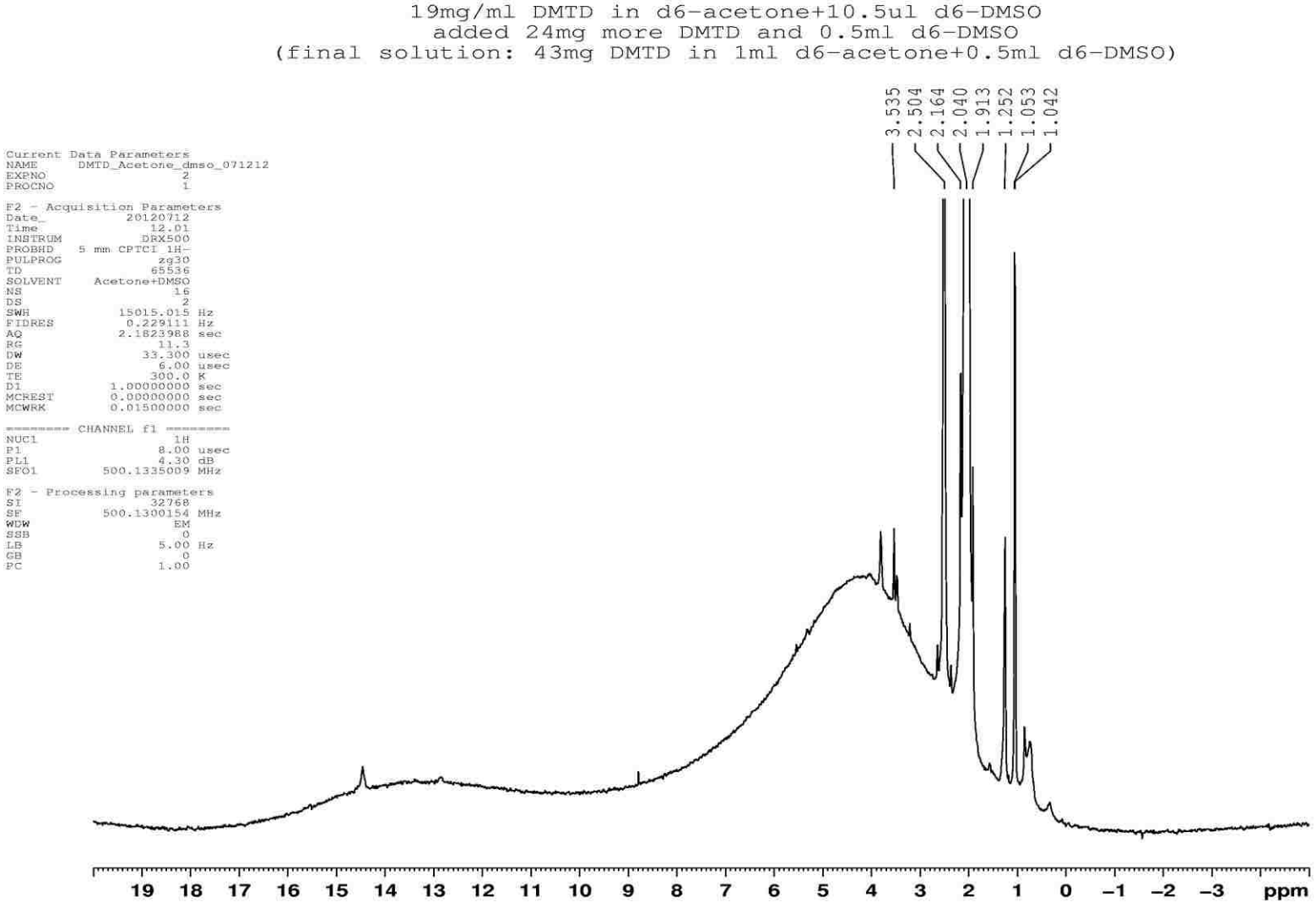


**Figure 1.16** Magnified baseline view of $^{1}$H NMR of MTT with DMSO in acetone-$d_6$

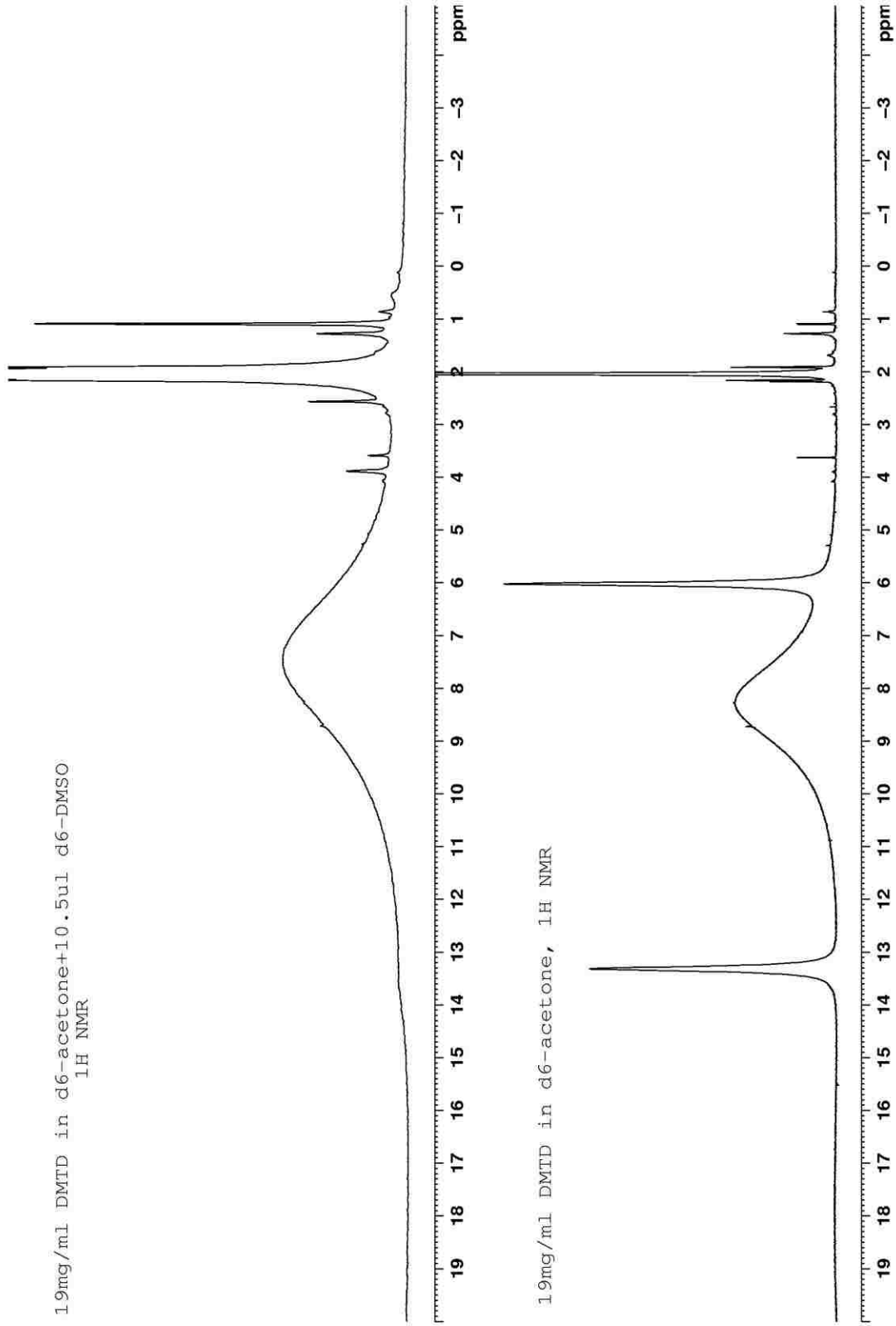


**Figure 1.17** $^{1}$H NMR compare of MTT in acetone-$d_6$ with and without DMSO

The S-H protons usually come at 1-2 ppm while the N-H protons come at about 9 ppm. In the proton spectrum of MTT in DMSO at 25 $^{o}$C, a N-H peak at 15ppm was observed which is typically a hydrogen bonded N-H (with water or DMSO). The free water in DMSO usually comes at 3.3 ppm which was observed as the 2$^{nd}$ peak at 25 $^{o}$C. The heating breaks the hydrogen bond and allows the N-H to exchange with the free water, therefore, two broad peaks were observed to be moving towards each other in the Varied Temperature NMR experiments. S-H only forms weak hydrogen bonds and at 25 $^{o}$C, the S-H was already exchanging with free water so no peak for the S-H was observed in the proton spectrum of MTT in DMSO at 25 $^{o}$C. At 120 $^{o}$C, only one broad peak at 3.7 ppm was observed because the protons were exchanging so fast now, that they all appear in the averaged position. This averaged position depends on how much the free water was present, plus the S-H at lower chemical shift, and also on how much the N-H protons were at higher shift. Note that the 15 ppm was not the true shift for N-H because of the hydrogen bonding. The true shift was near 9 ppm. Since there might be more free water in the system, the weighted average was at 3.7 ppm. Since "100% atom D type DMSO" was not used in the sample preparation for recording the NMR spectra, it was inferred that there could be either water in the solvent or hydrogen transfer between two MTT molecules which would explain the peak broadening in the NMR spectras. No water peak was observed in the proton spectrum of just the DMSO solvent. However, it would be interesting to observe the behavior of dry-MTT in 100% D-atom DMSO.

Dry MTT (9 mg) was dissolved in 0.6 ml 100% D-atom DMSO and transferred in a dry, nitrogen purged NMR tube after which proton spectrum was recorded, *Figure 1.18*. Only one broad peak spanning from 3-12 ppm was observed. On increasing the

concentration 46 mg of MTT in 0.6 ml of 100% D-atom DMSO, two distinct humps were observed, one around 3 and another around 13 ppm, *Figure 1.19*. These results indicate a possible proton transfer in the system such that the peaks observed are at the weighted average positions of the real 2 shifts. This corroborates our findings from the Varied Temperature NMR experiments. *Figure 1.20* shows the comparison spectras.

Due to the rapid proton exchange process on the two different $^{13}$Cs, the signals are just too broad to be seen. Therefore, it was proposed to add chromium acac [Cr(acac)] to the solution of MTT in DMSO to mask the effect of the prolonged relaxation time, to observe the $^{13}$C NMR. With Cr(acac), the relaxation time was enhanced. Thus, 45 mg of MTT was dissolved in 0.6 ml 100% D-atom DMSO and 1.5 mg of Cr(acac) was added and the spectra was recorded at 500 MHz and 25 $^{o}$C. The $^{1}$H NMR of MTT showed 2 broad peaks, as expected, *Figure 1.21* while the $^{13}$C NMR also depicted 2 peaks with the help of rapid scanning and pulse sequencing, *Figure 1.22*. When pulsing rapidly, the baseline was rolling so the "aring2" sequence is used to get rid of the rolling. Now the broad $^{13}$C peaks (linewidth over 2000 Hz) are pulled out of the baseline. The 2 peaks observed were at 158.5 ppm and 188.5 ppm, reinstating the structure of MTT in DMSO in the thiol-thione form where one of the hydrogen was on the sulfur and another, on the nitrogen. *Figure 1.23* shows the magnified spectra for the same.

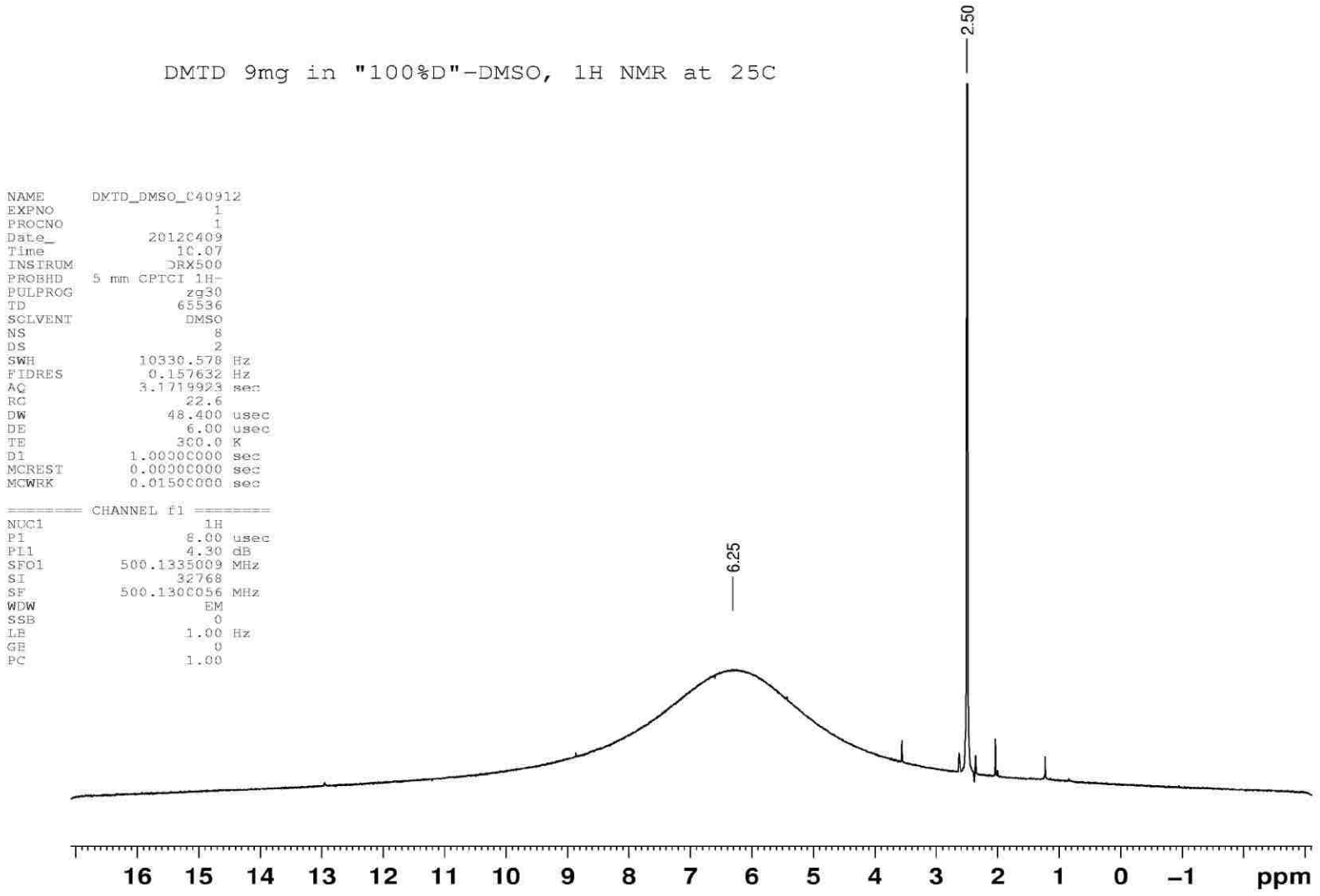


**Figure 1.18** $^{1}$H NMR of low conc. of MTT (9 mg) in DMSO at 25 $^{o}$C and 500 MHz

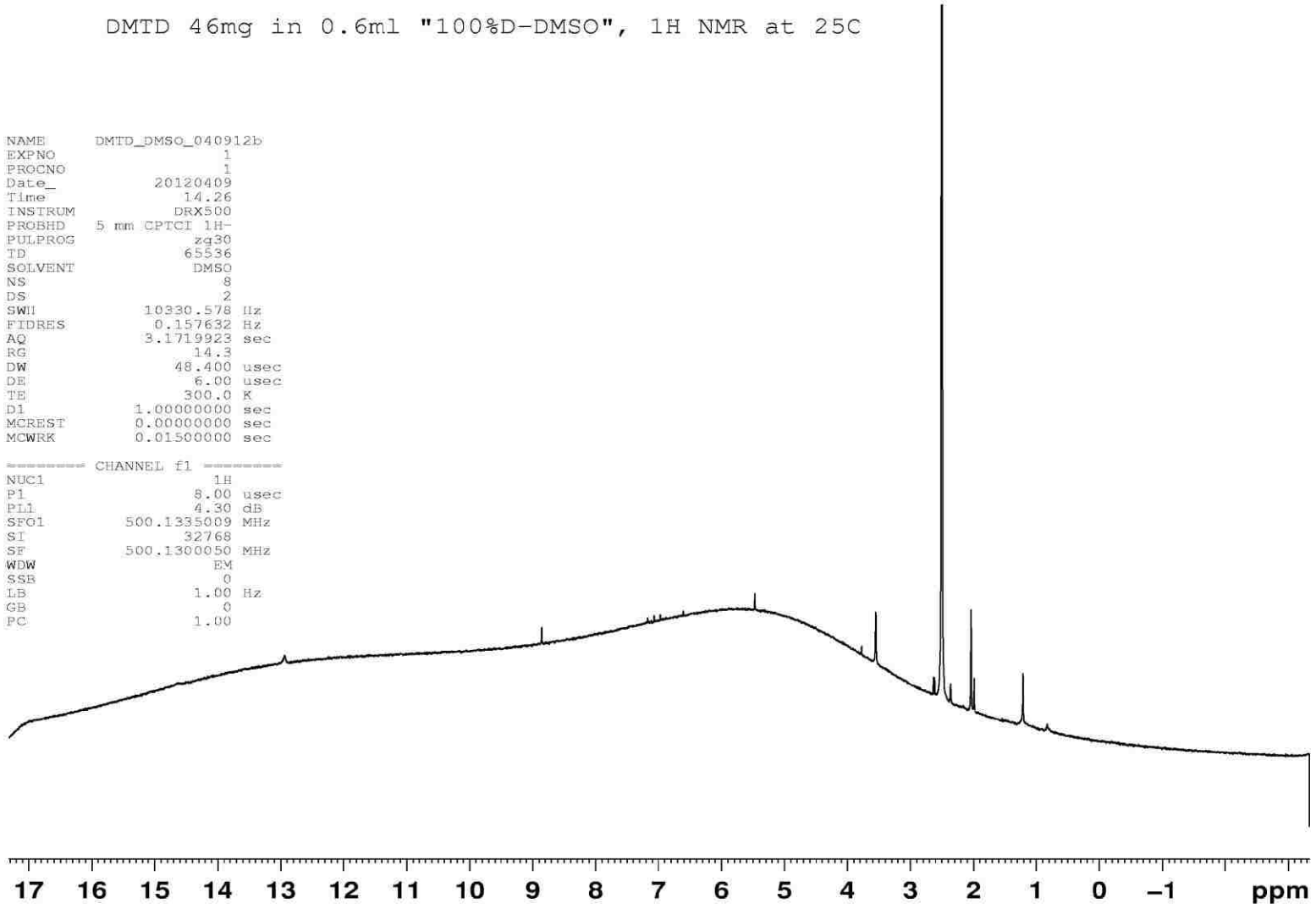


**Figure 1.19** $^{1}$H NMR of high conc. of MTT (46 mg) in DMSO at 25 $^{o}$C and 500 MHz

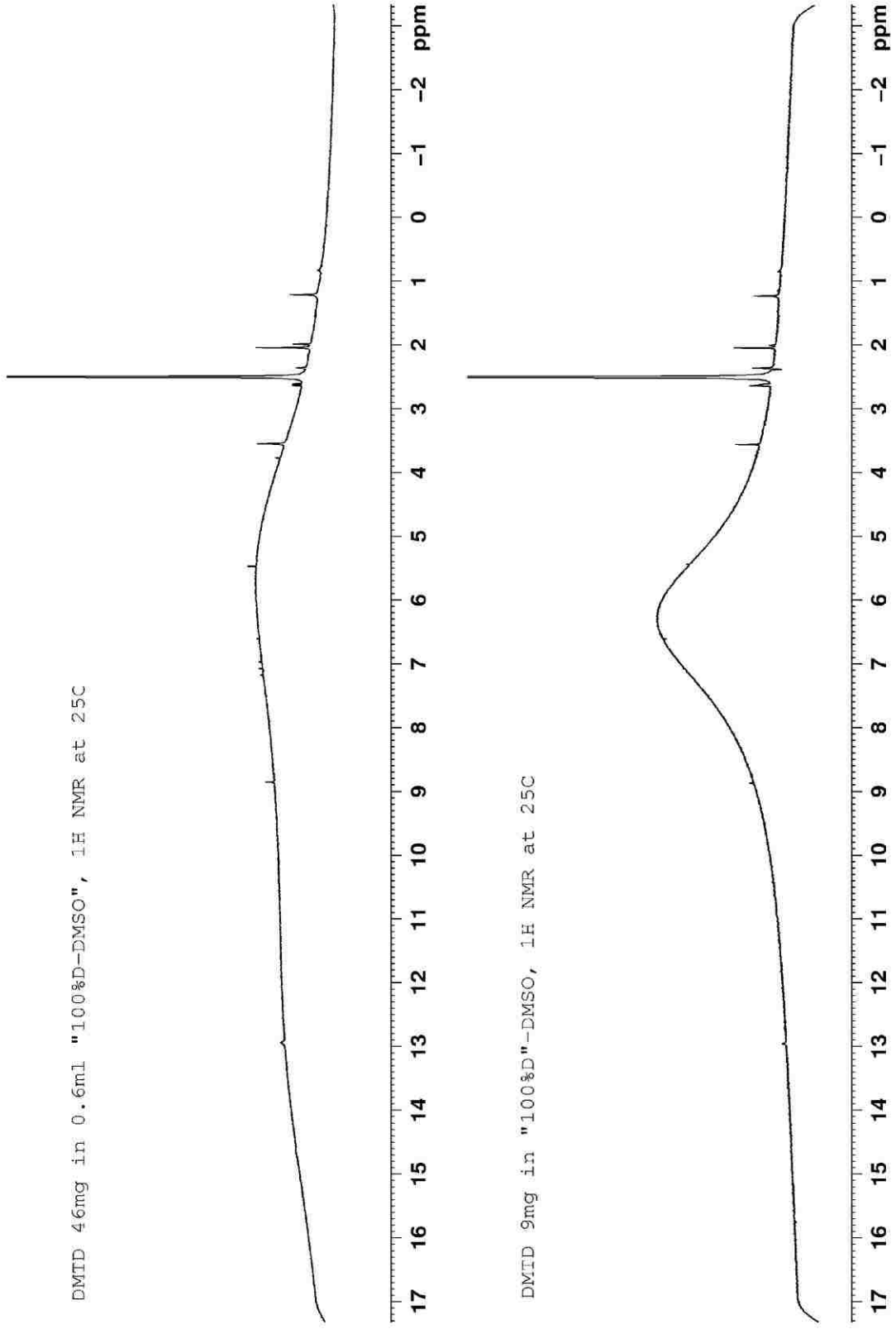


**Figure 1.20** Effect of MTT concentration in DMSO at 25 $^{o}$C and 500 MHz

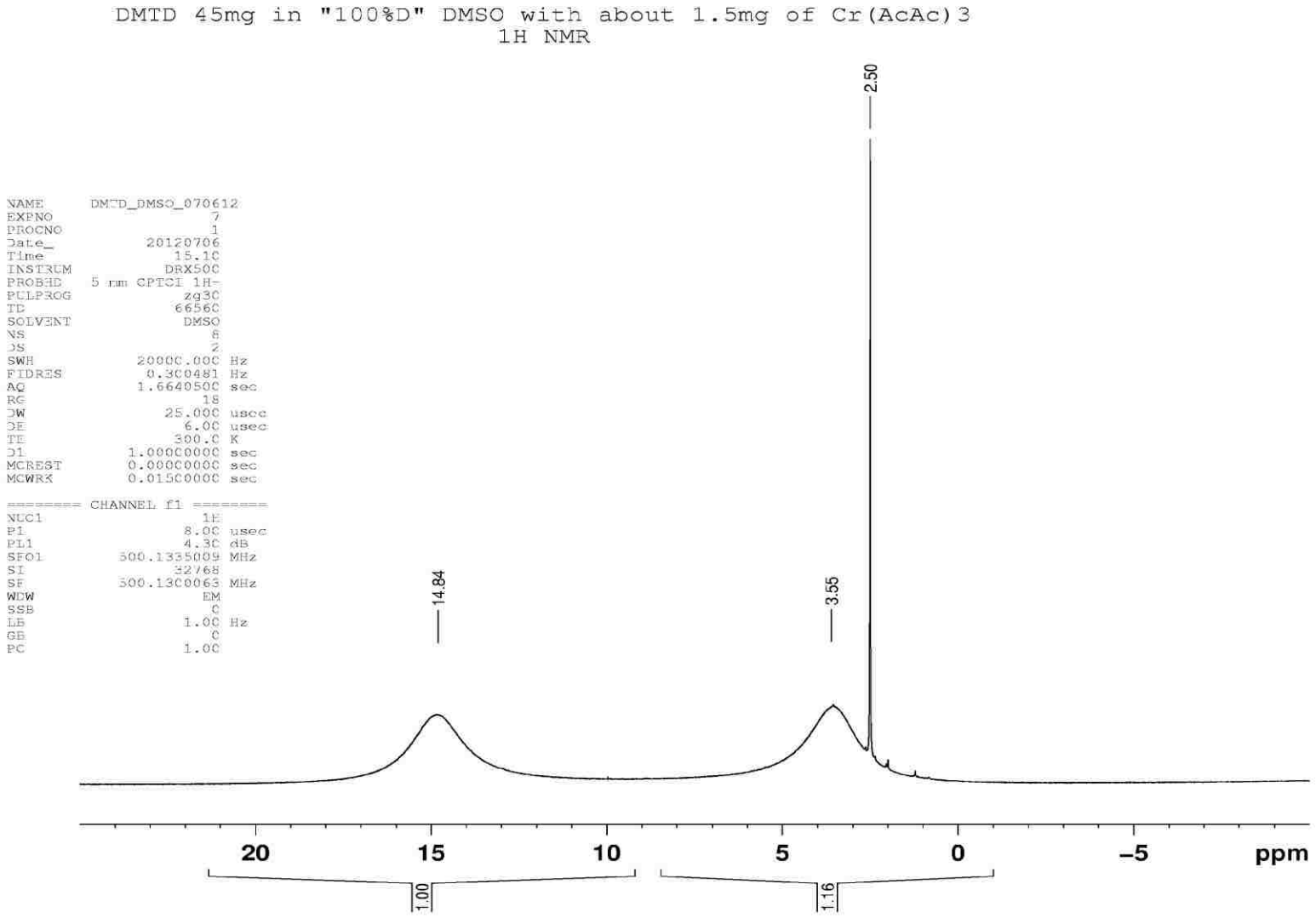


**Figure 1.21** $^{1}$H NMR of MTT in DMSO with chromium acac

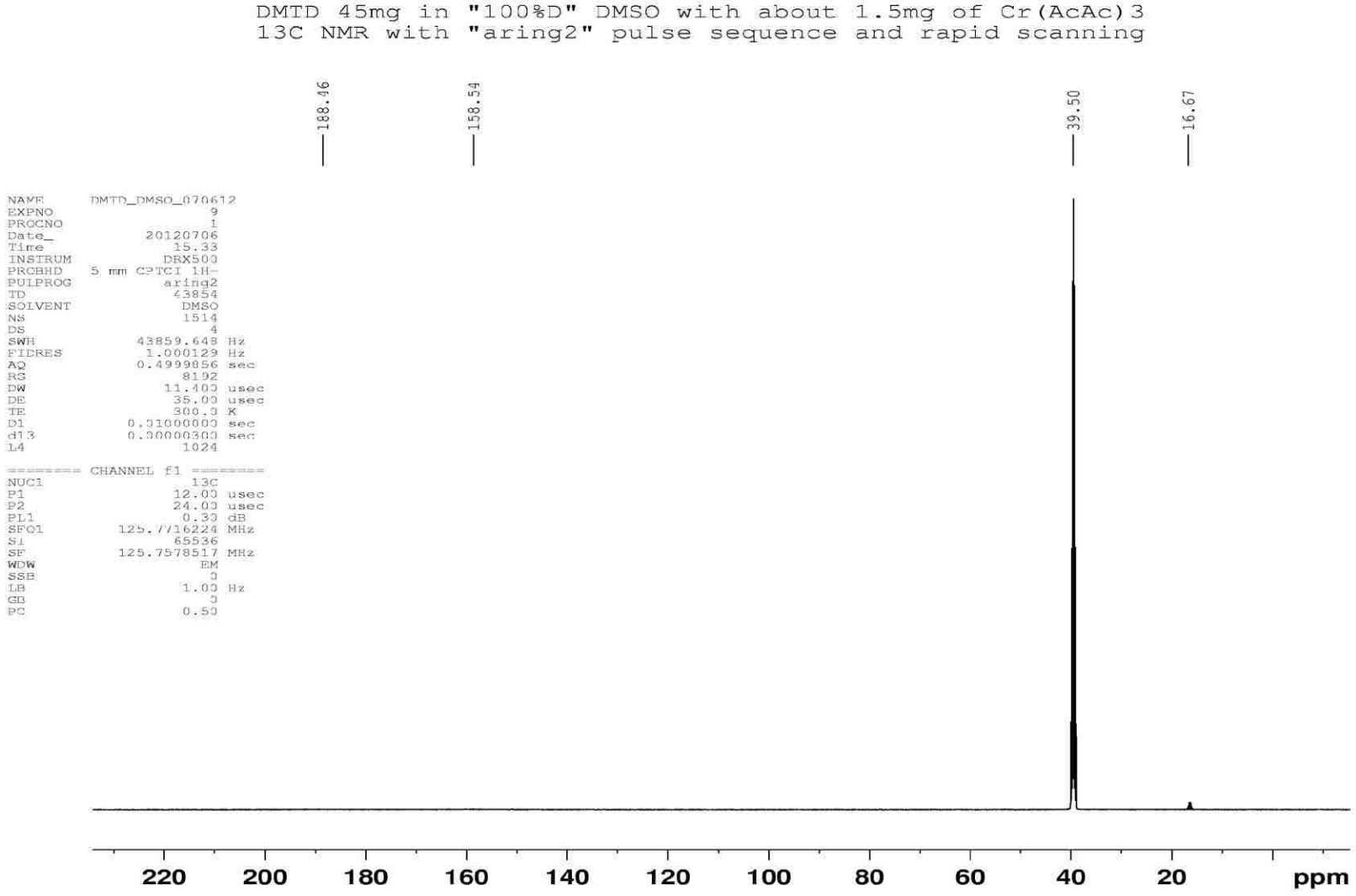


**Figure 1.22** $^{13}$C NMR of MTT in DMSO with chromium acac and rapid scanning

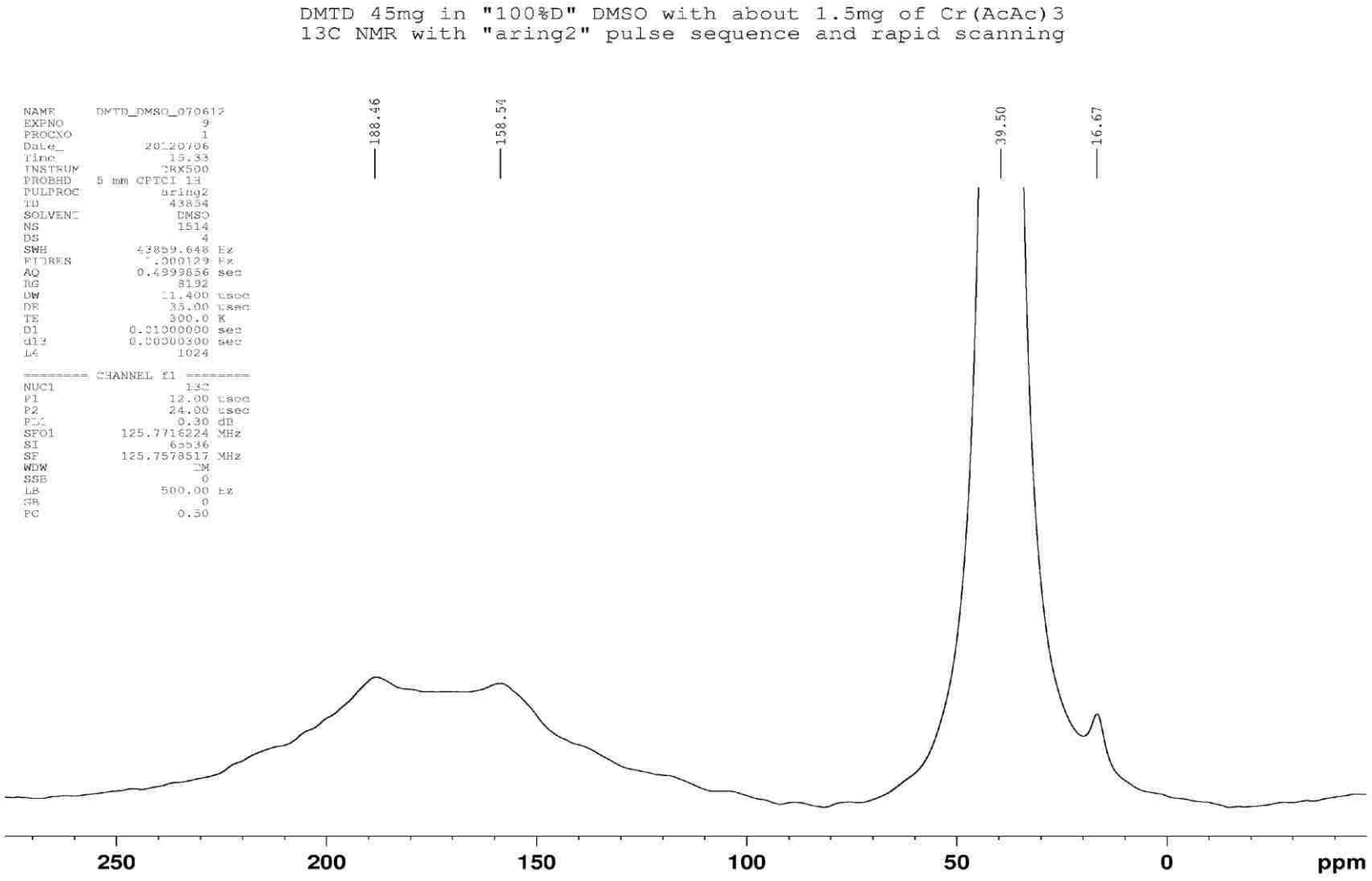


**Figure 1.23** Magnified baseline view with line broadening of 5 Hz for the $^{13}C$ NMR of MTT in DMSO with chromium acac and rapid scanning

Since the proton spectrum of MTT was only observable in DMSO, in another set of experiments, to provide evidence for a possible ligation between MTT and DMSO, it was proposed to observe the hydrogen peaks of DMSO without MTT and in presence of MTT, in ethanol-$d_6$. It be noted that the proton spectrum of MTT did not show any peaks in ethanol-$d_6$. A 1 ml sample of DMSO (13 mg, 0.000167 m) with 2 ml ethanol-$d_6$ was taken in an NMR tube for analysis. The proton spectrum depicted a single peak for DMSO at 2.6 ppm, *Figure 1.24* and integrating the peak with reference to the ethanol-hydrogen gave an integral value of 0.04, *Figure 1.26*. In another NMR tube, a 1 ml sample of 1:1 equimolar amount of MTT (25 mg, 0.000167 m) and DMSO (13 mg, 0.000167 m) was taken with 2 ml ethanol-$d_6$. The proton spectra for this sample showed that the DMSO peak at 2.6 ppm had shrunk in half and a new peak at 2.0 ppm was observed, *Figure 1.25*. On integrating the peaks, *Figure 1.27*, it was evident that even though equimolar amounts of MTT and DMSO were added to ethanol, 2 molecules of MTT were associating to 1 molecule of DMSO as the DMSO peak shrunk half in size. This corroborates with the proposed reaction mechanism for the formation of bis-MTT as the final product, as depicted in *Figure 1.32*. Whether the ligation is due to the S-S interaction or related to the proton transfer facilitated by oxygen of DMSO is still unclear and further experimentation is pivotal for a definite conclusion.

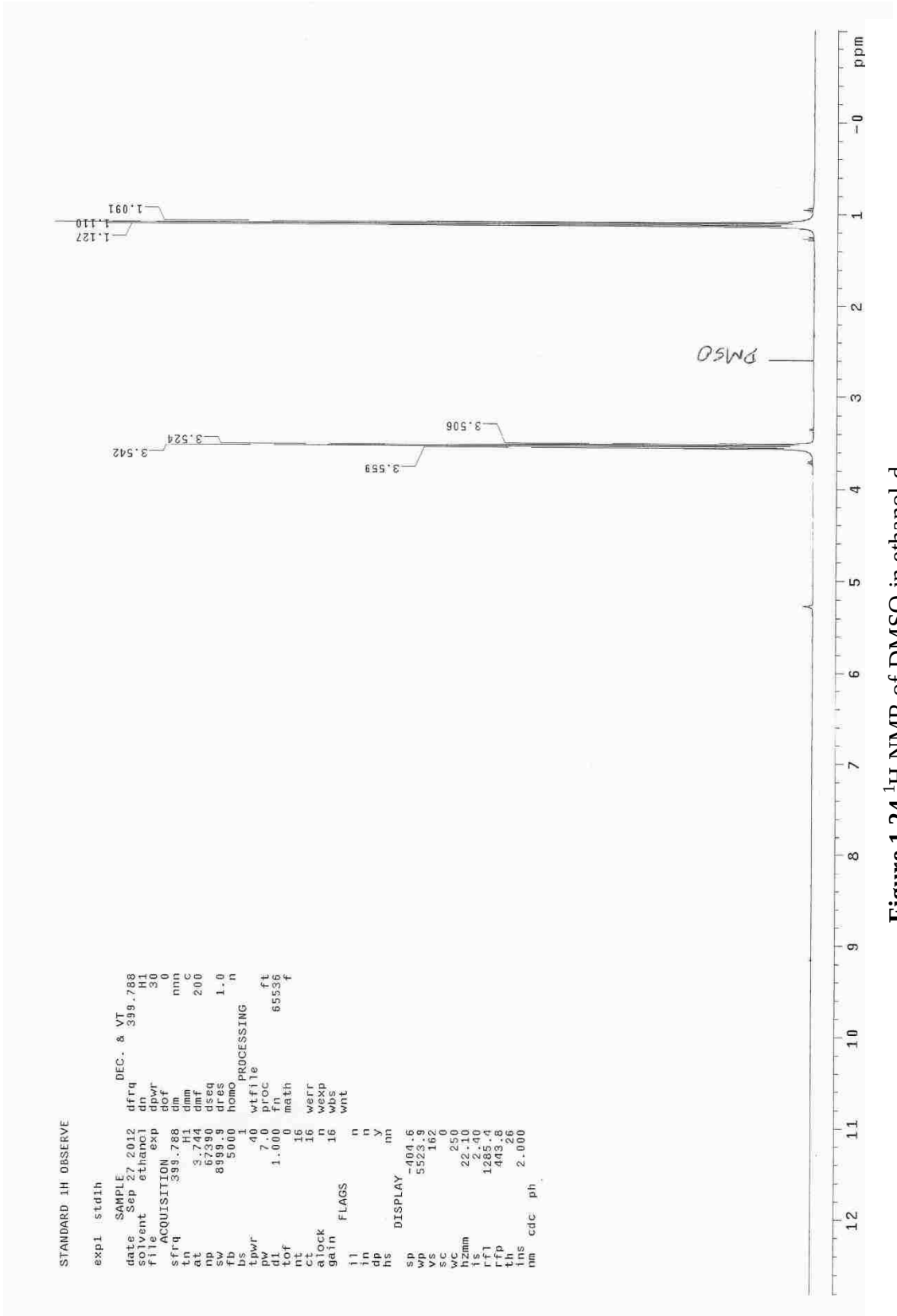


**Figure 1.24** $^{1}$H NMR of DMSO in ethanol-$d_6$

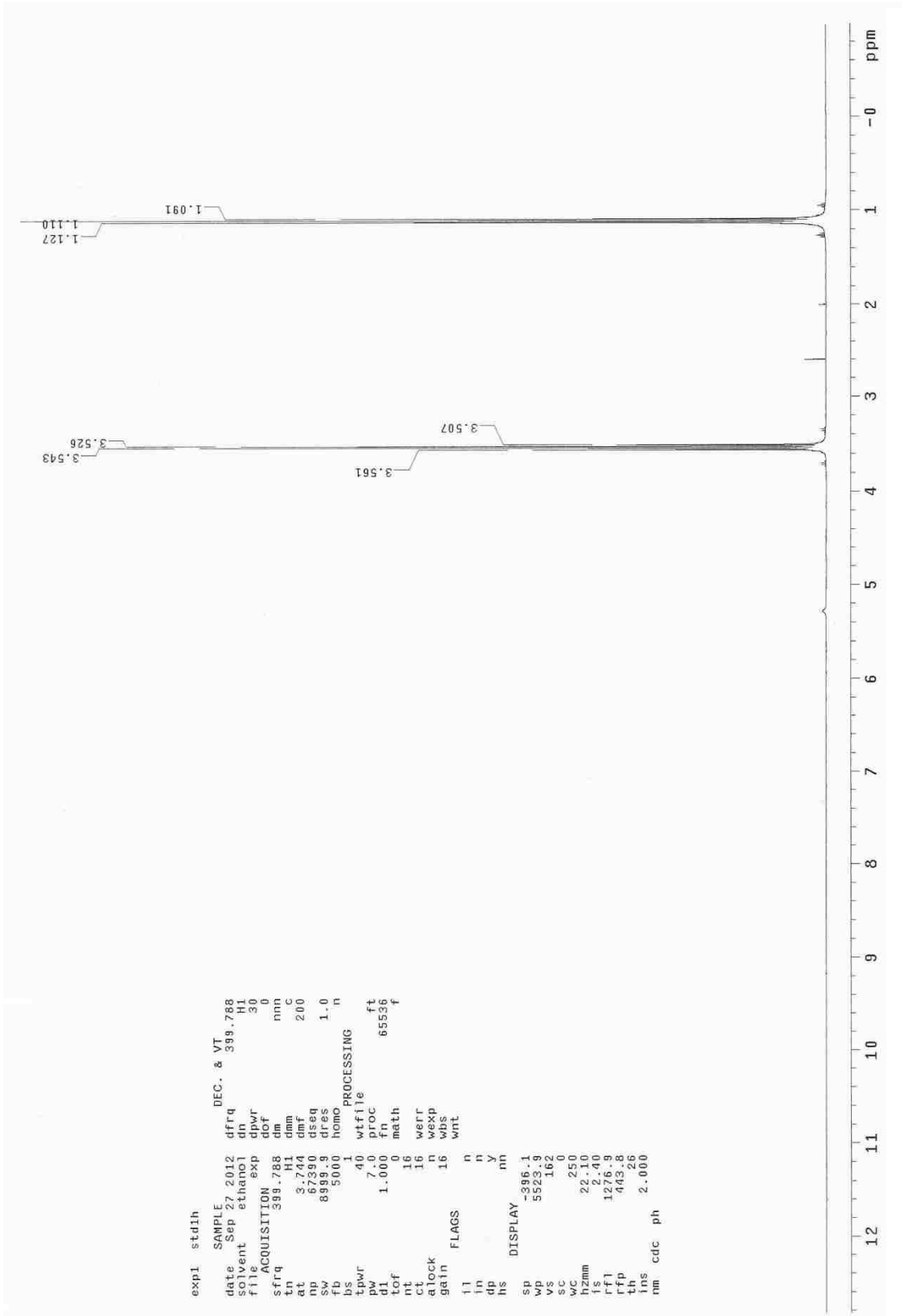


**Figure 1.25** $^{1}$H NMR of 1:1 equimolar amount of MTT + DMSO in ethanol-$d_6$

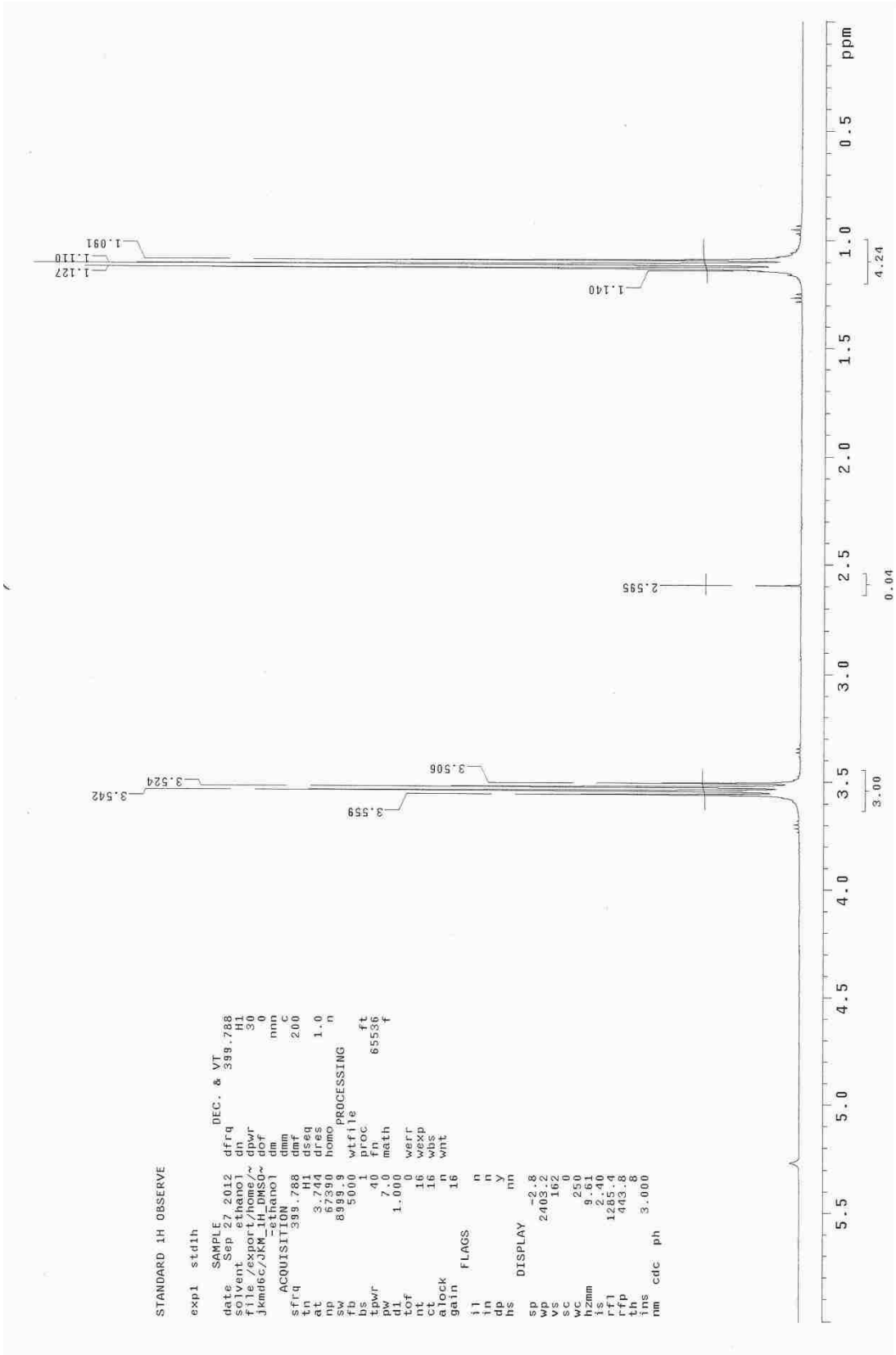


**Figure 1.26** Integrated $^{1}$H NMR of DMSO in ethanol-$d_6$

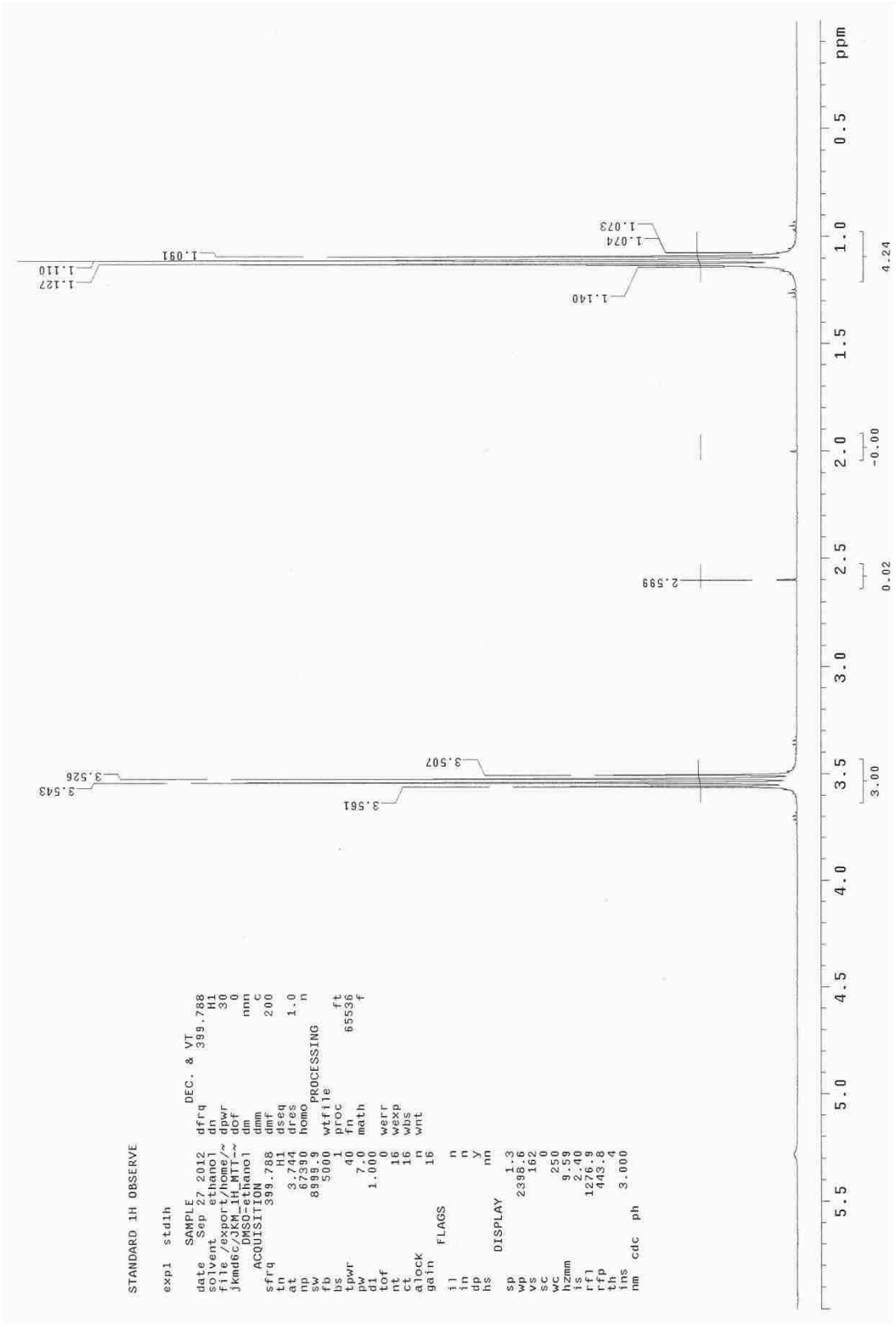


**Figure 1.27** Integrated $^{1}$H NMR of 1:1 equimolar amount of MTT + DMSO in ethanol-$d_6$

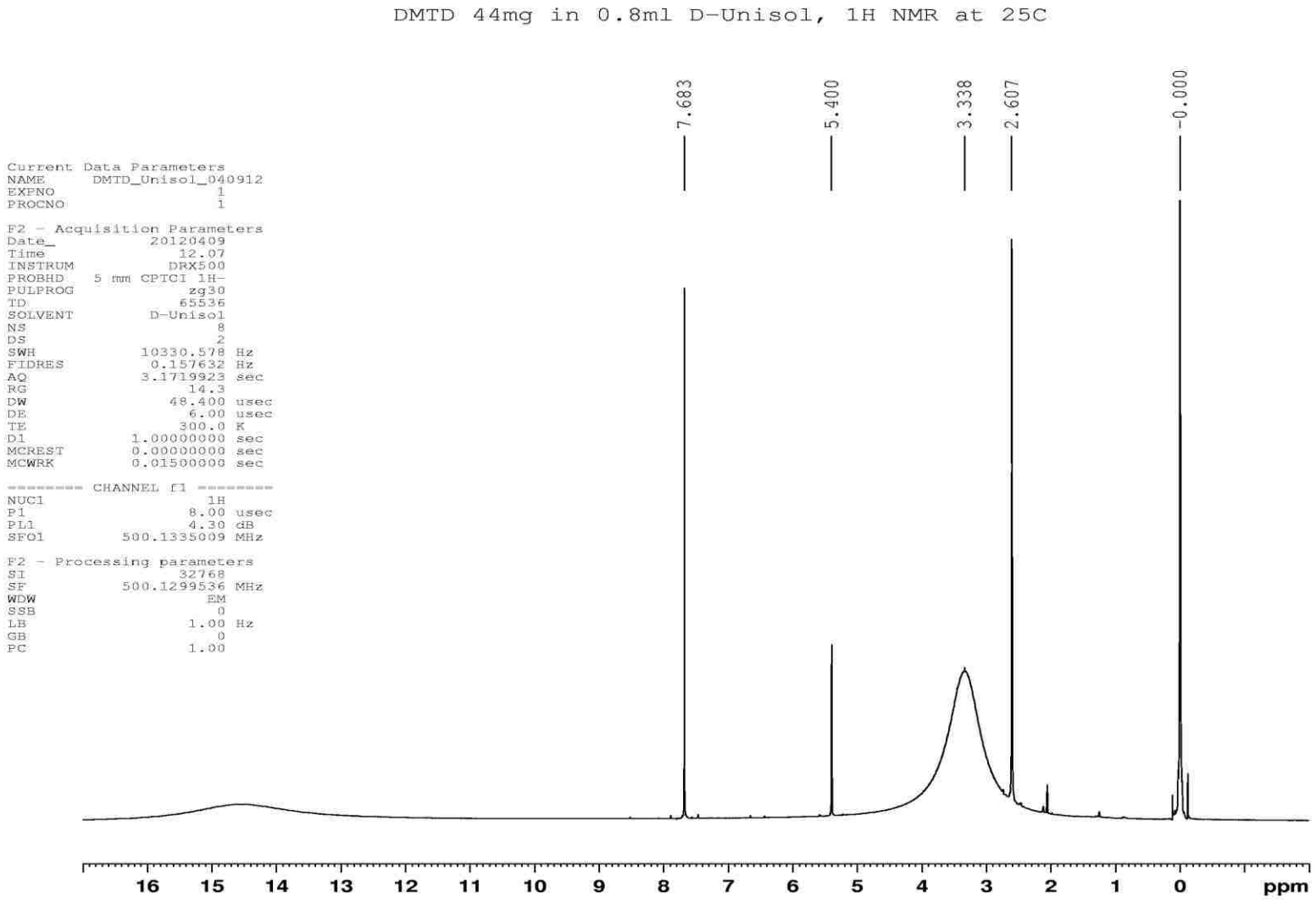


**Figure 1.28** $^{1}$H NMR of MTT in Unisol at 25 $^{o}$C and 500 MHz

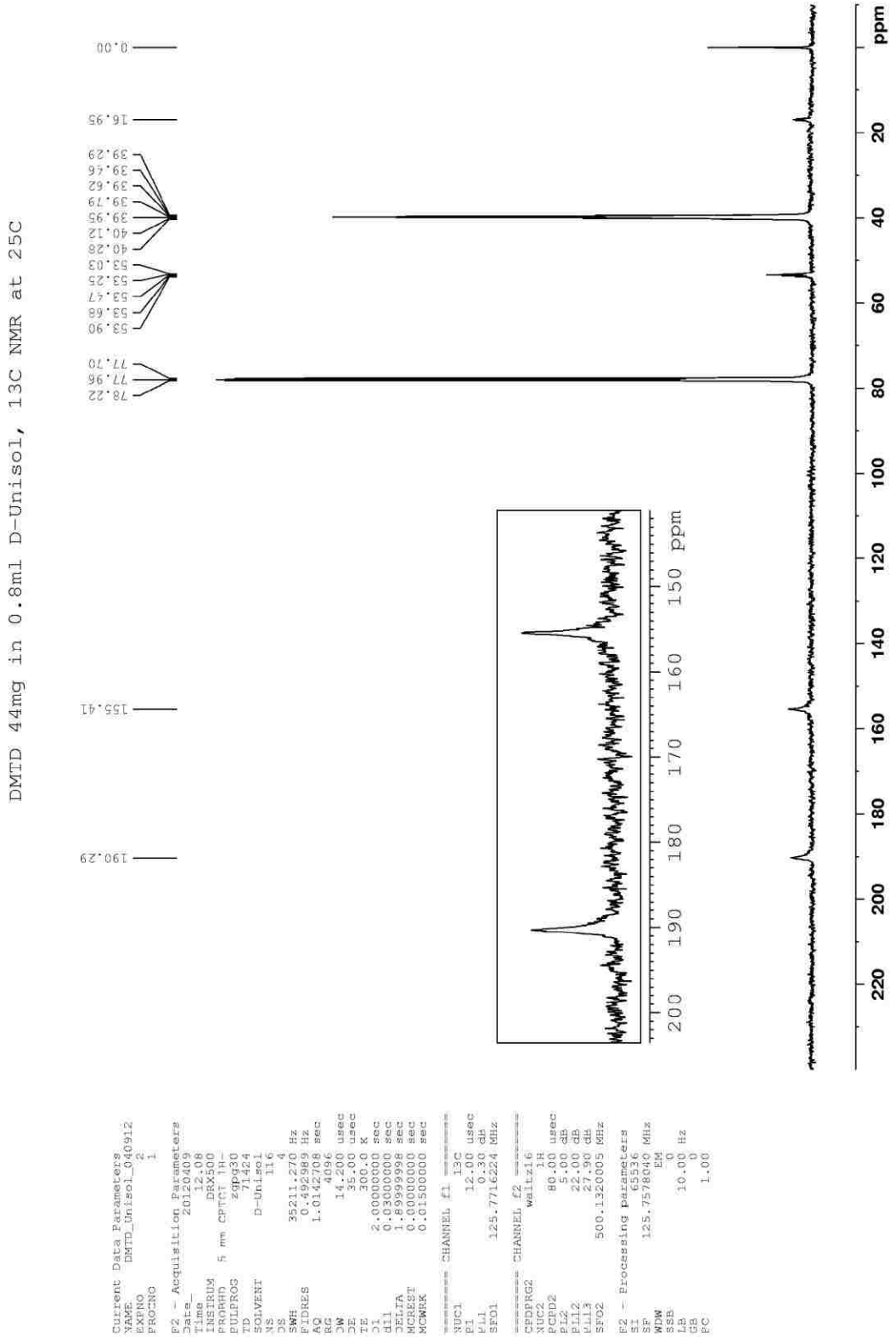


**Figure 1.29** $^{13}$C NMR of MTT in Unisol at 25 $^{o}$C and 500 MHz

As described in *Table 1*, both the $^{1}H$ and $^{13}C$ NMR were recorded in Unisol, as seen in *Figure 1.28* and *Figure 1.29*.

From all of the above results, it can be concluded that either rapid hydrogen exchange is happening or there is a pre-equilibrium product involving the MTT-DMSO adduct. If the condition is such that it allows the slowing down of the exchange we can observe two set of signals. One such condition is hydrogen bonding of the nitrogen or the sulfur. Hydrogen bonding occurs when there is water in the solvent or in solvent DMSO. Since the NMR solvents have only a small amount of water we can only see two $^{1}H$ peaks for MTT in the solvent (less than 20 mg). In acetone-$d_6$ (*Figure 1.13*) there are three peaks- the two sharp ones due to N-H and S-H and the broad one in the middle is weighted average peak due to the exchange. The N-H and S-H protons are not in their usual chemical shift positions, perhaps because they are hydrogen-bonded not with water but with acetone (enol form of acetone; acetone is known to undergo keto-enol conversion). Another condition to slow down the proton exchange is cooling, but it is not easy to do especially for DMSO which has such a high freezing point.

DMSO solvent is unique because it assists hydrogen transfer (*Figure 1.30, Figure 1.31*) and reacts with MTT to form bis-MTT (*Figure 1.32*). If the relative energies of *Intermediates 1 & 2* (*Figure 1.32*) are comparable, then equilibrium can exist such that both of those intermediates could be interchangeably formed, possibly leading to peak broadening as observed by $^{1}H$ NMRs. So it is difficult to observe two sharp peaks. Whether we can see two peaks in $^{1}H$ NMR depends on the concentration of MTT and dryness of DMSO. $^{1}H$ NMR of 9mg in "100%D" DMSO (*Figure 1.18*) showed only one broad peak indicating both N-H and S-H are involved in the hydrogen transfer assisted by

DMSO. After adding more MTT to 46mg there are two broad peaks observed. However, when there is a little water (VT-NMR study) or concentrated MTT solution with Cr(acac) present, we see two broad peaks.

Further research should shed more light on whether the proposed phenomena of proton/hydrogen transfer, *Figure 1.30* (less likely, higher energy pathway) *or Figure 1.31*, as well as the proposed disulfide bond formation, *Figure 1.32*, both of which lead to the final product of bis-MTT, are occurring in the MTT-DMSO system. If proven that the proton/hydrogen transfer was indeed occurring, the MTT-DMSO system can have significant applications in various fields. Ab-initio calculations of the energetics of the various tautomeric forms of MTT in DMSO are suggested to support the findings.

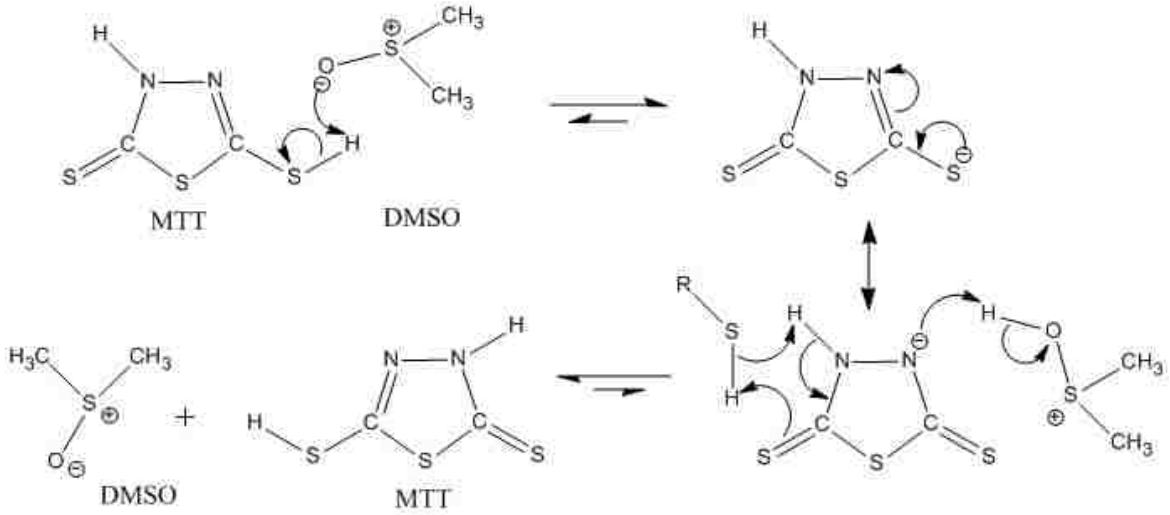


**Figure 1.30** Proposed mechanism-1 for the proton/hydrogen transfer phenomena occurring in the MTT-DMSO system

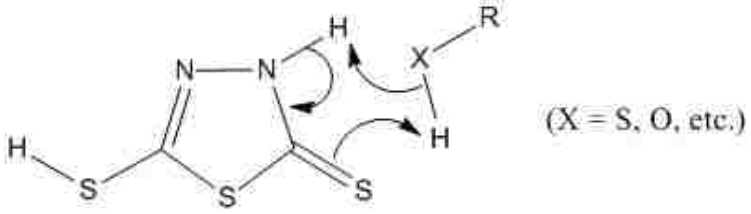


**Figure 1.31** Proposed mechanism-2 for the proton/hydrogen transfer phenomena occurring in the MTT-DMSO system

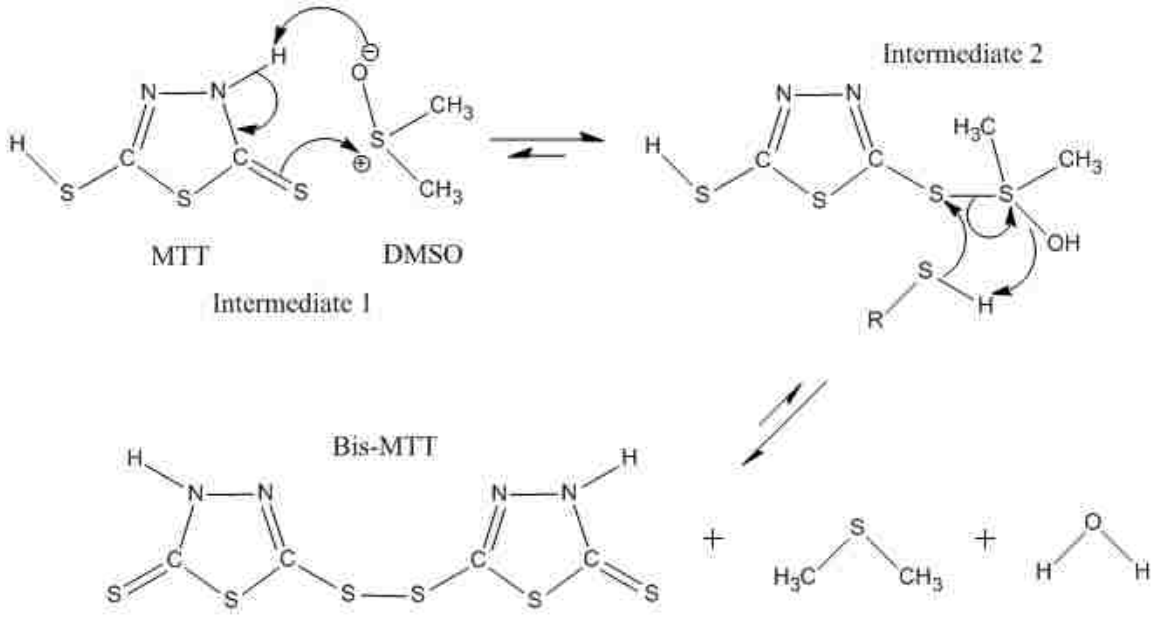


**Figure 1.32** Proposed mechanism for the disulfide bond formation occurring in the MTT-DMSO system

**1.3.2 Active Corrosion Inhibition Studies.** As a result of upcoming regulations on use of chromate based inhibitors, researchers put great efforts in order to develop environmental-friendly as well as more efficient corrosion inhibitors.[17] Organic inhibitors having the ability to chelate are considered to be a good approach and can provide protection against corrosion if they are designed to have certain functional groups which can attach to the metal substrate and a certain solubility parameter.[18] The ability of such designed molecules to move and reach the defected area and adsorb on the surface play an important role in the corrosion protection mechanism.[19] Thiadiazole derivatives consist of atoms that have lone pair electrons that help them to form coordinate bonds with the metal surface and can be designed to have low solubility. A series of thiadiazole derivatives can be synthesized with variable solubility parameters by

varying the length of the alkyl chain. These developed corrosion inhibitors may possess unique corrosion resistance. Their efficiency in coatings on bare steel and stainless steel can be evaluated by using electrochemical methods like EIS and salt spray test ASTM B-117.[20] Research studies for evaluating the active corrosion inhibition abilities of various derivatives of MTT are underway by fellow researchers, Yousef Dawib and Dr. Aysel Buyuksagis under the guidance of Dr. Michael R. Van De Mark.

**1.3.2.1 Electrochemical impedance spectroscopy (EIS).** This spectroscopic technique by which the active corrosion inhibition ability of MTT derivatives is to be tested, involves the measurement of alternating current impedance and its real and imaginary components Z' and Z'' of an electrochemical cell.[21] A sine-wave perturbation of small amplitude is employed on the electrode/solution interface. By plotting the data in Nyquist and Bode plot, one can obtain kinetic and mechanistic information that can be interpreted to calculate the coating resistance and coating capacitance.[22] Finally, the corrosion inhibitor efficiency can be easily calculated in view of the following formula:

$$\% \text{ Inhibition} = \frac{Rp - Rp^{o}}{Rp} \times 100 \qquad (1.3.2.1\ a)$$

Where –

$Rp^{o}$ is the polarization resistance without corrosion inhibitor

Rp is the polarization resistance with corrosion inhibitor

## 1.4 COLLOIDAL UNIMOLECULAR POLYMERS (CUPs)

Nanotechnology is the buzz word in science and the coatings industry today which is evident from the number of nanomaterial-related research publications, patents and the nanomaterial companies that have appeared in recent years. In every major field today, be it industry or academia, nano-projects not only receive a great deal of attention but also a significant portion of the resources available. The promise of this technology to deliver breakthrough coating performance in such areas as, scratch resistance, hardness, barrier properties, mechanical properties, etc. is the main reason for this high level of interest. Promoters of nanotechnology have done a great job of selling the idea that "smaller is better".[23]

The concept of nano is not entirely new to coating scientists and formulators as it has been known for decades that small particle size latexes are excellent film formers and provide excellent pigment binding ability in architectural paints.[24,25] This led to a boom in the introduction of nano-materials (100 nm or smaller) in the coatings industry. In early 21$^{st}$ century, a european luxury car manufacturer announced the use of nanoparticles in a clear-coat application, claiming to be the world's first water-based commercial automotive clear-coat that incorporates nanoparticles to achieve performance enhancements.[26] The particles are described as less than 20nm and the coating is cross-linked at 140 $^{o}$C. The new coating system was claimed to have 40 % better gloss retention compared to conventional clear-coats after numerous car wash tests. This performance was in reference to PPG industries announcement about the introduction of nanoparticles-based automotive clear-coats with the trade name "CeramiClear".[27]

Another example of nanoparticles is polyurethane dispersions which have been commonly used in coatings.[28] Although early work on applications of nanomaterials in coating has been spasmodic, there are many coatings scientists, formulators and researchers around the world today who are investigating different aspects of nano-dispersions in coatings. As a result, the conditions are mature enough for breakthroughs in this area over the next several years.

**1.4.1 Free Radical Polymerization.** The radical polymerization of acrylic monomers has been well investigated. Free radical polymerization[29,30,31,32,33] is a chain reaction in which the polymer is formed by the successive addition to the radical of vinyl-type building blocks. It involves three fundamental steps:

1. *Initiation*: The reaction of monomers may occur by the absorption of heat and/or light but often, an initiator is added to facilitate this process. The initiator (I) is a weak organic compound which can be decomposed thermally or photo-chemically to produce free radicals (R*). These radicals combine with monomers to form monomer radicals (M-R*) which can now react with other monomers to initiate the growth of polymeric chains.

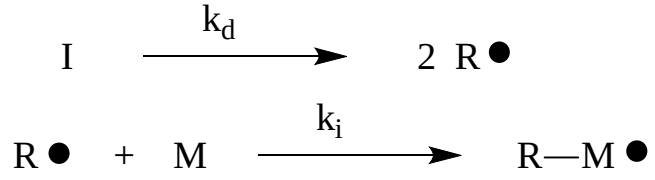


(1.4.1a)

2. *Propagation*: During propagation, monomers are added in rapid succession to the initiated monomer and the active center is continuously relocated at the

end of the growing polymer chain. This continues until the chain is terminated or transferred.

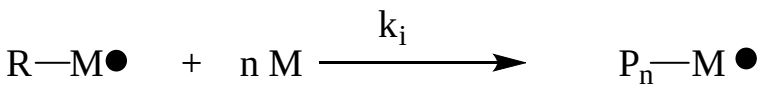


(1.4.1b)

3. *Termination*: Chain transfer agents are often used in this last step of a radical polymerization which can occur either by combination or disproportionation. In combination type of termination, two polymer chain radicals react/combine with each other and they annul the propagation step, giving the dead polymer (polymeric chain growth has ceased) as the end product. In disproportionation type of termination, the polymer chain radical reacts/combines with an initiator radical and yields a polymer as the final product.

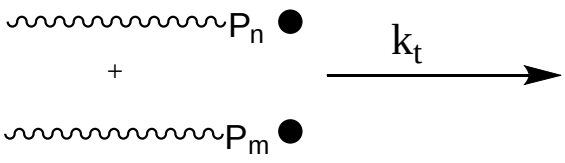


(1.4.1c)

**1.4.2 Acrylic CUPs.** The term Colloidal Unimolecular Polymer[34] (CUP) is introduced to describe a solid spherical single molecule polymer chain suspended in the continuous aqueous phase. CUPs contain a hydrophobic backbone and hydrophilic groups such as carboxylic acid salts. The polymers are synthesized by free radical polymerization and CUPs are formed by the water reduction process with subsequent removal of a volatile water loving solvent to yield a VOC free system. The nano-scale size of CUPs allows them to be thermodynamically stable in water due to the Brownian

motion of the water molecules around them.[35] The acrylic CUP resins prepared from high molecular weight polymers will give good lacquer performance while those of low molecular weight will give poor lacquer performance without a crosslinker. To evaluate and test the coating performance enhancements offered by crosslinkers to polymeric films, aziridine and melamine were used for the acrylic CUP resins.

**1.4.3 Aziridine.** The adverse effect on the environment and increasing costs of petrochemicals has led to the recent advances in the field of waterborne coatings technology.[36] Waterborne acrylics, urethanes, epoxy resins have provided formulations which are low in VOC, environmentally safe and user friendly. But these coatings still fall behind their solvent-borne counterparts in terms of chemical, corrosion and wear resistance and generally are low in gloss. Formulations based on two pack crosslinking coating systems provide a way of improving some of these drawbacks. Crosslinkers based on aziridine, which are three-membered organic heterocycles with a nitrogen atom in the ring are one such type of resins which greatly improve the coating properties.[37] *Figure 1.33* depicts the general structure of the Aziridine functional group.

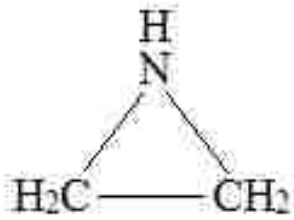


**Figure 1.33** Aziridine functional group

Aziridines are most commonly used in coatings systems based on carboxylated acrylics, carboxylated urethanes and vinyl acrylic. Polyfunctional aziridines greatly improve the moisture resistance, alkali resistance, ultraviolet light stability, gloss and adhesion of the final crosslinked coating.[38] The mechanism of crosslinking is the ring opening of aziridine through the reaction of carboxylic acid group on the acrylic resin with the aziridine to form an aminoester. Multifunctional aziridine can react through more than one site and give a crosslinked coating.[39] To effective crosslink the acrylic CUPs, a trifunctional aziridine CX-100 [trimethylolpropane tris(2-methyl-1-aziridinepropionate] from DSM NeoResins Inc. can be used to enhance the coating performance of CUPs.

**1.4.4 Melamine.** Melamine, which is an organic base and a trimer of cyanamide, is one of the most widely used crosslinkers for baked coating systems. The reaction of melamine with aldehydes, carboxylic acids or alcohols yields thermosetting polymers: melamine-formaldehyde type (MF) resins which have various applications as fabrics, dinnerware, glues, foams, counter tops, etc.[40,41] Resin systems with reactive functional groups such as hydroxyl, carboxylic acid and urethane can react with MF resins to give crosslinked products.[42] *Figure 1.34* depicts the general structure of the melamine functional group.

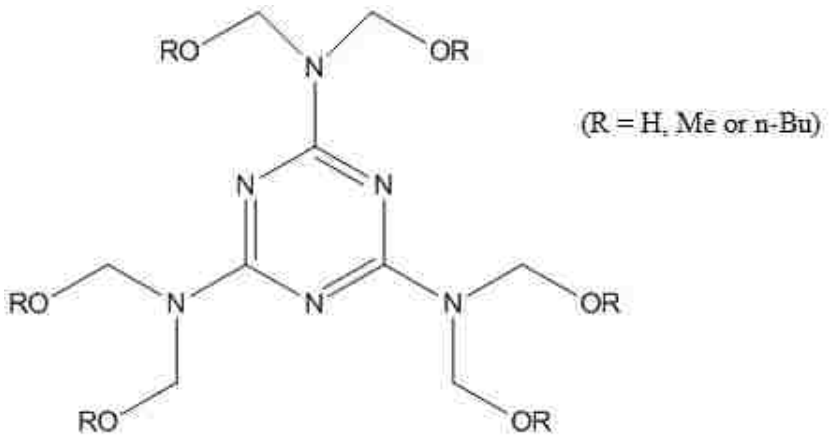


**Figure 1.34** Generalized structure of melamine-type crosslinker

The melamine used in the research study to crosslink acrylic CUPs was Cymel 373 from Cytec Industries Inc.: a methylated melamine formaldehyde with a medium degree of alkylation, medium to high methylol content and low imino functionality. Cymel 373 resin was soluble in water and was compatible with the acrylic CUPs. The acid functionality on the acrylic CUPs was sufficiently acidic to catalyze the curing reaction at a relatively low curing temperature. But usually sulfonic acid catalysts are added to the formulation to improve the curing characteristics.[43] The mechanism of crosslinking of Cymel 373 with the carboxylated acrylic CUPs involves the esterification or etherification of the methylated group by the acid functionality present on the acrylic polymer backbone.[44] The performance enhancements of melamine crosslinked CUPs are evaluated by means of testing protocols as per the specified ASTMs.

## REFERENCES


1. Sianawati, E. *Ph.D. Dissertation*: *Chemistry* **1997**, University of Missouri-Rolla.

2. Gourke, M. J. *Journal of Coatings Technology* **1977**, *49* (632), 69.

3. Technical Committee, New England Society for Coatings Technology. *J. Coat. Tech.* **1982,** *54* (684), 63-68.

4. Riggs, O. L.; Nathan, C. C. *Ed. NACE* **1973**, 7-27.

5. US Patent 5409528.

6. ASTM D-610: Standard Practice for Evaluating Degree of Rusting on Painted Steel Surfaces.

7. Sianawati, E.; Mistry, J. K.; Van De Mark, M. R. *European Coatings Journal* **2008**, *12*, 35-39.

8. Yakubovich, A. Y.; Ginsburg, V. A. *Zhurnal Obshchei Khimii* **1958**, *28*, 1031.

9. Sidky, M. M.; Mahran, M. R.; Zayed, M. F.; Abdou W. M.; Hafez, T. S. *Org. Preparations and Procedures Int.* **1982**, *14* (4), 225.

10. Masten, S. A.; "2,5-Dimercapto-1,3,4-thiadiazole: A review of Toxicological Literature", *National Toxicological Program/National Institutes of Health*, Jan. **2005**.

11. Kuodis, Z.; Rutavichyus, A.; Valiulene, S. *Chemistry of Heterocyclic compounds* **2000**, *36* (5), 598-602.

12. Truesdell, J. W.; Van De Mark, M. R. *Journal of Electrochemical Society* **1982**, *129* (12), 2673-2676.

13. Katritzky, A. R.; Wang, Z.; Offerman, R. J. *Journal of Heterocyclic Chemistry* **1990**, *27* (2), 139.

14. Kuodis, Z.; Rutavichyus, A; Valiulene, S. *Chemistry of Heterocyclic Compounds* **2001**, *36* (7), 857-861.

15. Durust, Y. *Phosphorus Sulfur Silicone* (ISSN: 1024-6507) **2009**, *184*, 2923.

16. Ferrari, M. B.; Fava, G. G.; Corrado, P. *Inorganica Chimica Acta* **1981**, 55(6), 167-169.

17. Braig, A.; *Proceedings: Electrochemical Society* **1998**, 97-41.

18. Sastri, V. S. *Corrosion inhibitors: Principles and Applications,* Wiley: New York, **1998**.

19. Behrens, R. A.; Braig, A. *Water-Borne and Higher-Solids Coatings Symposium* **1988**, *15th*, 170-207.

20. ASTM B-117: Standard Practice for Operating Salt Spray (Fog) Apparatus.

21. Rammelt, U.; Reinhard, G. *Progress in Organic Coatings* **1992**, *21*, 205-226.

22. Mishra, A. K.; Parashar, G.; Srivastva, D.; Kumar, P. *Paintindia* **2000**, *3*, 33-38.

23. Fernando, R. *Journal of Coatings Technology* **2004**, *1* (5), 32-38.

24. Schaller, E.J. *Journal of Paint Technology* **1968,** *40* (525), 433.

25. Boswell, S. T.; Craver, J. K.; Tess, R. W.; (Ed.) *Applied Polymer Science,* American Chemical Society, **1975**.

26. Mercedes-Benz corporate announcement, **2003**.

27. PPG Industries corporate announcement, **2003**.

28. Klempner, D; Frisch, K. *Advances in Urethane Science and Technology*, University of Detroit, Mercy, **2001**.

29. Flory, P. J. *Principles of Polymer Chemistry*, Cornell University Press, Ithaca, New York, **1953**.

30. Sanders, K., J. *Organic Polymer Chemistry*, Chapman and Hall, London, **1973**.

31. Rempp, E.; Merrill, E. W. *Polymer Synthesis*, Prentice Hall, New Jersey, **1981**.

32. Odian, G. *Principles of Polymerization*, Wiley Publications, New York, **1991**.

33. Painter, P. C. *Fundamentals of Polymer Science,* Technomic Publishing Company, Pennsylvania, **1997**.

34. Riddles, C. J.; Hua-Jung Hu, W. Z.; Van De Mark, M. R. *Polymer Preprints* **2011,** *52* (2), 232-233.

35. Chen, M; Van De Mark, M. R. *Polymer Preprints* **2011,** *52* (2), 336-337.

36. Liebscher H. *Progress in Organic Coatings* **2000**, 40 (1-4), 75-83.

37. Steuerle, U.; Feuerhake, R. *Ullmann's Encyclopedia of Industrial Chemistry*, Wiley-VCH, Weinham, **2006**.

38. Jin, Y.; Zhang, R.; Wei, D. Q. *China Leather* **1998**, *27* (11), 9.

39. Xie, F.; Liu, Z.; Wei, D. *Chinese Journal of Polymer Science* **2002**, *20* (1), 65-70.

40. Blakey, W. *Journal of Oil and Color Chemists' Association* **1943**, 26(281), 187-93.

41. Wicks, Z. W.; Jones, F. N.; Pappas, S. P.; Wicks, D. A. *Organic Coatings*, John Wiley & Sons Publications, **2007**.

42. Blank, W. J. *Journal of Coatings Technology* **1979,** *51* (656), 61-70.

43. Product datasheet: *Cymel 373*, Cytec Industries Inc. **2010**.

44. Czech, Z. *Polymer International* **2003**, *52*, 347-357.

**PAPER**

# I. CHELATING COMPOUNDS AS POTENTIAL FLASH RUST INHIBITORS IN WATER BORNE COATING SYSTEMS

**Emerentiana Sianawati, Jigar K. Mistry and Michael R. Van De Mark***

*Missouri S&T Coatings Institute & Department of Chemistry,*
*Missouri University of Science & Technology, Rolla, MO-65409, USA.*

**(Published as an Article in the *European Coatings Journal, 2008*)**

## 1. ABSTRACT

Flash rusting is an objectionable property of waterborne coatings. Designing a flash rust inhibitor which forms a tight chelated complex with the metal substrate, thereby preventing it from corroding, would prove to be an effective additive.

## 2. INTRODUCTION

Waterborne coatings on ferrous substrates usually show flash rusting which decreases the adhesion of the coating and the corrosion products can form a stain. Conventional flash rust inhibitors show system dependency and their effectiveness varies with the type of pigment, extender or the resin used and henceforth have to be used in

excess. Nitrites, commonly used as flash rust inhibitors leach out over a period of time and can cause blistering[1]. This study investigates chelating compounds as potential flash rust inhibitors. Compounds being evaluated include amine alcohols, diamines and sulfur containing amines. A new corrosion inhibitor 2,5-(S-acetic acid)-dimercapto-1,3,4-thiadiazole ($H_2$ADTZ) was synthesized. The performance characteristics of this new-generation additive as a flash rust inhibitor were evaluated in water borne systems by a spectrophotometer.

## 3. EXPERIMENTAL

All panels were coated with a wire-wound bar # 40 and exposed to either Test Condition A or Test Condition B and allowed to dry for 24 hours before making any measurements. The cold rolled matt finished steel panels were Q-Panel R-46 and the aluminum panels were A-46 mill finish, also from Q-Panel.

### **3.1** Test Condition A - for evaluation of flash rust inhibition by amines and amine alcohols

Coated steel panels of paints with the amine and amine alcohol inhibitors were placed directly into the highly regulated constant humidity/temperature cabinet for 2 hours at 95 ± 3 % R.H. and 30 $^{o}$C. The samples were then removed and allowed to dry for 48 hours at 23 $^{o}$C and 65 ± 3 % R.H. to ensure a consistent extent of drying. The relative humidity was controlled during the drying period by use of an enclosure measuring 5'x6'x10' containing both a humidifier and a source of dry air. The flow rate of the dry air was varied as needed to maintain the humidity at 65 ± 3 %.

**3.2** Test Condition B – for evaluation of flash rust inhibition by $H_2$ADTZ, Sodium Nitrite, N,N-dimethyl-1,3-propanediamine and 2-Amino-2-methylethanol

Coated steel panels of paints with $H_2$ADTZ, sodium nitrite, N,N-dimethyl-1,3-propanediamine and 2-amino-2-methylethanol were placed directly on a tray in the constant humidity chamber at 95% relative humidity at 30 $^{o}$C for 30 minutes and then removed and allowed to dry at 40-50% relative humidity at 22 $^{o}$C for 24 hours.

**3.3** Spectrophotometric measurement for flash rust and stain determination

Measurements were made using nine readings per panel with a 1cm diameter window using a Minolta 2002 or a Byk Color-guide color computer. All evaluations are based upon 3 panels being tested per formulated coating to minimize error due to application or surface condition variation. Also, for the spectrophotometric method to be accurate, complete hide by the coating is necessary. The Hunter Whiteness Index was measured for the samples to determine the extent of flash rusting.

**3.4** Extent of flash rusting calculation

The percentage of flash rusting reported was obtained from the following equation:

% Flash Rusting = [(Standard – Sample) / (Standard – Blank)] * 100

where the values for the standard, sample and the blank were the Hunter Whiteness Index values measured spectrophotometrically for the respective panels. The blank was defined as a steel panel coated with the paint of same thickness containing no inhibitor and

exposed to the same drying condition. The standard was the paint applied the same as the blank except to an Aluminum panel.

**3.5** Adhesion

The adhesion of the coatings was evaluated using ASTM cross hatch method # D3359-08[3]. For each panel tested, three adhesion test areas were measured. All adhesion numbers reported were based on the average value of the three numbers.

**3.6** Atomic absorption measurement

The coating was removed from a 4.5 cm x 8 cm (1.77 inch x 3.15 inch) area of the panels with methylene chloride. It was collected in a crucible and ashed at 500 $^{o}$C. The ashed sample was digested with 10 ml of 50 wt% nitric acid atleast 3 times until the solution color did not change and finally with 6 ml 50 wt% of hydrochloric acid. The sample was diluted with de-ionized water, filtered and brought to a volume of 100 ml. Further dilution with water was made as needed before the iron concentration measurement was determined by atomic absorption on a Perkin Elmer AA Model 2380 spectrometer.

**3.7** Synthesis of $H_2$ADTZ[4]

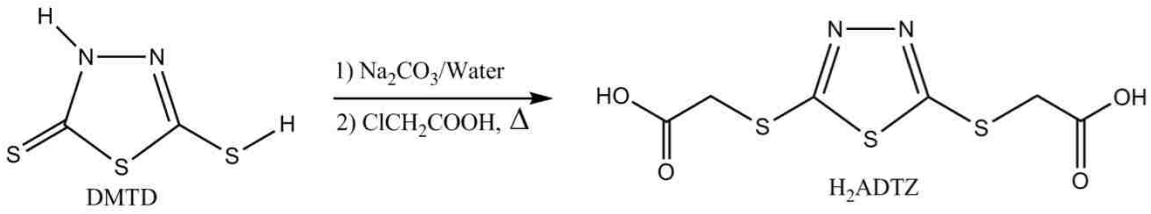


**Scheme 1.** Synthesis of $H_2$ADTZ from DMTD

To a stirred aqueous solution of chloroacetic acid (94.5 g, 1 mol) and sodium carbonate (53 g, 0.5 mol), 2,5-dimercapto-1,3,4-thiadiazole (75 g, 0.5 mol) was added. The reaction mixture was stirred and refluxed for 3 hours, then it was cooled and filtered. Ethanol was added to the reaction mixture, yielding a white precipitate. The product 2,5-(S-acetic acid)-dimercapto-1,3,4-thiadiazole ($H_2$ADTZ) was then washed with ethanol and dried under vacuum. The yield was 120.3 g (90.5%). The melting point of the compound was 164~165 $^{o}$C. The $^{1}$H and $^{13}$C NMR as well as IR results were consistent with the literature.[4]

## 4. RESULTS AND DISCUSSION

**4.1** Evaluation of the performance characteristics of chelating compounds as flash rust inhibitors

The evaluation of various chelating amines and amine alcohols as flash rust inhibitors was done using spectrophotometric and atomic absorption methods[2]. The Hunter Whiteness Index was measured for the samples to determine the extent of flash rusting which is represented by the % Staining while the Atomic Absorption Method was used to measure the actual amount of corrosion which is represented by the % Rust. All chelating amines and amine alcohol inhibitors were post added into a paint made with Paint Formula I at 1 w/w%.

As seen from Table I, since all the inhibitors showed the formation of % Rust less than the control, it can be inferred that all of the above inhibitors formed complexes with the metal substrate. The presence of the methyl group of 1,2-propanediamine increased

the mobility of the chelated complexes of corrosion products in the coated film and caused more flash rusting and staining. The same argument applies for triethylenetetraamine, multiple ligating sites were not found to be effective in inhibiting flash rusting. The presence of two methyl groups on the nitrogen of N,N-dimethyl-1,3-propanediamine and the bridge formed by the chelation of 2-methylpentamethylenediamine with the metal substrate helped form an effective hydrophobic layer at the surface which reduced the corrosion rate. 1,2-ethanediamine and 2-methylpentamethylenediamine showed no visible sign of rust or stain spotting and would therefore qualify as a good inhibitor by the ASTM D610-08 method, which is a subjective and operator dependent method. Yet, 1,2-ethanediamine had a higher stain value as measured by Hunter Whiteness and caused the paint to be slightly yellow compared to the original, which is unaccounted by the ASTM method. N,N-Dimethyl-1,3-propanediamine also exhibited no sign of spotting or staining. Triethylenetetraamine performed the worst in the series for inhibition. Thus, triethylenetetraamine and 1,2-propanediamine were not able to prohibit the migration of the corrosion products to the surface of the coating which would appear as a stain. Since corrosion is a function of pH, as the pH increases, the rate of corrosion decreases. The inhibition capability by the above inhibitors was partly the effect of the pH and also the formation of chelating complexes on the metal substrate. Above pH 9.5, the paint is corrosive to the skin. Therefore, any paint with the above inhibitors at this level will have an unacceptable pH for commercial purposes.

**Table 1.** The effect of diamine and tetraamine inhibitors on flash rust staining development –

| **Inhibitors** | **pH** | **Cross Hatch Adhesion** | **% Rust** | **% Staining** |
|---|---|---|---|---|
| 1,2-ethanediamine | 10.6 | 4.5 | 4.4 | 28.8 |
| 1,2-propanediamine | 10.4 | 3.0 | 34.0 | 282.4 |
| N,N-dimethyl-1,3-propanediamine | 10.6 | 4.0 | 0.7 | 8.4 |
| 2-methylpentamethylenediamine | 10.9 | 4.0 | 0.8 | 6.4 |
| Triethylenetetraamine | 10.3 | 3.0 | 62.6 | 391.5 |

**4.2** Amine alcohols –

The first series of amine alcohols studied were ethanolamine, diethanolamine and triethanolamine. As seen from the Table II, ethanolamine exhibited inhibition potential equivalent to 1,2-ethanediamine in preventing staining. In rust inhibition however, ethanolamine performed poorer than 1,2-ethanediamine. As the substitution on the nitrogen increased, the rust and the staining inhibition decreased. This might be partly because the more substituted amines form more soluble chelating complexes which migrate in the coated film to form a stain. Diethanolamine and triethanolamine inhibited some flash rust formation but caused significantly more staining than the blank. Since ethylene glycol and other simple primary alcohols do not inhibit flash rusting, it is likely that the alcohol group was too weakly ligating and resulted in more water solubility.

**Table 2.** Percent rust, staining, adhesion and pH of 2-carbon amine alcohols –

| Inhibitors | pH | Cross Hatch Adhesion | % Rust | % Staining |
|---|---|---|---|---|
| Ethanolamine | 10.4 | 4.0 | 8.5 | 27.9 |
| Diethanolamine | 9.8 | 4.5 | 14.6 | 130.9 |
| Triethanolamine | 9.1 | 3.0 | 67.9 | 233.1 |

The second series of amine alcohols investigated was the derivatives of amine propanol. As seen from the Table III, 2-Methylaminoethanol, which is a secondary amine, had the best rust and staining inhibition properties. 3-Aminopropanol, which would form a 5-membered bridged complex with the metal substrate, had as good a potential in inhibiting rust as 2-Methylaminoethanol, but had slightly less potential in inhibiting staining. Compared to the other two inhibitors in the series, 1-Amino-2-propanol had the least inhibiting properties. Overall, these compounds were good rust and staining inhibitors. The pH of these amine alcohols was strongly basic similar to the diamine compounds, which might be partly responsible for the inhibitory characteristic. The inhibition results were however, better than mono- and diamine. Unlike the ethanolamine series, these compounds were more hydrophobic as a complex due to the increased aliphatic component of the added $CH_2$.

**Table 3.** Percent rust, staining, adhesion and pH of 3-carbon amine alcohols –

| Inhibitors | pH | Cross Hatch Adhesion | % Rust | % Staining |
|---|---|---|---|---|
| 3-Aminopropanol | 10.6 | 3.5 | 1.5 | 4.8 |
| 1-Amino-2-propanol | 10.3 | 4.0 | 5.0 | 4.6 |
| 2-Methylaminoethanol | 10.6 | 4.0 | 1.4 | -2.6 |

The third series of amine alcohols investigated was the addition of substituents onto the nitrogen and carbon adjacent to the amine: 2-amino-2methyl-propanol, N,N-diethylethanolamine and N-methyldiethanolamine. As seen from the Table IV, the addition of two methyl groups to ethanolamine on the carbon adjacent to the nitrogen decreased the staining and corrosion by a factor of two. The addition of a methyl on the nitrogen of diethanolamine again decreased corrosion but increased staining. It should be noted that the pH of these systems is dependent on the molecular weight of the inhibitor and the number of amine groups. Since corrosion is pH dependent, it will have an effect on both the amount of corrosion and potentially on the amount of stain. The adhesion of the coatings containing all of these inhibitors was very good regardless of the amount of rust or staining produced.

**Table 4.** Percent rust, staining, adhesion and pH of bulky amine alcohol inhibitors –

| Inhibitors | pH | Cross Hatch Adhesion | % Rust | % Staining |
|---|---|---|---|---|
| 2-Amino-2methyl-propanol | 10.2 | 4.0 | 3.3 | 12.9 |
| N,N-diethylethanolamine | 10.1 | 4.0 | 4.9 | 44.6 |
| N-methyldiethanolamine | 9.5 | 4.5 | 8.5 | 64.7 |

**4.3** $H_2$ADTZ –

The inhibitors that performed well in the series of chelating amines and amine alcohols were evaluated against $H_2$ADTZ for their inhibitory capabilities using the spectrophotometric method. The inhibitory properties of sodium nitrite, commonly used as a flash rust inhibitor in waterborne coating systems, were also evaluated. The Hunter Whiteness Index was measured for the samples to determine the extent of flash rusting and reported as % Flash Rust Stain. The inhibitors were post added into paints made with Paint Formula II and Paint Formula III and were modified to a constant pH of 8.2 using glacial acetic acid and ammonium hydroxide. This pH modification was done to help level the effect of pH on corrosion rate, however, it does increase the electrolyte concentration which will also have an effect on corrosion rate. The pH of 8.2 was selected to emulate common architectural paints.

As seen from the Table 5, N,N-dimethyl-1,3-propanediamine and 2-Methylaminoethanol were found to be effective at 1.4 % w/w concentration. The high level required here may be the result of the increased electrolyte effect. Sodium nitrite was reasonably effective at a low level but less effective at increased concentrations. This again can be explained by the fact that sodium nitrite, being a salt, acts like an electrolyte. $H_2$ADTZ was found to inhibit flash rusting even at 0.05 % w/w in Paint Formula III. For Paint Formula II, it required 0.25 % w/w of $H_2$ADTZ to see significant inhibition of flash rusting.

**Table 5.** Effectiveness of various flash rust inhibitors as compared to $H_2$ADTZ –

| | | **Paint Formula II** | | **Paint Formula III** | |
|---|---|---|---|---|---|
| **Inhibitor** | **Concentration (% w/w)** | **Avg. Hunter Whiteness** | **% Flash Rust Stain** | **Avg. Hunter Whiteness** | **% Flash Rust Stain** |
| | | | | | |
| Sodium Nitrite | 0.1 | 91.47 | 18.83 | 91.84 | 18.02 |
| | 0.3 | 91.09 | 19.67 | 91.31 | 19.19 |
| | 0.6 | 90.92 | 20.05 | 88.88 | 24.55 |
| | | | | | |
| N,N-dimethyl-1,3-propanediamine | 0.5 | 54.61 | 100.22 | 69.36 | 67.65 |
| | 0.8 | 79.64 | 44.95 | 91.10 | 19.66 |
| | 1.4 | 91.06 | 19.74 | 92.27 | 17.07 |
| | | | | | |
| 2-Methylaminoethanol | 0.5 | 91.69 | 18.35 | 91.3 | 19.21 |
| | 0.8 | 91.98 | 17.71 | 92.33 | 16.94 |
| | 1.4 | 90.65 | 20.65 | 92.94 | 15.58 |
| | | | | | |
| $H_2$ADTZ | 0.05 | 67.58 | 71.58 | 92.84 | 15.81 |
| | 0.1 | 71.47 | 62.99 | 93.15 | 15.12 |
| | 0.25 | 85.78 | 31.39 | 93.34 | 14.71 |

## 5. CONCLUSIONS

To be an effective flash rust inhibitor in water-borne coating systems, the inhibitor must prevent the electro-chemical reactions occurring on the metal substrate and stop the migration of the corrosion products to the surface of the film to prevent staining.

For all the amine alcohol compounds studied, corrosion product formation and staining inhibition in the latex paints was dependent on the both the chelating groups as well as the aliphatic characteristics of the ligating compound. The presence of groups which increased the metal complex solubility increased staining. This study indicates a general direction to begin synthesis of new inhibitors. The use of amines results in an increased pH which was problematic. Nitrites have limits due to their water solubility and potential to cause blisters. The use of sulfur containing ligating groups shows potential as effective flash rust inhibitors. Further research should yield improved cost effective additives without increasing the pH significantly.

## 6. REFERENCES

1.) U.S. Patent 5409528.

2.) M. R. Van De Mark, E. Sianawati, P. Duncan, N. R. Mason; "Development and Evaluation of a new Spectrophotometric Integration Technique for Flash Rust Staining Determination", Constituent Society Paper, Vol. 65, No. 827, Dec. 1993.

3.) ASTM D-3359: Cross-hatch Adhesion Method.

4.) X. H. Lou, Y. Zhu, H. Gao, A. X. Zhu, Y. T. Fan, H. W. Hou, h. J. Lu; Chinese Journal of Inorganic Chemistry, Vol. 21, No. 5, May 2005.

## 7. FIGURE

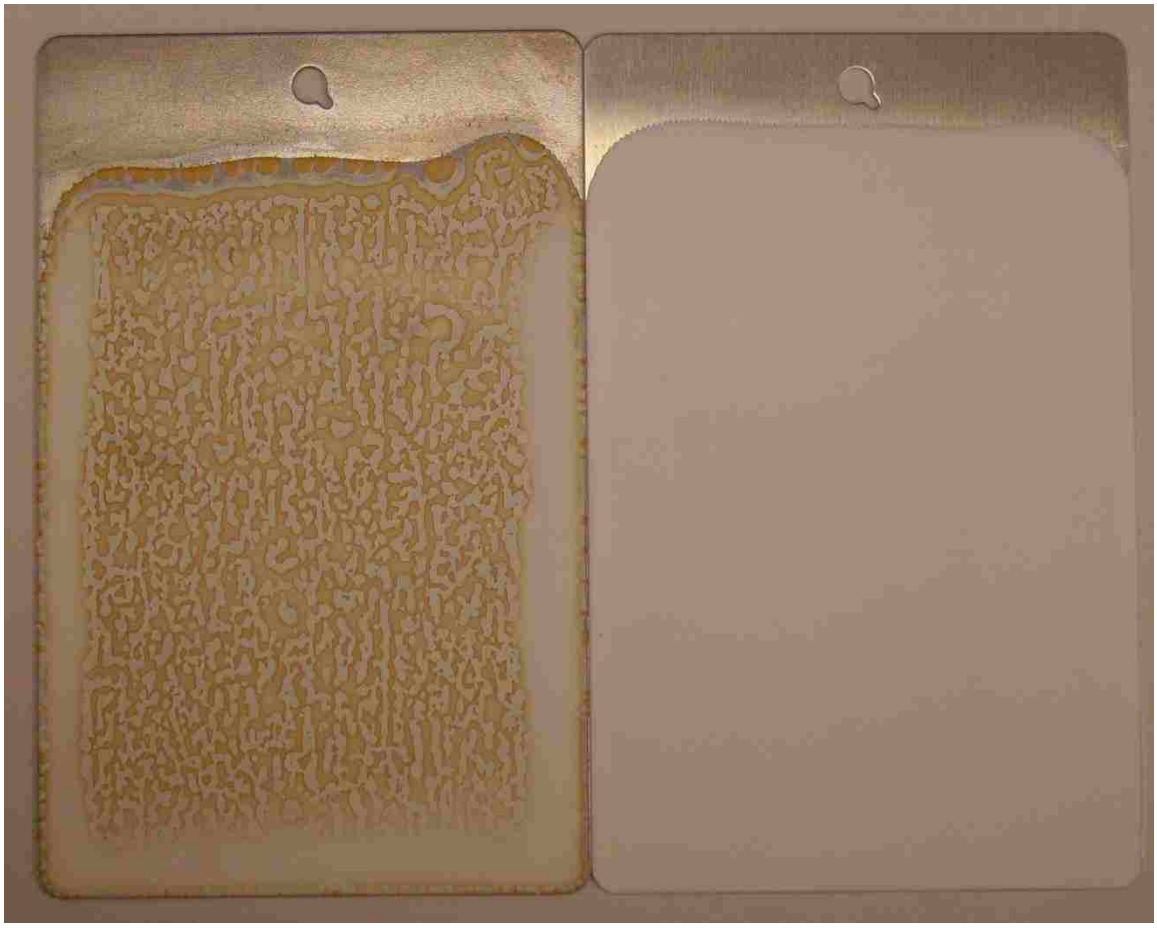

**Figure 1.** Flash rusting and staining patterns developed on paint films on steel panel without (left) and with (right) inhibitor $H_2$ADTZ

# 8. SUPPORTING INFORMATION

**Table S.1** Paint Formulation-I

| Materials | Lbs | Gal |
|---|---|---|
| Natrosol 250 HBR[a] | 0.5 | 0.05 |
| Propylene Glycol | 28.81 | 3.33 |
| Water | 212.5 | 25.51 |
| Triton CF-10[b] | 5.8 | 0.65 |
| Foamaster AP[c] | 2.22 | 0.29 |
| ND2-Polywet[d] | 7.39 | 0.81 |
| TiPure R-900[e] | 401.27 | 12.05 |
| *High Speed Grind, 30 min.* | | |
| Texanol[f] | 14.11 | 1.79 |
| Foamaster AP[c] | 1.58 | 0.21 |
| Ucar 1018[g] | 470.86 | 55.32 |
| Total | 1145 | 100.01 |

**Table S.2** Paint Formulation-II

| Materials | Lbs | Gal |
|---|---|---|
| Natrosol 250 HBR[a] | 1.5 | 0.25 |
| Propylene Glycol | 13.02 | 1.5 |
| Water | 171.3 | 20.55 |
| Tamol 850h | 1.981 | 0.2 |
| Triton CF-10[b] | 3.154 | 3.5 |
| Foamaster AP[c] | 1.912 | 0.25 |
| TiPure R-902[e] | 258.7 | 7.38 |
| Atomite[j] | 86.2 | 3.69 |
| *High Speed Grind, 30 min.* | | |
| Texanol[f] | 12.52 | 1.5 |
| Ucar 625[b] | 449.4 | 51.65 |
| Water | 114.2 | 13.7 |
| Total | 1113.9 | 101.02 |

**Table S.3** Paint Formulation-III

| Materials | Lbs | Gal |
|---|---|---|
| Natrosol 250 HBR[a] | 1.5 | 0.25 |
| Propylene Glycol | 26.04 | 3 |
| Water | 226.5 | 27.2 |
| Tamol 850h | 1.981 | 0.2 |
| Triton CF-10[b] | 3.154 | 3.5 |
| Foamaster AP[c] | 1.912 | 0.25 |
| TiPure R-902[e] | 262.9 | 7.5 |
| Atomite[j] | 140.2 | 6 |
| *High Speed Grind, 30 min.* | | |
| Texanol[f] | 12.52 | 1.5 |
| Neocar Acrylic 820[b] | 315.4 | 36.67 |
| Water | 150.83 | 18.1 |
| Total | 1143 | 101.02 |

## 9. APPENDIX

a. Aqualon Co.

b. The Dow Chemical Co.

c. Henkel Process Chemical, Inc.

d. Uniroyal Chemicals.

e. DuPont.

f. Eastman Chemical Products, Inc.

g. Drew Chemicals.

# II. 5-MERCAPTO-1,3,4-THIADIAZOLE-2(3H)-THIONE: SYNTHESIS AND STRUCTURE OF ALKYLATED DERIVATIVES

**Jigar K. Mistry, Richard Dawes*, Amitava Choudhury and Michael R. Van De Mark***

*Missouri S&T Coatings Institute & Department of Chemistry,*

*Missouri University of Science & Technology, Rolla, MO-65409, USA.*

**(Accepted for publication as an Article in the *Journal of Heterocyclic Chemistry)***

## 1. GRAPHICAL ABSTRACT

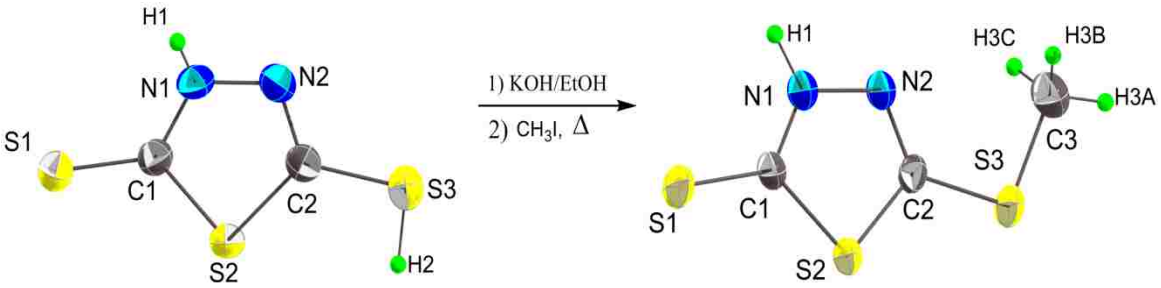


**Keywords:** 1,3,4-thiadiazolidine-2,5-dithione; 2,5-dimercapto-1,3,4-thiadiazole; 5-mercapto-1,3,4-thiadiazole-2(3H)-thione; 2,5-bis(thioaceticacid)-1,3,4-thiadiazole; MTT.

*Corresponding authors: dawesr@mst.edu, mvandema@mst.edu

## 2. ABSTRACT

The observed structure of 1,3,4-thiadiazolidine-2,5-dithione **(**also known as 2,5-dimercapto-1,3,4-thiadiazole (DMTD or DMcT)) has been previously reported in three different tautomeric forms including –dithiol and –dithione. This report examines the relative stability of each form and also reports synthesis and characterization of the structures of mono- and dialkylated forms of 5-mercapto-1,3,4-thiadiazole-2(3H)-thione (abbreviated as MTT). The methods of X-ray crystallography, NMR spectroscopy and ab-initio electronic structure calculations were combined to understand the reactivity and structure of each compound.

## 3. INTRODUCTION

1,3,4-Thiadiazolidine-2,5-dithione (CAS 1072-71-5) is also known as 2,5-dimercapto-1,3,4-thiadiazole, DMTD or bismuththiol. Its derivatives find application as raw material for various organic syntheses, analytical reagents, fuel additives, lubricant additives, intermediates for other pharmaceutical compounds, chelating compounds for metals, and flash-rust and corrosion inhibitors in coatings.

In our previous work of evaluating the corrosion inhibition performance of 2,5-bis(thioaceticacid)-1,3,4-thiadiazole for its use as a potential flash-rust inhibitor and a corrosion inhibitor in coatings,[1] the compound 5-mercapto-1,3,4-thiadiazole-2(3H)-thione (MTT) was used as a starting material. The structure of MTT is often reported in the literature in its tautomeric –dithiol form or in the –dithione form. In fact it has been shown to have three tautomeric structures,[2-4] with structure 1 being the most commonly reported in the literature.

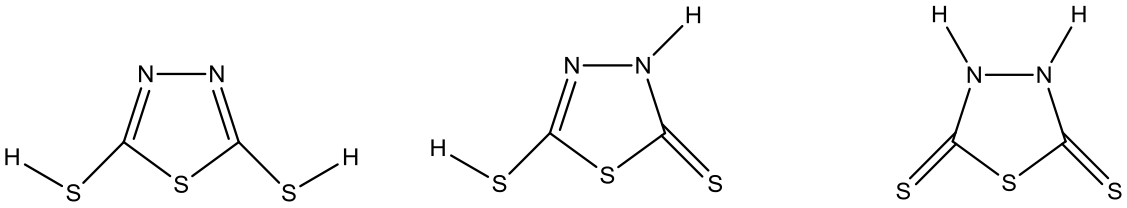


**Figure 1.** Three tautomeric forms of MTT.

An X-ray crystal structure of MTT was reported in 1976 consistent with structure 2.[5] Several recent reports refer to the structure of MTT as that of structure 3.[6-8] In order to synthesize and evaluate the various mono- and di-substituted derivatives of MTT as potential anti-flash-rust and anti-corrosives for coatings, it was important to know and understand the substitution mechanism of this compound and its various derivatives as well as to determine the structures and their stability. This report addresses the structure and various substitution products of MTT by combining results of ab-initio electronic structure calculations, X-ray crystallography and nuclear magnetic resonance spectroscopy to validate and better understand the chemistry of MTT.

## 4. RESULTS AND DISCUSSION

MTT as well as the mono-alkylated structure can exist in various tautomeric forms and the di-alkylated structure can exist in three structurally isomeric forms. The stability of each tautomer was evaluated through ab-initio electronic structure calculations. These calculations are presented considering MTT first, followed by the alkylated derivatives.

## 4.1 Structure of 5-mercapto-1,3,4-thiadiazole-2(3H)-thione [MTT]

Table 1 lists the results of various levels of calculation for the three contending tautomeric forms of MTT. Structure **2** is predicted to be the lowest energy structural isomer by all of the computational methods employed. The highest level explicitly-correlated coupled-cluster (F12) calculations (see Table 1) with corrections for solvation in ethanol predict structures **1** and **3** to lie about 4.7 and 5.9 kcal/mol higher in energy, respectively. Finite temperature effects at 298 K were estimated and added to the energies using harmonic-oscillator rigid-rotor approximate free-energy corrections obtained from force-field analyses at the B3LYP/aug-cc-pVTZ and MP2/aug-cc-pVTZ levels. Energies for the explicitly correlated F12 methods were combined with thermal corrections from the MP2 calculations. A correction for solvation modeled (PCM) at the B3LYP/aug-cc-pVTZ level (including geometric relaxation) was added to both the DFT and F12 results. The X-ray crystal structure determined in this study is shown in Figure 2. Our newly determined structure is in close agreement with that previously reported by J.W. Bats.[5]

**Table 1**. Calculated relative energies (kcal/mol) for structures **1-3** including thermal corrections at 298 K, and the effects of solvation in ethanol [designated by (s)].

| Method | Structure 1 | Structure 2 | Structure 3 |
|---|---|---|---|
| B3LYP/6-31G(d)[a] | 8.57 | 0.00 | 6.03 |
| B3LYP/AVTZ[a] | 7.43 | 0.00 | 6.82 |
| B3LYP/AVTZ (s)[a] | 8.52 | 0.00 | 2.77 |
| MP2/AVDZ[b] | 4.48 | 0.00 | 9.51 |
| MP2/AVTZ[b] | 4.04 | 0.00 | 10.08 |
| MP2-F12/VDZ-F12[b] | 3.57 | 0.00 | 10.50 |
| CCSD(T)-F12a/VDZ-F12[b] | 3.59 | 0.00 | 9.92 |
| CCSD(T)-F12b/VDZ-F12[b] | 3.57 | 0.00 | 9.99 |
| CCSD(T)-F12a/VDZ-F12 (s)[b] | 4.68 | 0.00 | 5.87 |

All F12 calculations used structures optimized at the MP2/AVTZ level (see text). (s) including implicit PCM solvation model for ethanol. [a] Thermal corrections computed at B3LYP/AVTZ level. [b] Thermal corrections computed at MP2/AVTZ level.

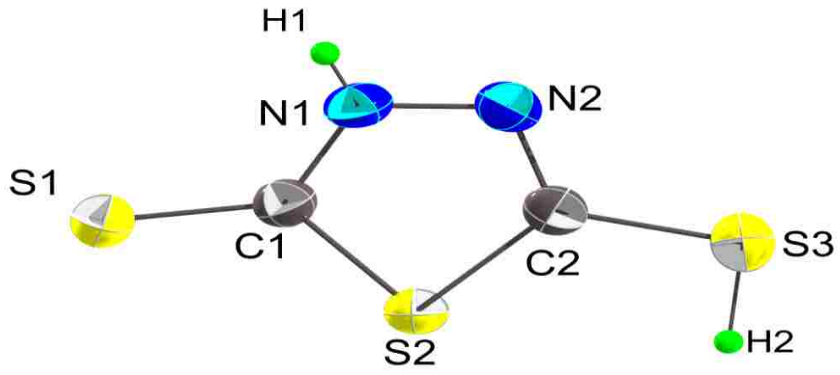


**Figure 2.** Thermal ellipsoids for MTT as observed through X-ray crystallography.

## 4.2 Mono-alkylation of MTT

The mono-alkylation of MTT can produce four possible structures (4-7). Structures 4 and 5 derive from S-alkylation while structures 6 and 7 come from N-alkylation.

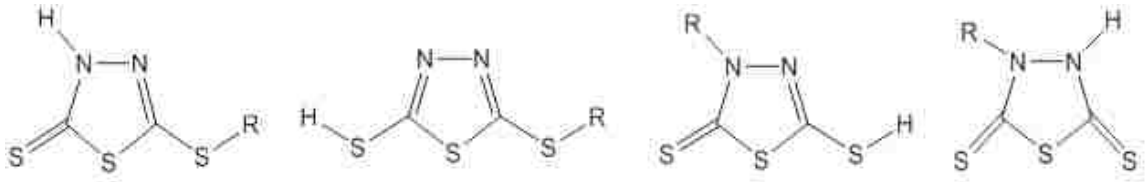

**Structure 4** **Structure 5** **Structure 6** **Structure 7**

***[R = Alkyl]***

**Figure 3.** Four possible mono-substituted products of MTT.

The precursors to structures **4-7** are the anions which could exist as either structure **8** or **9**. The highest-level ab-initio calculations for structures **8** and **9** predict that structure **8** is more stable by 7.37 kcal/mol (Table 2) and thus, the proton is lost from the sulfur and not the nitrogen during alkylation.

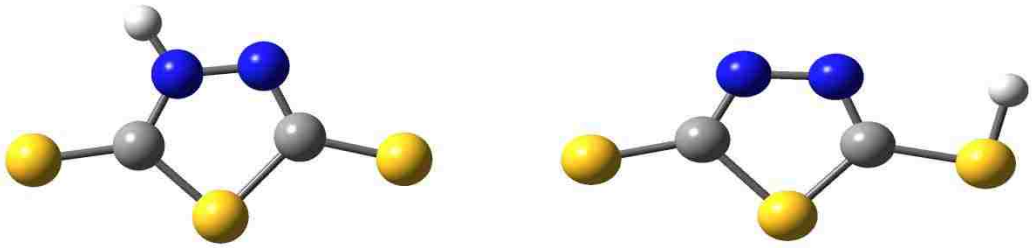

**Structure 8** **Structure 9**

**Figure 4.** Two possible anionic forms of MTT.

**Table 2**. Calculated relative energies (kcal/mol) for anion structures **8** and **9** including thermal corrections at 298 K, and the effect of solvation in ethanol [designated by (s)].

| Method | Structure 8 | Structure 9 |
|---|---|---|
| B3LYP/6-31G(d)[a] | 0.00 | 15.50 |
| B3LYP/AVTZ[a] | 0.00 | 13.68 |
| B3LYP/AVTZ (s)[a] | 0.00 | 10.62 |
| MP2/AVDZ[b] | 0.00 | 11.22 |
| MP2/AVTZ[b] | 0.00 | 10.74 |
| MP2-F12/VDZ-F12[b] | 0.00 | 10.25 |
| CCSD(T)-F12a/VDZ-F12[b] | 0.00 | 10.44 |
| CCSD(T)-F12b/VDZ-F12[b] | 0.00 | 10.44 |
| CCSD(T)-F12a/VDZ-F12 (s)[b] | 0.00 | 7.37 |

All F12 calculations used structures optimized at the MP2/AVTZ level (see text). (s) including implicit PCM solvation model for ethanol.[a] Thermal corrections computed at B3LYP/AVTZ level.[b] Thermal corrections computed at MP2/AVTZ level.

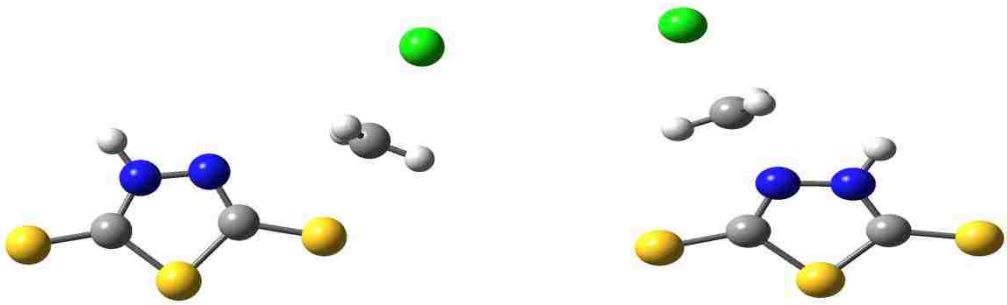

**Structure 10** **Structure 11**

**Figure 5**. The $S_N2$ transition structures for two possible alkylation sites- at the sulfur (structure **10**) or at the nitrogen (structure **11**).

$S_N2$ reaction transition structures (TS) **10** and **11** were located corresponding to methylation of **8** at the S or N positions respectively, using chloromethane (rather than iodomethane which was used in the experiment, to reduce the number of electrons in the calculations) as the alkylating agent. Methylation at the S-position is strongly preferred with **10** predicted to be 6.21 kcal/mol lower in free energy than **11** for the highest level calculations (including the preferential solvation of **11**).

**Table 3.** Calculated relative energies (kcal/mol) for $S_N2$ transition structures **10** and **11** including thermal corrections at 298 K, and the effect of solvation in ethanol [designated by (s)].

| **Method** | **TS (Structure 10)** | **TS (Structure 11)** |
|---|---|---|
| B3LYP/AVTZ[a] | 0.00 | 7.44 |
| B3LYP/AVTZ (s)[a] | 0.00 | 5.77 |
| MP2/AVTZ[b] | 0.00 | 7.21 |
| MP2-F12/VDZ-F12[b] | 0.00 | 7.54 |
| CCSD(T)-F12a/VDZ-F12[b] | 0.00 | 7.89 |
| CCSD(T)-F12b/VDZ-F12[b] | 0.00 | 7.89 |
| CCSD(T)-F12a/VDZ-F12 (s)[b] | 0.00 | 6.21 |

All F12 calculations used structures optimized at the MP2/AVTZ level (see text). (s) including implicit PCM solvation model for ethanol. [a] Thermal corrections computed at B3LYP/AVTZ level. [b] Thermal corrections computed at MP2/AVTZ level.

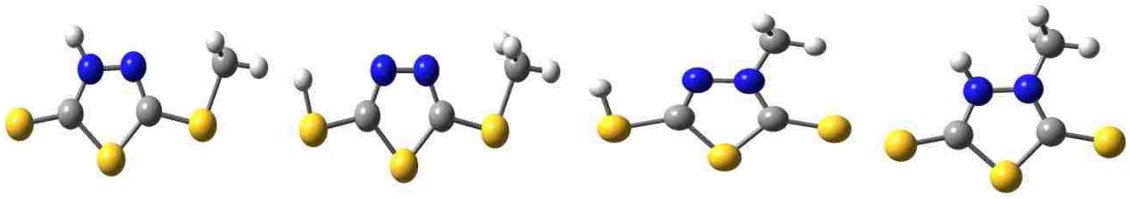

**Structure 12** **Structure 13** **Structure 14** **Structure 15**

**Figure 6.** Four potential mono-alkylation structures **12 - 15**.

**Table 4.** Calculated relative energies (kcal/mol) for structures **12-15** including thermal corrections at 298 K, and the effect of solvation in ethanol [where designated by (s)].

| **Method** | **Structure 12** | **Structure 13** | **Structure 14** | **Structure 15** |
|---|---|---|---|---|
| B3LYP/6-31G(d)[a] | 0.00 | 8.33 | 1.06 | 6.31 |
| B3LYP/AVTZ[a] | 0.00 | 7.21 | 1.92 | 7.72 |
| B3LYP/AVTZ (s)[a] | 0.00 | 8.58 | 2.72 | 4.39 |
| MP2/AVDZ[b] | 1.56 | 5.77 | 0.00 | 9.23 |
| MP2/AVTZ[b] | 0.02 | 3.83 | 0.00 | 9.60 |
| MP2-F12/VDZ-F12[b] | 0.00 | 3.38 | 0.61 | 10.55 |
| CCSD(T)-F12a/VDZ-F12[b] | 0.00 | 3.35 | 1.03 | 10.25 |
| CCSD(T)-F12b/VDZ-F12[b] | 0.00 | 3.34 | 1.01 | 10.30 |
| CCSD(T)-F12a/VDZ-F12 (s)[b] | 0.00 | 4.72 | 1.83 | 6.93 |

All F12 calculations used structures optimized at the MP2/AVTZ level (see text). (s) including implicit PCM solvation model for ethanol.[a] Thermal corrections computed at B3LYP/AVTZ level.[b] Thermal corrections computed at MP2/AVTZ level.

Methylation of **8** through TS **10** or **11** leads to product structures **12** and **15** respectively, while methylation of disfavored anion **9** at the two positions would lead to structures **13** and **14**. Table 4 compares the calculated energies of all four possible products. Structure **12** is predicted to be the most stable of all four of the methylated structures. Looking at the reaction scheme, structure **12** is strongly favored both kinetically and thermodynamically. The lower energy anion **8**, reacts through the lower energy TS **10** to form the most stable product **12**. Not surprisingly the product of the first methylation step was confirmed by X-ray crystallography (Figure 7) and $^{13}C$ NMR spectroscopy to be structure **12**.

The $T_1$-diagnostic is around 0.02 for all calculated structures supporting the reliability of single-reference methods to describe these systems. Calculated $^{13}C$ NMR shifts (relative to TMS) were obtained for structures **12** and **13** using the GIAO method[20] with B3LYP and the 6-31G* basis set. Calculated shifts for the ring carbons are 159.6 and 186.0 ppm (structure **12**) and 158.6 and 167.1 ppm (structure **13**). The calculated values for structure **12** agree closely with experimentally recorded values of 159.4 and 187.6 ppm.

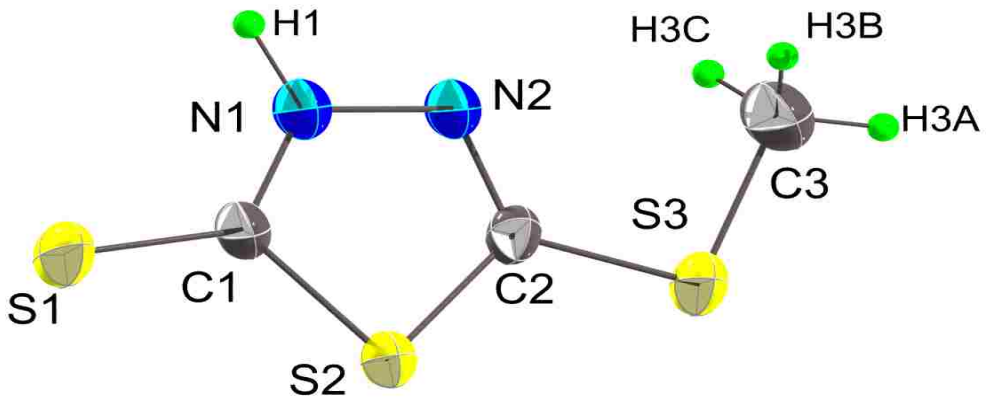


**Figure 7.** Thermal ellipsoids for Me-MTT as observed through X-ray crystallography.

## 4.3 Di-alkylation of MTT

The di-alkylation of MTT was analogously investigated. From structure **12** (mono-alkylated MTT), a second alkylation can occur at two possible alkylation sites- either at the sulfur (forming structure **16**) or at the nitrogen (forming structure **17**).

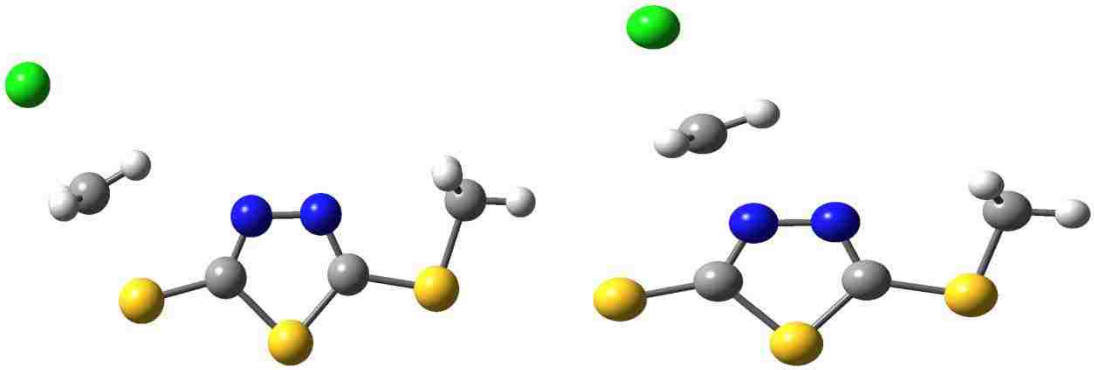

**Structure 16** **Structure 17**

**Figure 8.** The transition structures for di-alkylation of MTT.

Considering a second methylation step starting from **12** and again using chloromethane as the alkylating agent (to simplify the calculations), TS structures **16** and **17** were located connecting **12** with product structures **19** and **20** respectively. Table 5 compares calculated energies for TSs **16** and **17**. Methylation at the S position appears to be kinetically favored as **16** is predicted to be lower in estimated free energy at 298 K than **17** for the B3LYP and CCSD(T)-F12 calculations. The differences in this case are only 1.0 and 0.6 kcal/mol (B3LYP and CCSD(T)-F12) while MP2 calculations actually favor **17**. Preferential solvation of **16** contributes the most to the net difference of 1.62 kcal/mol at the CCSD(T)-F12a (s) level. Given the smaller differences in barrier heights (than for the first methylation step) and the discrepancy with the MP2 results, additional DFT calculations were performed using iodomethane and the midix basis set. Including

solvation by ethanol and thermal corrections at 298 K, the difference in barrier heights increases to 3.48 kcal/mol, making methylation at the S position more strongly kinetically favored. Table 6 compares the energies of di-methylation structures **18** - **20**.

**Table 5.** Calculated relative energies (kcal/mol) for $S_N2$ transition structures **16** and **17** including thermal corrections at 298 K, and the effect of solvation in ethanol [where designated by (s)].

| Method | TS (Structure 16) | TS (Structure 17) |
|---|---|---|
| B3LYP/AVTZ[a] | 0.00 | 1.04 |
| B3LYP/AVTZ (s)[a] | 0.00 | 2.02 |
| MP2/AVTZ[b] | 0.79 | 0.00 |
| MP2-F12/VDZ-F12[b] | 0.40 | 0.00 |
| CCSD(T)-F12a/VDZ-F12[b] | 0.00 | 0.64 |
| CCSD(T)-F12b/VDZ-F12[b] | 0.00 | 0.61 |
| CCSD(T)-F12a/VDZ-F12 (s)[b] | 0.00 | 1.62 |
| B3LYP/midix (s) iodo[c] | 0.00 | 3.48 |

All F12 calculations used structures optimized at the MP2/AVTZ level (see text). (s) including implicit PCM solvation model for ethanol.[a] Thermal corrections computed at B3LYP/AVTZ level.[b] Thermal corrections computed at MP2/AVTZ level. DFT calculation using iodomethane (see text).

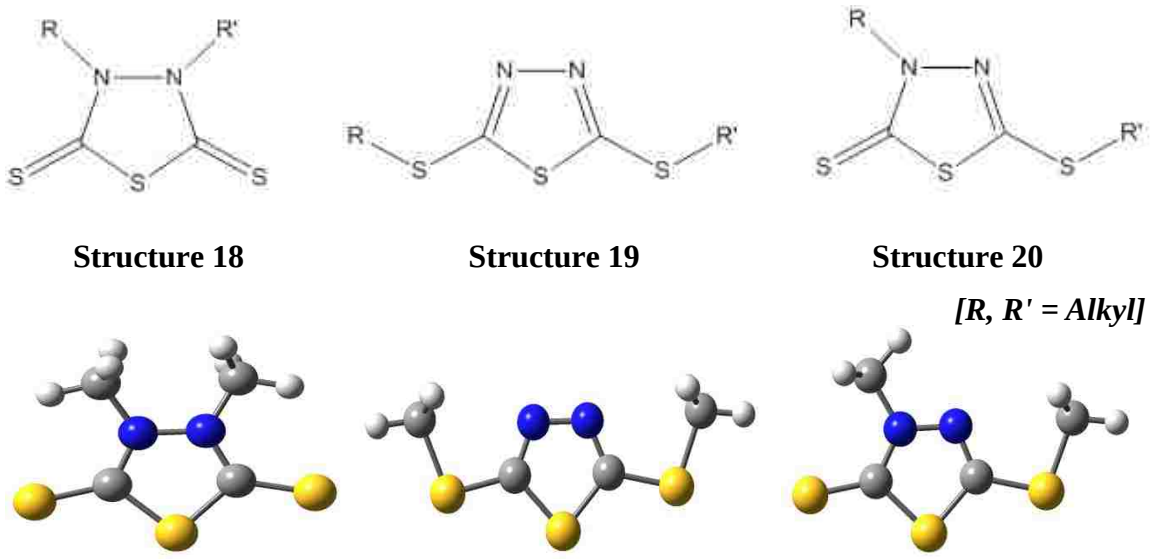


**Structure 18** **Structure 19** **Structure 20**

***[R, R' = Alkyl]***

**Figure 9.** Three possible structures of the di-substituted product of MTT.

**Table 6.** Calculated relative energies (kcal/mol) for structures **18**, **19** and **20** including thermal corrections at 298 K, and the effect of solvation in ethanol [designated by (s)].

| Method | Structure 18 | Structure 19 | Structure 20 |
|---|---|---|---|
| B3LYP/6-31G(d)[a] | 8.89 | 7.89 | 0.00 |
| B3LYP/AVTZ[a] | 10.34 | 5.89 | 0.00 |
| B3LYP/AVTZ (s)[a] | 7.09 | 6.76 | 0.00 |
| MP2/AVDZ[b] | 9.42 | 6.43 | 0.00 |
| MP2/AVTZ[b] | 11.23 | 4.45 | 0.00 |
| MP2-F12/VDZ-F12[b] | 12.16 | 3.40 | 0.00 |
| CCSD(T)-F12a/VDZ-F12[b] | 11.75 | 2.93 | 0.00 |
| CCSD(T)-F12b/VDZ-F12[b] | 11.82 | 2.93 | 0.00 |
| CCSD(T)-F12a/VDZ-F12 (s)[b] | 8.50 | 3.81 | 0.00 |

All F12 calculations used structures optimized at the MP2/AVTZ level (see text). (s) including implicit PCM solvation model for ethanol. [a] Thermal corrections computed at B3LYP/AVTZ level. [b] Thermal corrections computed at MP2/AVTZ level.

TSs **16** and **17** connect **12** with **19** and **20** respectively while **18** is included for comparison. Structure **19** is predicted to be significantly less stable (~3.8 kcal/mol) than **20** yet has been confirmed through X-ray crystallography as the only detectable product structure. The highest level calculations reported here are expected to be quite reliable especially for estimating the relative energies of product structures. The best calculations using chloromethane do predict **19** as the kinetically favored product and DFT calculations for iodomethane favor it even more. The barrier for methyl transfer converting **19** into **20** was computed (at the B3LYP/AVTZ level) to be 55.5 kcal/mol which supports the idea that once **19** is formed it will not easily convert to the more stable **20**.

Since 2,5-bis(methylthio)-1,3,4-thidiazole-2-thiol is a liquid compound, a crystal structure for the di-alkylation product of MTT namely 2,5-bis(thioaceticacid)-1,3,4-thiadiazole [$H_2$ADTZ] was obtained to reconfirm the above results that both of the substitutions occur on sulfur. Both $^{1}$H and $^{13}$C NMR spectra of dimethylated MTT and $H_2$ADTZ are consistent with the X-ray determined structure **19**. 2,5-bis(methylthio)-1,3,4-thidiazole-2-thiol (dimethylated MTT) showed $^{13}$C peaks in d-DMSO at 165.56 ppm (-N=C-S-Me), and 15.60 (-CH3) and GC-MS parent peak at 177 (isotopic abundance peaks due to sulfur at 178 & 179) and significant m/z peaks at 146, 147 (due to the loss of two methyl groups) which confirmed the identity of the compound as 2,5-bis(methylthio)-1,3,4-thiadiazole. 2,5-bis(thioaceticacid)-1,3,4-thiadiazole [$H_2$ADTZ] showed $^{13}$C peaks in d-DMSO at 165.56 ppm (-N=C-S-), 169.11 ppm (-COOH) and 35.74 ppm (-$CH_2$-).

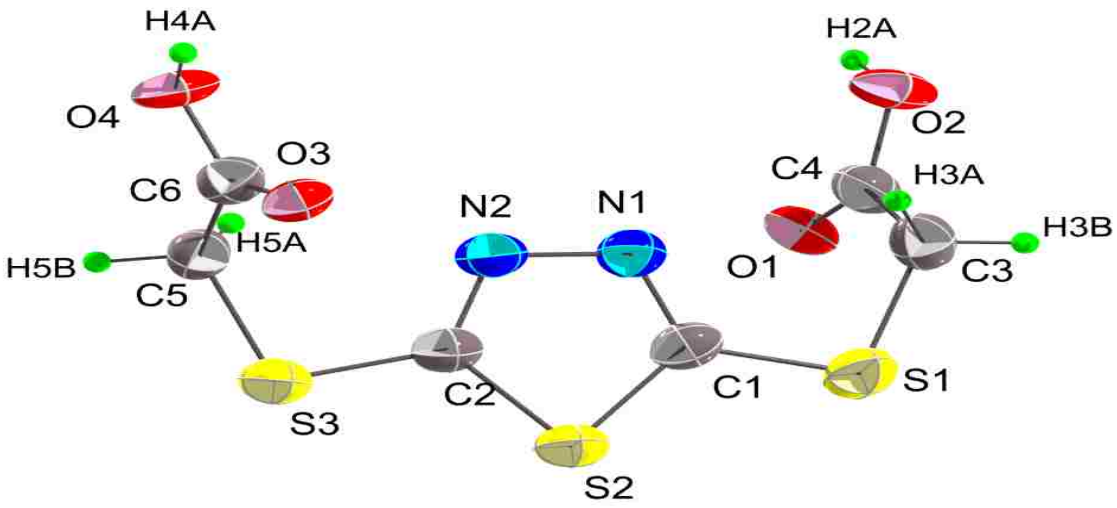


**Figure 10.** Thermal ellipsoid for 2,5-bis(thioaceticacid)-1,3,4-thiadiazole [$H_2$ADTZ] as observed through X-ray crystallography.

## 5. CONCLUSIONS

A combined study by means of X-ray crystallography, $^{13}C$ nuclear magnetic resonance spectroscopy and ab-initio electronic structure calculations was performed, determining the structure of 5-mercapto-1,3,4-thiadiazole-2(3H)-thione and its substituted derivatives conclusively and explaining the chemistry of its reaction mechanisms.

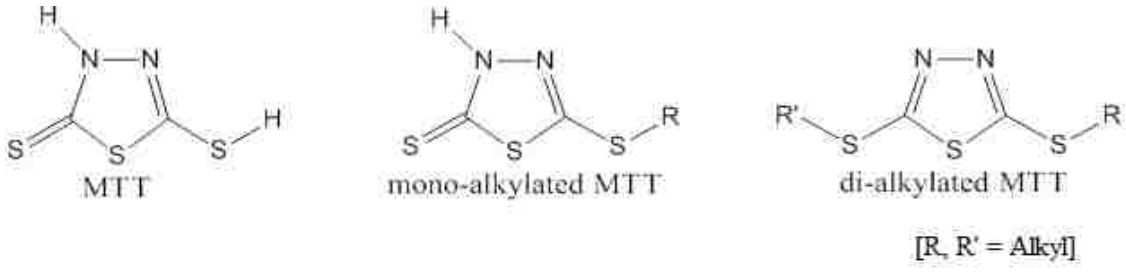


**Figure 11**. The results of X-ray crystallography, NMR spectroscopy and ab-initio electronic structure calculations indicate the preferred structures of MTT, mono-alkylated MTT and di-alkylated MTT.

# 6. EXPERIMENTAL

**6.1 Materials.** The starting material 5-mercapto-1,3,4-thiadiazole-2(3H)-thione (MTT) was obtained from R. T. Vanderbilt who lists the chemical as 2,5-dimercapto-1,3,4-thiadiazole (Structure **1**) and was re-crystallized from benzene before use. All the solvents were dried and distilled before use unless otherwise specified. All other chemicals were procured from Fisher or Aldrich and used as received.

**6.2 X-ray crystallography.** Intensity data sets for all the compounds were collected on a Bruker Smart Apex diffractometer using SMART software.[9] Suitable crystals were selected and mounted on a glass fiber using epoxy-based glue. The data were collected at room temperature employing a scan of 0.3° in ω with an exposure time of 20 s/frame. The cell refinement and data reduction were carried out with SAINT,[10] the program SADABS was used for the absorption correction.[10] The structure was solved by direct methods using SHELXS-97[11,12] and difference Fourier syntheses. Full-matrix least-squares refinement against $|F^2|$ was carried out using the SHELXTL-PLUS[11,12] suite of programs. All non-hydrogen atoms were refined anisotropically. Hydrogen atoms were placed geometrically and held in the riding mode during the final refinement. However, hydrogen atoms on N and S in case of 5-mercapto-1,3,4-thiadiazole-2(3H)-thione and on N in the case of 5-(methylthio)-1,3,4-thidiazole-2-thiol were well located from the difference Fourier map and refined subsequently.

Crystallographic data (excluding structure factors) for the structures in this paper have been deposited with the Cambridge Crystallographic Data Centre as supplementary publication nos. CCDC 883750 [5-mercapto-1,3,4-thiadiazole-2(3H)-thione], CCDC

883751 [5-(methylthio)-1,3,4-thidiazole-2(3H)-thione] and CCDC 883752 [2,5-(S-acetic acid)dimercapto-1,3,4-thiadiazole]. Copies of the data can be obtained, free of charge, on application to CCDC: 12 Union Road, Cambridge CB2 1EZ, UK, (fax: +44-(0)1223-336033 or e-mail: deposit@ccdc.cam.ac.uk).

**6.3 NMR spectroscopy.** The instrument used for recording the $^{1}$H-NMR and $^{13}$C-NMR data for liquid state NMR was 400 MHz Varian FT/NMR spectrometer. The reference peak used was δ for TMS at 0.0 ppm.

**6.4 NMR of MTT.** The Bruker DRX300 spectrometer with CP-MAS and 7mm diameter solid rotor was used for the solid state NMR. Measurements were made at 5 kHz spinning and the reference peak used was δ for glycine C=O carbon at 176.03 ppm. 5-mercapto-1,3,4-thiadiazole-2(3H)-thione (MTT) showed $^{13}$C peaks at 159.60 ppm (-N=C-SH) and 189.07 ppm (-N-C=S). The 400 MHz Varian FT/NMR spectrometer was used for the $^{13}$C-NMR liquid state NMR using ethanol-D6 as solvent and the spectra showed $^{13}$C peaks at 148.50 ppm (-N=C-SH) and 190.20 ppm (-N-C=S) confirming the structure to be in the thiol-thione form (one H on sulfur and another on nitrogen). MTT was observed to form disulfides in DMSO and thus, DMSO was not considered a suitable solvent for recording the NMR spectra even though some researchers have reported the $^{1}$H-NMR and $^{13}$C-NMR spectra of MTT in DMSO-d6.[13]

**6.5 Ab-initio electronic structure calculations.** A variety of ab initio electronic structure calculations were performed to study candidate starting material structures **1-3**. From the starting material, two consecutive methylation reactions were studied comparing at each stage the relative energies of possible anions formed by deprotonation as well as $S_N2$ transition structures leading to possible product structures. The Gaussian09[14] and Molpro2010[15] software packages were used for all the calculations reported here. Geometry optimizations and harmonic vibrational frequency calculations were used to locate and confirm minimum energy configurations for each structure. Structures were optimized using the B3LYP[16] hybrid density functional (DFT) method with the 6-31G* and aug-cc-pVTZ basis sets as implemented in the Gaussian program. Additional optimizations were performed using Møller-Plesset second-order perturbation theory (MP2)[17] with Dunning's double and triple-zeta augmented correlation-consistent basis sets (aug-cc-pVDZ and aug-cc-pVTZ).[18] Some high-level explicitly correlated F12[19] single-point-energy calculations were performed using the structures previously determined at the MP2/aug-cc-pVTZ level. Peterson's specialized double-zeta F12 basis set VDZ-F12[20] was used to compute energies with the MP2-F12 and CCSD(T)-F12 methods. The Molpro program was used for all explicitly correlated F12 calculations. For all structures the effect of solvation was estimated (allowing structural relaxation) at the B3LYP/aug-cc-pVTZ level using the implicit Polarizable Continuum Model (PCM) solvation model as parameterized for ethanol in the Gaussian09 program.[21] The $T_1$-diagnostic was recorded to confirm the applicability of the single-reference methods used in this study.

**6.6 Synthesis of mono-Methylated MTT[6] (**Structure **12).** To a stirred aqueous solution of potassium hydroxide (0.1 mol, 5.61g) in absolute ethanol (2.17 mol, 99.97 g), 5-mercapto-1,3,4-thiadiazole-2(3H)-thione (0.1 mol, 15.02g) was added. The reaction mixture was stirred for half an hour before methyl iodide (0.11 mol, 15.61g) was added to the mixture and refluxed for 6 hours, and then it was cooled and filtered. The filtered product 5-(methylthio)-1,3,4-thidiazole-2(3H)-thione (mol. wt. 164.27) was crystallized from benzene to yield a yellowish needle-shaped precipitates which were dried under vacuum. The yield was 74% (12.15 g). The melting point of the compound was found to be 137-138 $^{o}$C. 5-(methylthio)-1,3,4-thidiazole-2(3H)-thione showed $^{13}$C peaks in d-DMSO at 159.39 (-N=C-S-Me), 187.51 (-N-C=S) and 14.67 ppm (-CH3); $^{1}$H peaks in d-DMSO at 2.52 (S-$CH_3$) and 14.30 ppm (N-H); IR bands at 3050, 1480, 1365, and 1100 $cm^{-1}$; MS peaks at 164, 91, 88, 73 and 59 m/z.

**Scheme 1**: Synthesis of mono-Methylated MTT.

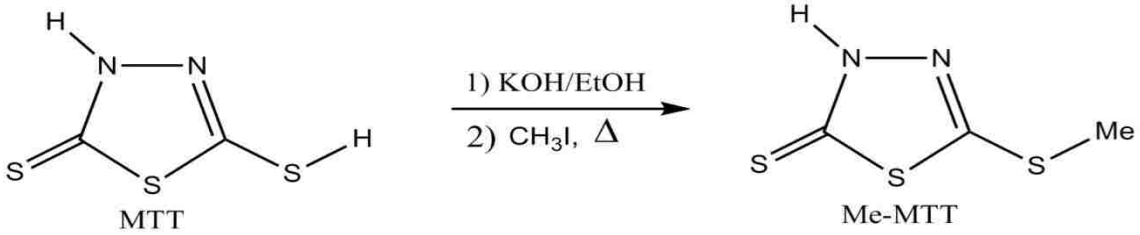


**6.7 Synthesis of di-Methylated MTT[22] (**Structure **19).** To a stirred aqueous solution of 100 ml DI/distilled water with sodium hydroxide (0.3 mol, 12g) in 1,4-dioxane (0.12 mol, 100 ml), 5-mercapto-1,3,4-thiadiazole-2(3H)-thione (0.1 mol, 15.02g) was added. The reaction mixture was stirred for 30 minutes before methyl iodide (0.21 mol, 29.80g) was added to the mixture and refluxed for 6 hours, after which the reaction

product was cooled, poured into water and extracted twice with diethyl ether, dried over anhydrous sodium sulfate, filtered and rotavaped to give a yellowish liquid product 2,5-bis(methylthio)-1,3,4-thiadiazole (mol. wt. 178.30). The yield was 79% (14.08 g). The boiling point of the compound was found to be 311-313 $^{o}$C. 2,5-Bis(methylthio)-1,3,4-thidiazole was a yellowish liquid which showed $^{13}$C peaks in d-DMSO at 165.56 ppm (-N=C-S-Me), and 15.60 (-$CH_3$); $^{1}$H peaks in d-DMSO at 2.55 ppm (-$CH_3$) and GC-MS parent peak at 177 (isotopic abundance peaks due to Sulfur at 178 & 179) and significant m/z peaks at 146, 147 (due to the loss of 2 Methyl groups) which confirmed the identity of the compound as 2,5-bis(methylthio)-1,3,4-thiadiazole.

Di-alkylation of MTT can also be achieved by sequential alkylation of mono-alkylated MTT, but one-pot dimethylation procedure is convenient and therefore, preferred. Di-methylated MTT has been synthesized in good yields by taking mono-methylated MTT in 1:1 water-dioxane mixture with sodium hydroxide as the base and iodomethane as the alkylating agent.

**Scheme 2**: Synthesis of di-Methylated MTT.

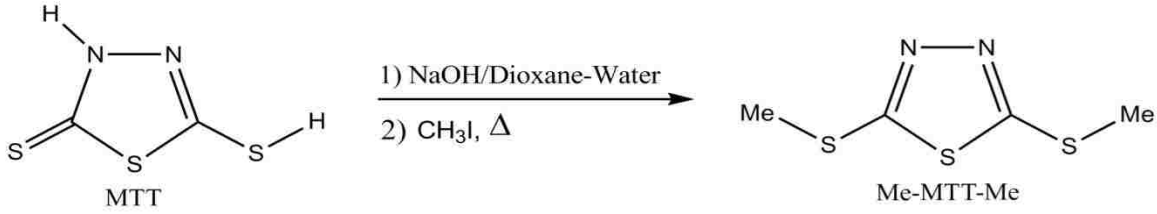


MTT Me-MTT-Me

### 6.8 Synthesis of 2,5-bis(thioaceticacid)-1,3,4-thiadiazole [$H_2$ADTZ] [1]

**(**Figure **10).** To a stirred aqueous solution of chloroacetic acid (94.5 g, 1 mol) and sodium carbonate (53 g, 0.5 mol), 5-mercapto-1,3,4-thiadiazole-2(3H)-thione (75 g, 0.5 mol) was

added. The reaction mixture was stirred and refluxed for 3 hours, then it was cooled and filtered. Ethanol was added to the reaction mixture, yielding a white precipitate. The product 2,5-(S-acetic acid)-dimercapto-1,3,4-thiadiazole ($H_2$ADTZ) (mol. wt. 266.32) was then washed with ethanol and dried under vacuum to give a white solid ($H_2$ADTZ). The yield was 83% (110.51 g). The melting point of the compound was found to be 164-165 $^{o}$C. 2,5-bis(thioaceticacid)-1,3,4-thiadiazole showed $^{13}$C peaks in d-DMSO at 164.56 (-N=C-S-), 169.11 (-COOH) and 35.74 ppm (-$CH_2$-); $^{1}$H peaks in d-DMSO at 4.11 (-$CH_2$) and 11.46 ppm (-OH); IR bands at 3410, 2920, 2830, 1750 and 1600 cm$^{-1}$.

**Scheme 3**: Synthesis of 2,5-bis(thioaceticacid)-1,3,4-thiadiazole [$H_2$ADTZ].

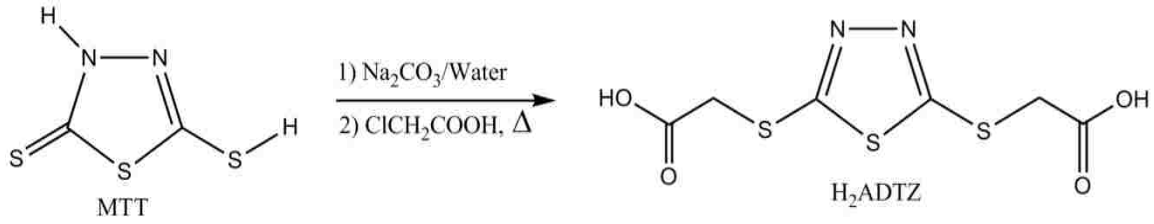

**Scheme 4.** Proposed mechanism for reactions of MTT.

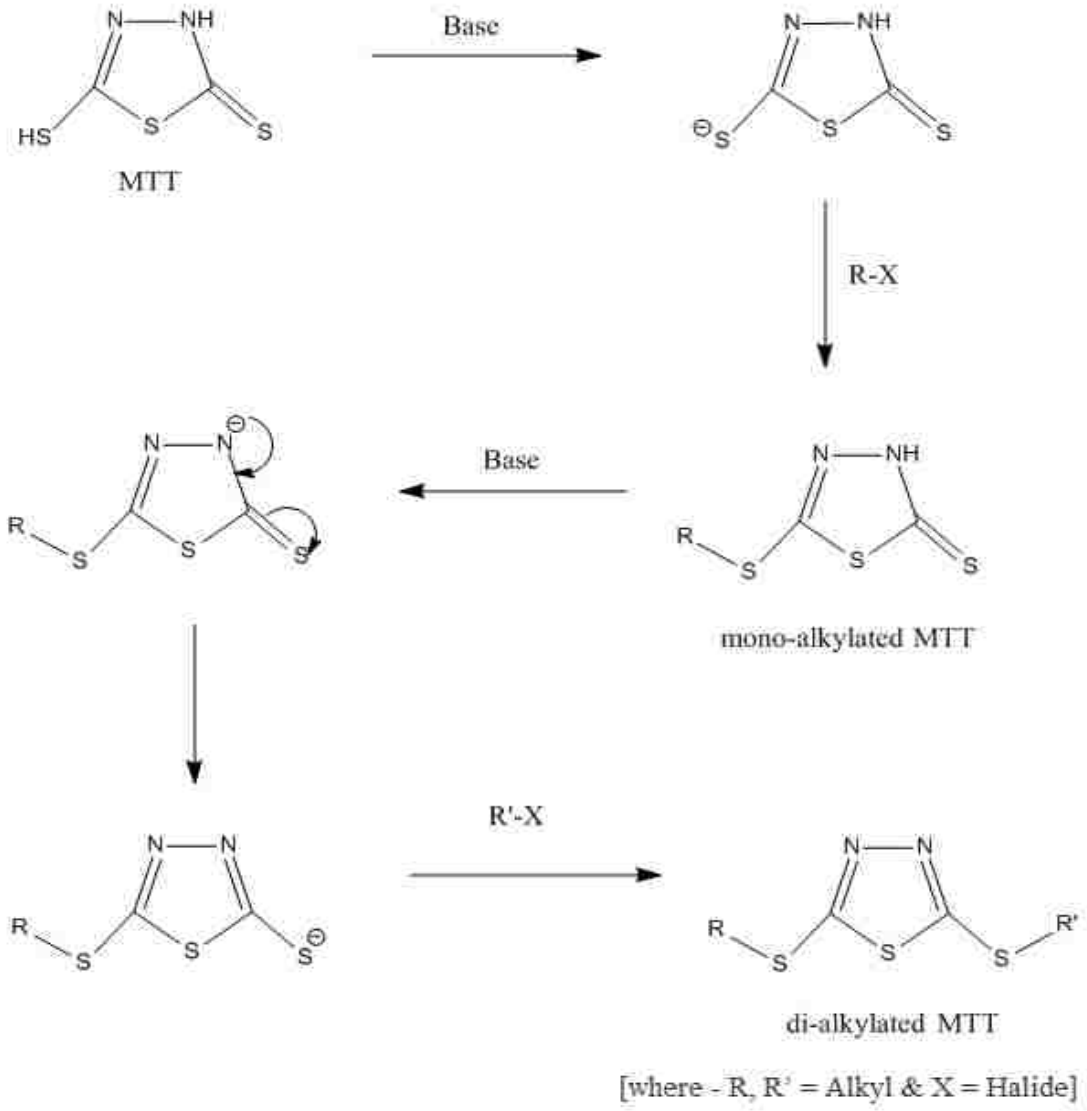

## 7. REFERENCES


1. Sianawati, E.; Mistry, J. K.; Van De Mark, M. R. European Coatings Journal 2008, 12, 35.

2. Yakubovich, A. Y.; Ginsburg, V. A. Zhurnal Obshchei Khimii 1958, 28, 1031.

3. Sidky, M. M.; Mahran, M. R.; Zayed, M. F.; Abdou W. M.; Hafez, T. S. Org. Preparations and Procedures Int. 1982, 14(4), 225.

4. Masten, S. A. Review of Toxicology Studies: 2,5-Dimercapto-1,3,4-Thiadiazole for National Toxicology Program, Jan. 2005.

5. Bats, J. W. Acta Crystallogrica; Sect.B:Struct.Crystallogr.Cryst.Chem. 1976, 32, 2866.

6. Katritzky, A. R.; Wang, Z.; Offerman, R. J. Journal of Heterocyclic Chemistry 1990, 27(2), 139.

7. Kuodis, Z.; Rutavichyus, A; Valiulene, S. Chemistry of Heterocyclic Compounds 2000, 36(5), 598.

8. Durust, Y. Phosphorus Sulfur Silicone (ISSN: 1024-6507) 2009, 184, 2923.

9. Bruker (2002). SMART. Bruker AXS Inc., Madison, Wisconsin, USA.

10. Bruker (2008). SAINT and SADABS. Bruker AXS Inc., Madison, Wisconsin, USA.

11. Sheldrick, G. M. *SHELXS-97 and SHELXTL-97*, University of Göttingen: 1997.

12. Sheldrick, G. M. Acta Cryst. 2008, A64, 112-122.

13. Salimon, J.; Salih, N.; Hameed, A.; Ibraheem, H.; Yousif, E. Journal of Applied Sciences Research 2010, 6(7), 866.

14. Frisch, M. J.; Trucks, G. W.; Schlegel, H. B.; Scuseria, G. E.; Robb, M. A.; Cheeseman, J. R.; Scalmani, G.; Barone, V.; Mennucci, B.; Petersson, G. A.; Nakatsuji, H.; Caricato, M.; Li, X.; Hratchian, H. P.; Izmaylov, A. F.; Bloino, J.; Zheng, G.; Sonnenberg, J. L.; Hada, M.; Ehara, M.; Toyota, K.; Fukuda, R.; Hasegawa, J.; Ishida, M.; Nakajima, T.; Honda, Y.; Kitao, O.; Nakai, H.; Vreven, T.; Montgomery, J. A., Jr.; Peralta, J. E.; Ogliaro, F.; Bearpark, M.; Heyd, J. J.; Brothers, E.; Kudin, K. N.; Staroverov, V. N.; Kobayashi, R.; Normand, J.; Raghavachari, K.; Rendell, A.; Burant, J. C.; Iyengar, S. S.; Tomasi, J.; Cossi, M.; Rega, N.; Millam, N. J.; Klene, M.; Knox, J. E.; Cross, J. B.; Bakken, V.; Adamo, C.; Jaramillo, J.; Gomperts, R.; Stratmann, R. E.; Yazyev, O.; Austin, A. J.; Cammi, R.; Pomelli, C.;

Ochterski, J. W.; Martin, R. L.; Morokuma, K.; Zakrzewski, V. G.; Voth, G. A.; Salvador, P.; Dannenberg, J. J.; Dapprich, S.; Daniels, A. D.; Farkas, O.; Foresman, J. B.; Ortiz, J. V.; Cioslowski, J.; Fox, D. J. Gaussian 09, Revision B.01; Gaussian, Inc.: Wallingford, CT, 2010.

15. MOLPRO, a package of *ab initio* programs designed by H.-J. Werner and P. J. Knowles, Version 2010.1, R. Lindh, F. R. Manby, M. Schütz *et al.*

16. Becke, A. D. J. Chem. Phys. 1993, 98, 5648.

17. Head-Gordon, M.; Head-Gordon, T. Chem. Phys. Lett. 1994, 220, 122.

18. Kendall, R. A.; Dunning, Jr. T. H.; Harrison, R. J. J. Chem. Phys. 1992**,** 96, 6796.

19. Adler, T. B.; Knizia, G.; Werner, H. J. J. Chem. Phys. 2007, 127, 221106.

20. Peterson, K. A; Adler, T. B.; Werner, H. J. J. Chem. Phys. 2008, 128, 084102.

21. (a) Ditchfield, R. Mol. Phys. 1974, 27, 789. (b) Wolinski, K.; Hilton, J. F.; Pulay, P. J. Am. Chem. Soc. 1990, 112, 8251.

22. Tashbaev, G. A.; Nasyrov, I.M.; Zakharov, K. S.; Zegel'man, L.A. Izvestiya Akademii Nauk Tadzhikskoi SSR, Otdelenie Fiziko-Matematicheskikh, Khimicheskikh i Geologicheskikh Nauk 1991, 1, 88.

# 8. SUPPORTING INFORMATION

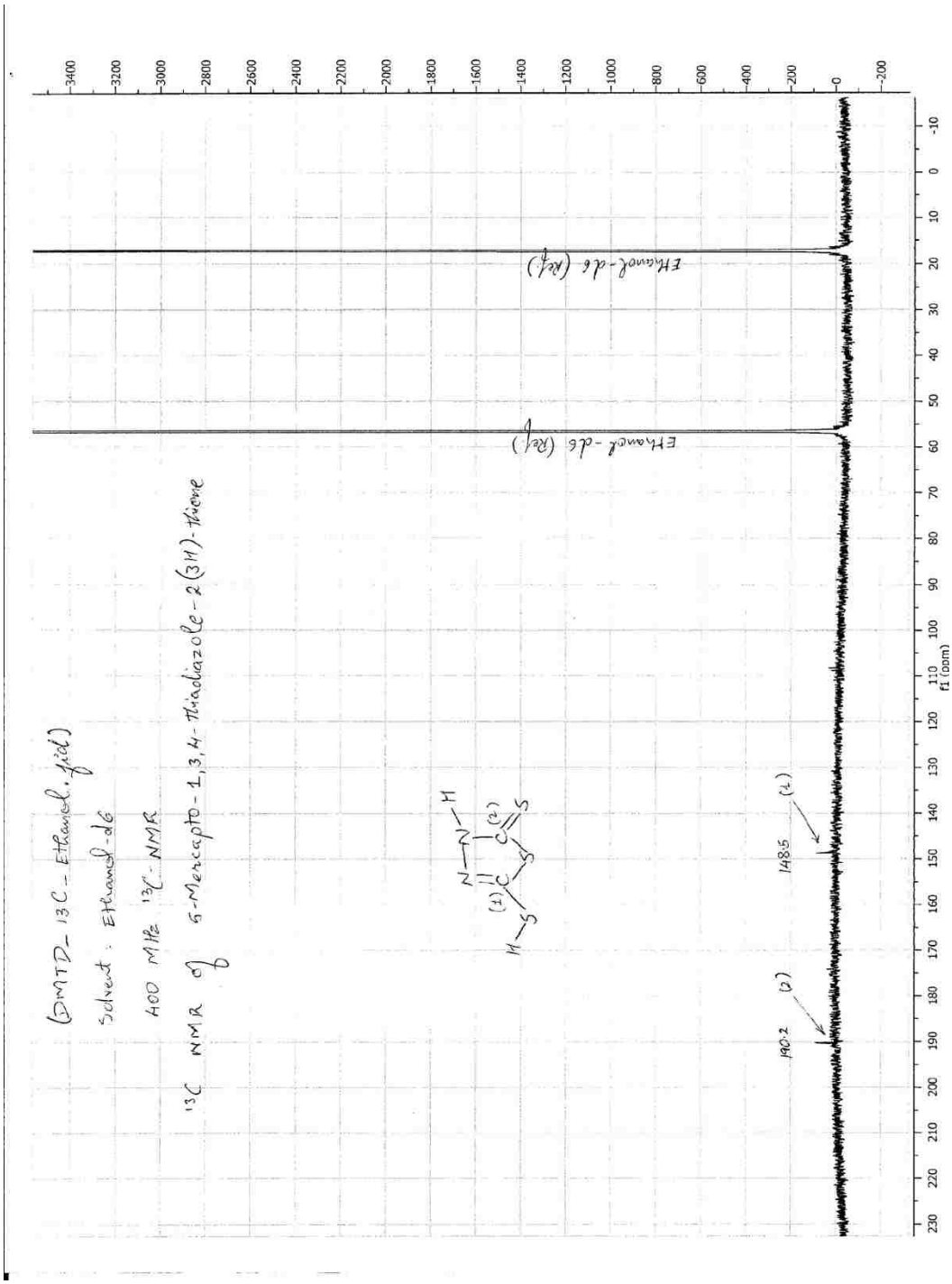


**Figure S.1** $^{13}$C liquid state NMR of MTT. The two carbon peaks observed here corroborate our findings that MTT exists in the thiol-thione form.

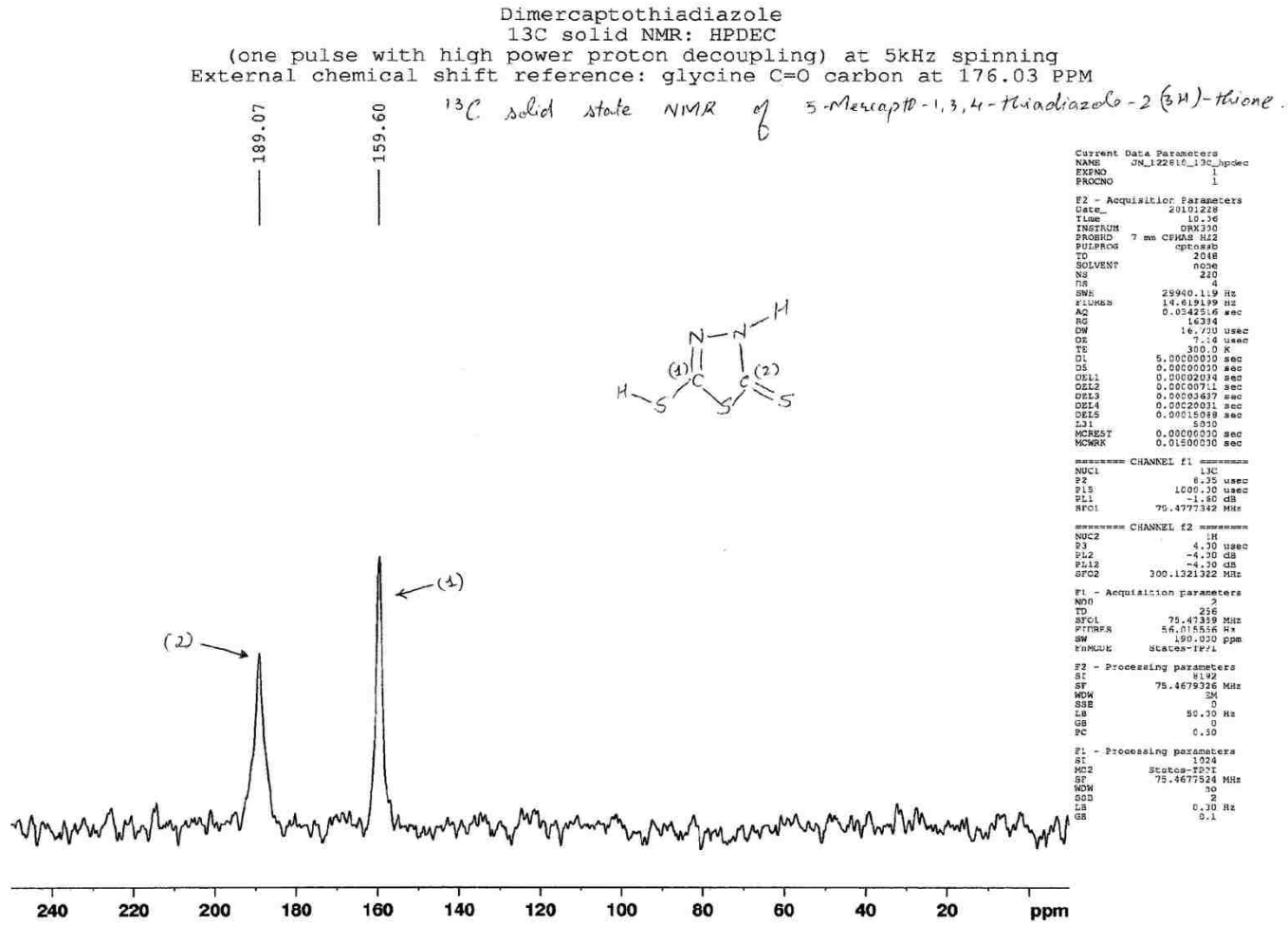


**Figure S.2** $^{13}$C solid state NMR of MTT. The nmr spectra is consistent with the findings that MTT exists in the thiol-thione form

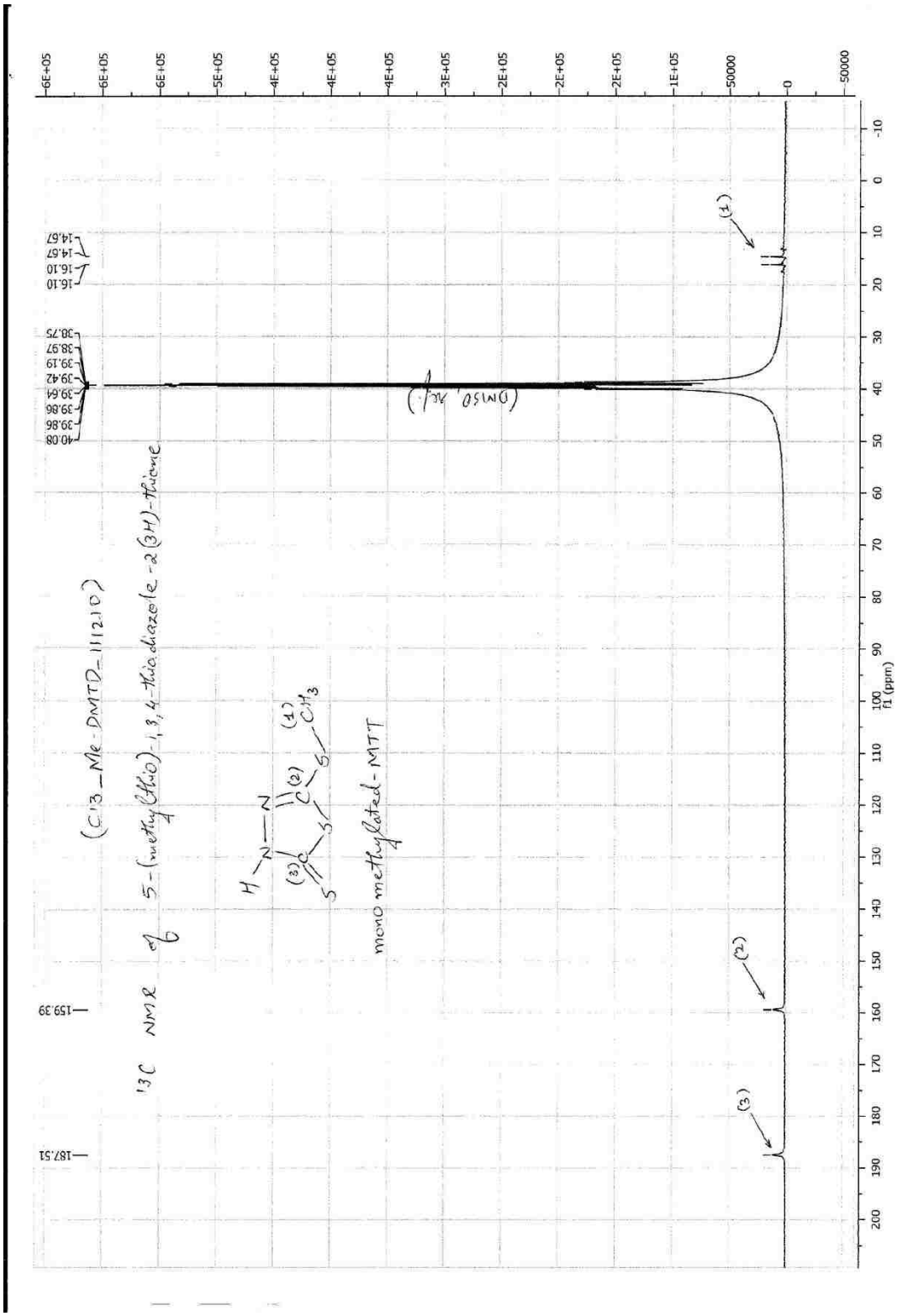


**Figure S.3** $^{13}$C liquid state NMR of mono-methylated MTT. The 3 distinctive peaks and their positions confirm that the 1$^{st}$ substitution is on sulfur for Me-MTT

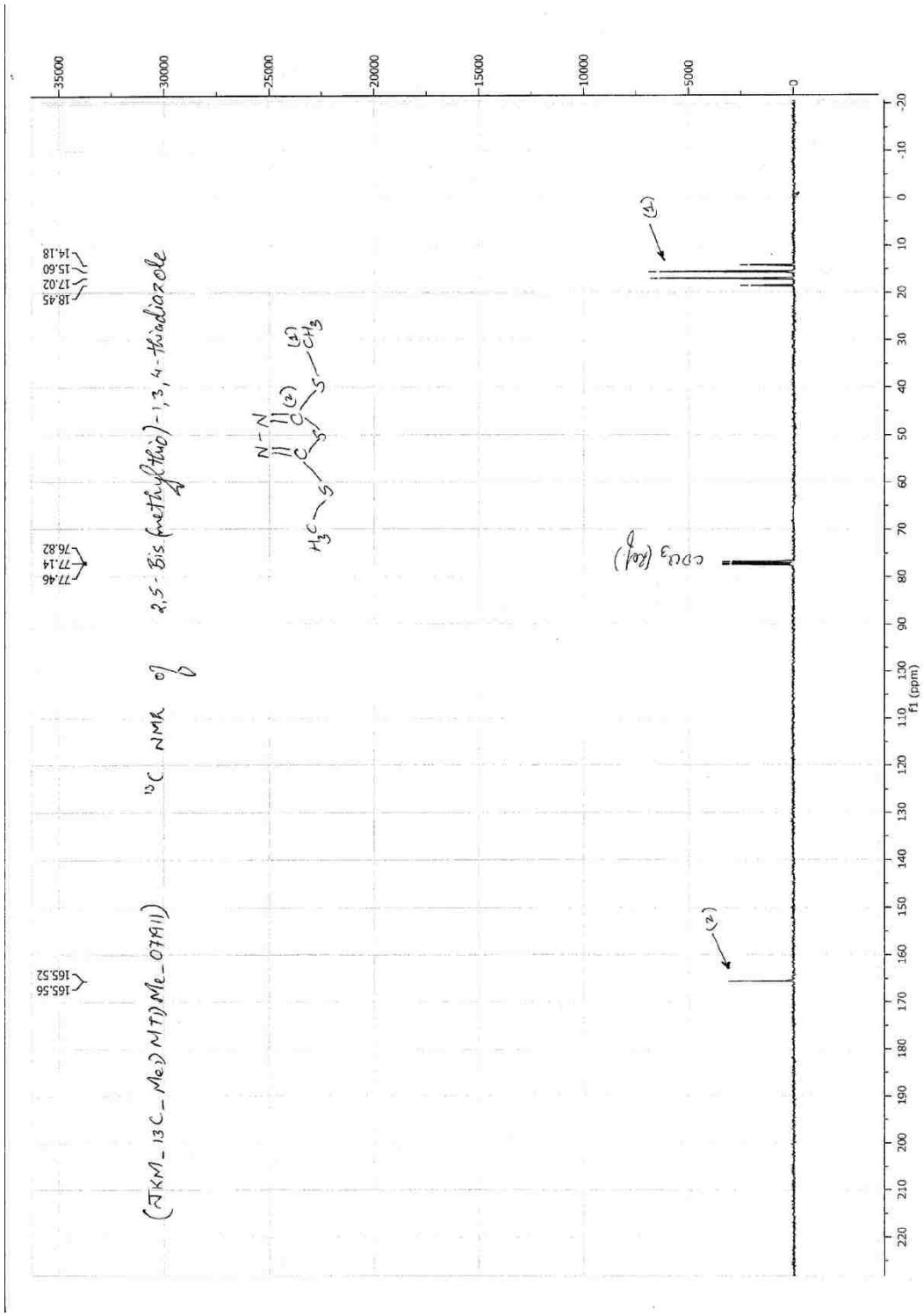


**Figure S.4** $^{13}$C liquid state NMR of di-methylated MTT. The spectra is proof that the 2$^{nd}$ substitution on MTT also occurs on sulfur to form the product Me-MTT-Me

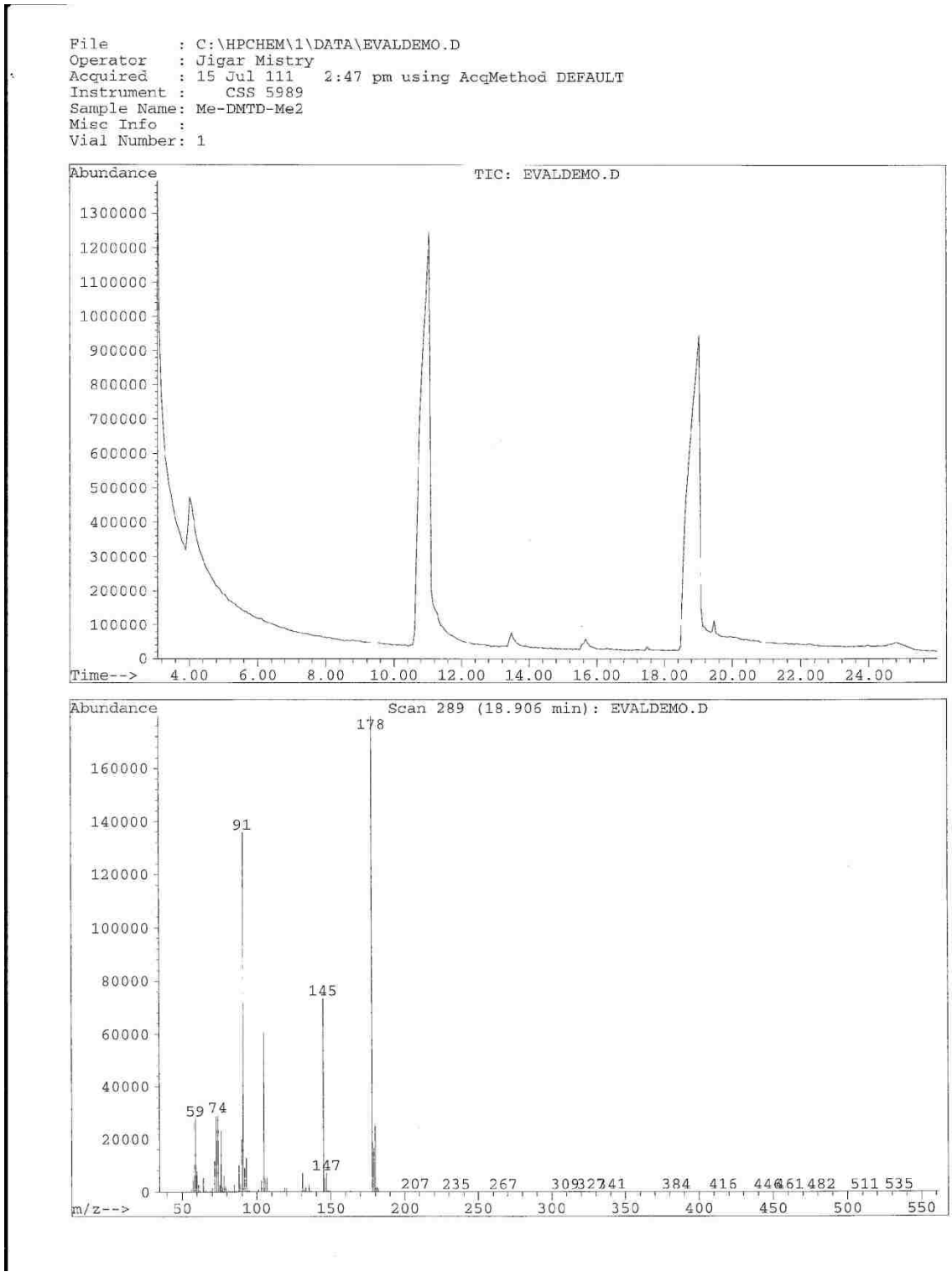


**Figure S.5** GC-MS of di-methylated MTT

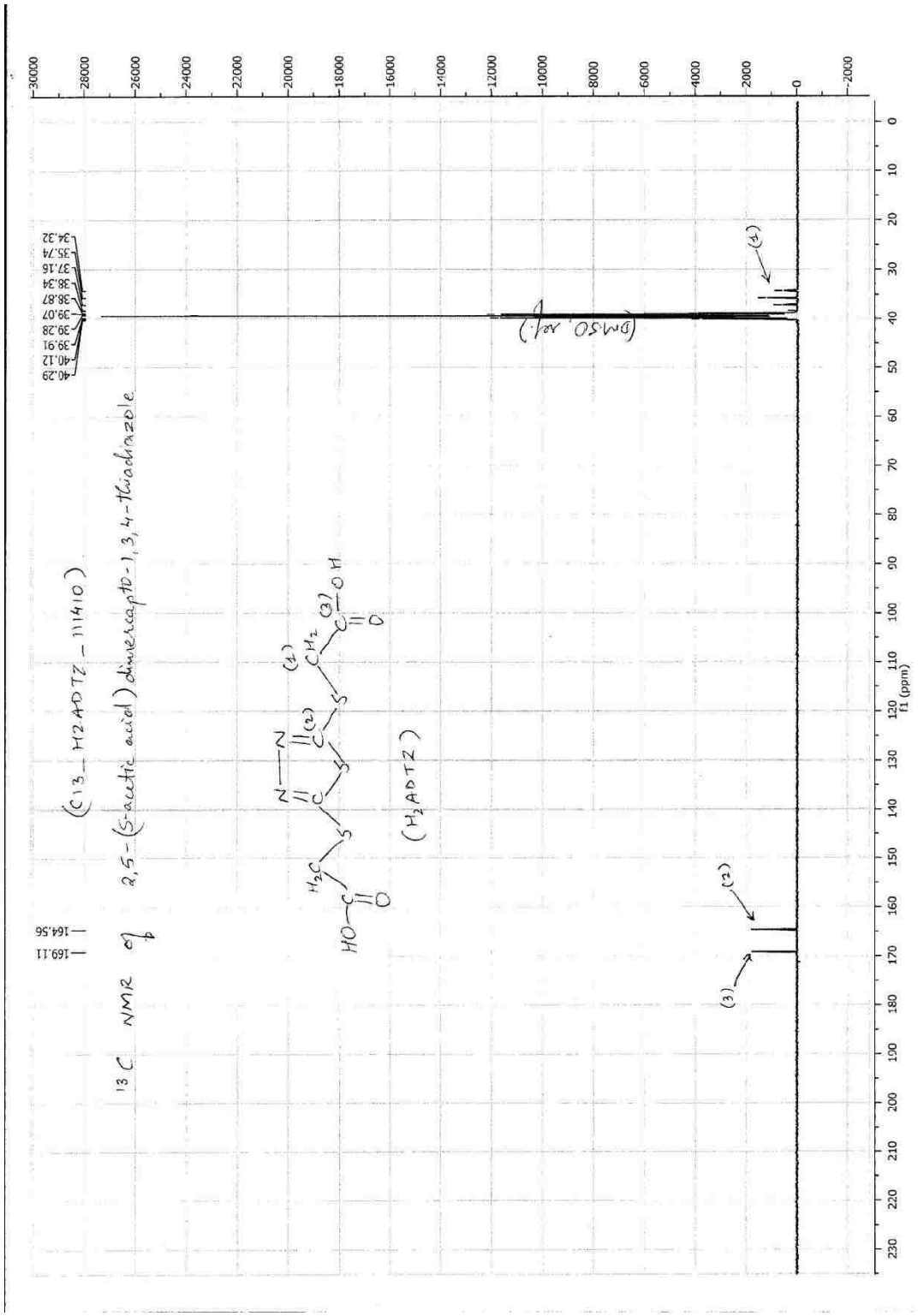


**Figure S.6** $^{13}C$ liquid state NMR of $H_2ADTZ$. This spectra corroborates the findings that both the substitutions on MTT occurs on the sulfur

Crystal data and structure refinement parameters for DMTD, Me-DMTD and H2ADTZ

| | *DMTD* | *Me-DMTD* | *H2ADTZ* |
|---|---|---|---|
| Empirical formula | C2 H2 N2 S3 | C3 H4 N2 S3 | C6 H6 N2 O4 S3 |
| Formula weight | 150.24 | 164.26 | 266.31 |
| Temperature (K) | 298(2) | 298(2) | 298(2) |
| Wavelength(Å) | 0.71073 | 0.71073 | 0.71073 |
| Crystal system | Monoclinic | Monoclinic | Orthorhombic |
| space group | P2(1)/c | P2(1)/c | Fdd2 |
| Unit cell dimensions | | | |
| a (Å) | 6.2250(10) | 4.133(3) | 22.069(10) |
| b (Å) | 10.5764(17) | 9.511(6) | 36.776(16) |
| c (Å) | 9.2450(18) | 17.101(11) | 5.163(2) |
| α (°) | 90 | 90 | 90 |
| β (°) | 113.643(2) | 102.025(9) | 90 |
| γ (°) | 90 | 90 | 90 |
| Volume (A^3) | 557.58(17) | 657.5(7) | 4191(3) |
| Z (Mg) | 4 | 4 | 16 |
| Calculated density (m^3) | 1.79 | 1.659 | 1.688 |
| Absorption coefficient(mm^-1) | 1.19 | 1.017 | 0.702 |
| F(000) | 304 | 336 | 2176 |
| Crystal size(mm) | 0.10 x 0.05 x 0.03 | 0.17 x 0.04 x 0.04 | 0.10 x 0.05 x 0.03 |
| Theta range for data collection(°) | 3.08 to 28.30 | 2.44 to 26.00 | 2.15 to 28.28 |
| Completeness to theta (%) | 99.9 | 97.9 | 99.8 |
| Reflections collected/unique | 6767/1391 [R(int)=0.0436] | 6307/1263 [R(int)=0.0663] | 12676/2578 [R(int)=0.0996] |
| Absorption correction | Semi-empirical from equivalents | Semi-empirical from equivalents | Semi-empirical from equivalents |
| Max. and min. transmission | 0.9697 and 0.8943 | 0.9605 and 0.8461 | 0.9820 and 0.9357 |
| Refinement method | Full-matrix least-squares on F^2 | Full-matrix least-squares on F^2 | Full-matrix least-squares on F^2 |
| Data/restraints/parameters | 1391/0/72 | 1263/0/77 | 2578/1/138 |
| Goodness-of-fit on F^2 | 1.071 | 1.104 | 0.977 |
| Final R indices [I>2sigma(I)] | R1=0.0422, wR2=0.0973 | R1=0.0928, wR2=0.2298 | R1=0.0542, wR2=0.0989 |
| R indices (all data) | R1=0.0580, wR2=0.1054 | R1=0.1016, wR2=0.2367 | R1=0.1114, wR2=0.1185 |
| Largest diff. peak and hole(e.A^-3) | 0.406 and -0.263 | 1.576 and -0.449 | 0.285 and -0.228 |

**Table S.1** X-ray crystallographic structure refinement parameters for MTT (DMTD), Me-MTT (Me-DMTD) and $H_2$ADTZ

Bond lengths [A] and angles [deg] for sad1

**DMTD**

| | |
|---|---|
| S(1)-C(1) | 1.666(3) |
| S(2)-C(1) | 1.734(3) |
| S(2)-C(2) | 1.738(3) |
| S(3)-C(2) | 1.738(3) |
| S(3)-H(2) | 1.15(3) |
| N(1)-C(1) | 1.333(3) |
| N(1)-N(2) | 1.361(3) |
| N(1)-H(1) | 0.69(3) |
| C(2)-N(2) | 1.288(3) |
| | |
| C(1)-S(2)-C(2) | 89.69(13) |
| C(2)-S(3)-H(2) | 95.7(15) |
| C(1)-N(1)-N(2) | 119.9(2) |
| C(1)-N(1)-H(1) | 124(2) |
| N(2)-N(1)-H(1) | 116(2) |
| N(2)-C(2)-S(3) | 121.3(2) |
| N(2)-C(2)-S(2) | 114.5(2) |
| S(3)-C(2)-S(2) | 124.12(16) |
| N(1)-C(1)-S(1) | 127.7(2) |
| N(1)-C(1)-S(2) | 106.76(19) |
| S(1)-C(1)-S(2) | 125.58(16) |
| C(2)-N(2)-N(1) | 109.1(2) |

**Me-DMTD**

| | |
|---|---|
| C(1)-N(1) | 1.335(8) |
| C(1)-S(1) | 1.665(6) |
| C(1)-S(2) | 1.742(6) |
| N(1)-N(2) | 1.378(7) |
| N(1)-H(1) | 0.93(9) |
| N(2)-C(2) | 1.301(8) |
| C(2)-S(3) | 1.727(6) |
| C(2)-S(2) | 1.743(6) |
| S(3)-C(3) | 1.787(7) |
| C(3)-H(3A) | 0.9600 |
| C(3)-H(3B) | 0.9600 |
| C(3)-H(3C) | 0.9600 |
| | |
| N(1)-C(1)-S(1) | 126.9(5) |
| N(1)-C(1)-S(2) | 107.7(4) |
| S(1)-C(1)-S(2) | 125.4(4) |
| C(1)-N(1)-N(2) | 119.0(5) |
| C(1)-N(1)-H(1) | 123(5) |
| N(2)-N(1)-H(1) | 118(5) |
| C(2)-N(2)-N(1) | 109.1(5) |
| N(2)-C(2)-S(3) | 125.1(5) |
| N(2)-C(2)-S(2) | 114.7(4) |
| S(3)-C(2)-S(2) | 120.2(3) |
| C(1)-S(2)-C(2) | 89.5(3) |
| C(2)-S(3)-C(3) | 100.3(3) |
| S(3)-C(3)-H(3A) | 109.5 |
| S(3)-C(3)-H(3B) | 109.5 |
| H(3A)-C(3)-H(3B) | 109.5 |
| S(3)-C(3)-H(3C) | 109.5 |
| H(3A)-C(3)-H(3C) | 109.5 |
| H(3B)-C(3)-H(3C) | 109.5 |

**H2ADTZ**

| | |
|---|---|
| C(1)-N(1) | 1.295(6) |
| C(1)-S(1) | 1.737(5) |
| C(1)-S(2) | 1.739(5) |
| N(1)-N(2) | 1.382(5) |
| N(2)-C(2) | 1.302(5) |
| C(2)-S(2) | 1.720(5) |
| C(2)-S(3) | 1.745(5) |
| S(1)-C(3) | 1.800(5) |
| C(3)-C(4) | 1.479(7) |
| C(3)-H(3A) | 0.9700 |
| C(3)-H(3B) | 0.9700 |
| C(4)-O(1) | 1.207(5) |
| C(4)-O(2) | 1.306(5) |
| O(2)-H(2A) | 0.8200 |
| S(3)-C(5) | 1.785(4) |
| C(5)-C(6) | 1.496(6) |
| C(5)-H(5A) | 0.9700 |
| C(5)-H(5B) | 0.9700 |
| C(6)-O(3) | 1.208(5) |
| C(6)-O(4) | 1.305(5) |
| O(4)-H(4A) | 0.8200 |
| | |
| N(1)-C(1)-S(1) | 125.3(4) |
| N(1)-C(1)-S(2) | 114.1(3) |
| S(1)-C(1)-S(2) | 120.6(3) |
| C(1)-N(1)-N(2) | 112.7(4) |
| C(2)-N(2)-N(1) | 112.0(4) |
| N(2)-C(2)-S(2) | 114.8(4) |
| N(2)-C(2)-S(3) | 124.2(3) |
| S(2)-C(2)-S(3) | 120.9(3) |
| C(2)-S(2)-C(1) | 86.4(2) |
| C(1)-S(1)-C(3) | 99.0(2) |
| C(4)-C(3)-S(1) | 114.1(4) |
| C(4)-C(3)-H(3A) | 108.7 |
| S(1)-C(3)-H(3A) | 108.7 |
| C(4)-C(3)-H(3B) | 108.7 |
| S(1)-C(3)-H(3B) | 108.7 |
| H(3A)-C(3)-H(3B) | 107.6 |
| O(1)-C(4)-O(2) | 123.3(5) |
| O(1)-C(4)-C(3) | 126.2(5) |
| O(2)-C(4)-C(3) | 110.5(5) |
| C(4)-O(2)-H(2A) | 109.5 |
| C(2)-S(3)-C(5) | 98.6(2) |
| C(6)-C(5)-S(3) | 115.4(3) |
| C(6)-C(5)-H(5A) | 108.4 |
| S(3)-C(5)-H(5A) | 108.4 |
| C(6)-C(5)-H(5B) | 108.4 |
| S(3)-C(5)-H(5B) | 108.4 |
| H(5A)-C(5)-H(5B) | 107.5 |
| O(3)-C(6)-O(4) | 122.5(4) |
| O(3)-C(6)-C(5) | 126.3(4) |
| O(4)-C(6)-C(5) | 111.2(4) |
| C(6)-O(4)-H(4A) | 109.5 |

**Table S.2** Bond length and bond angles, as determined by X-ray crystallography for MTT (DMTD, Me-MTT (Me-DMTD) and $H_2$ADTZ

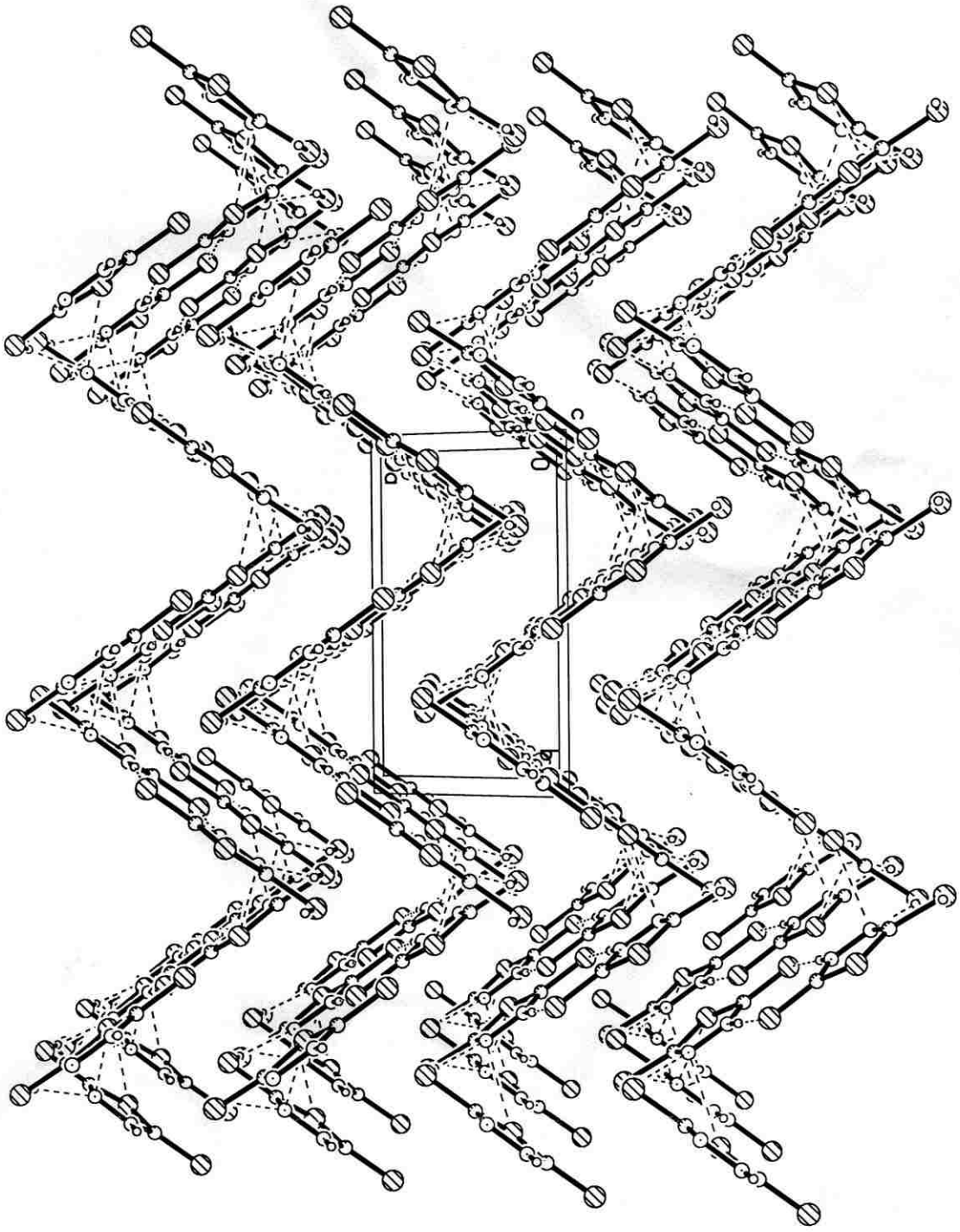


**Figure S.7** A 3-D arrangement of MTT molecules in its crystal form, as portrayed from the results of X-ray crystallography

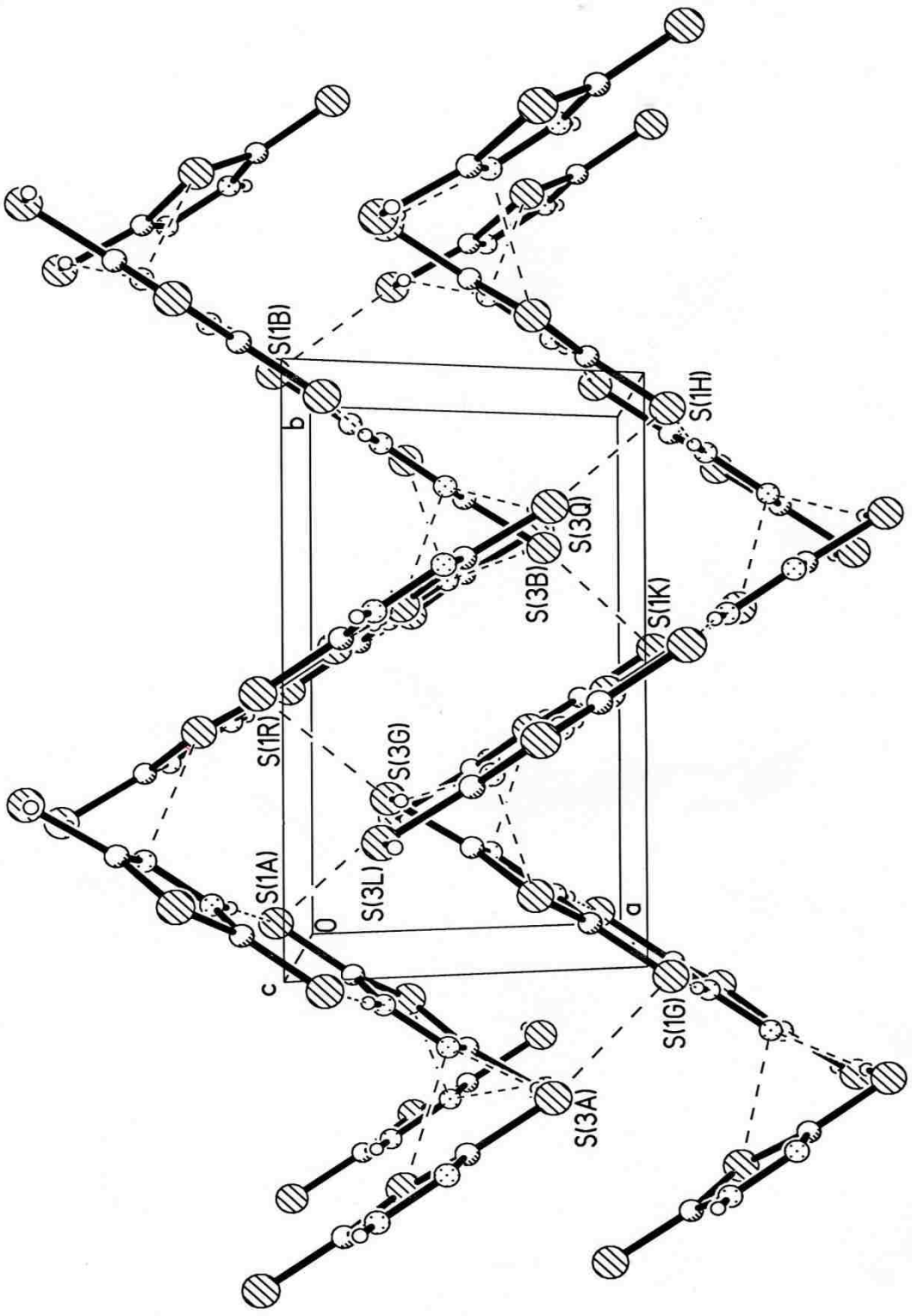


**Figure S.8** π- π interactions between the centroids of the 5-membered MTT ring and that of another ring from the neighboring layer

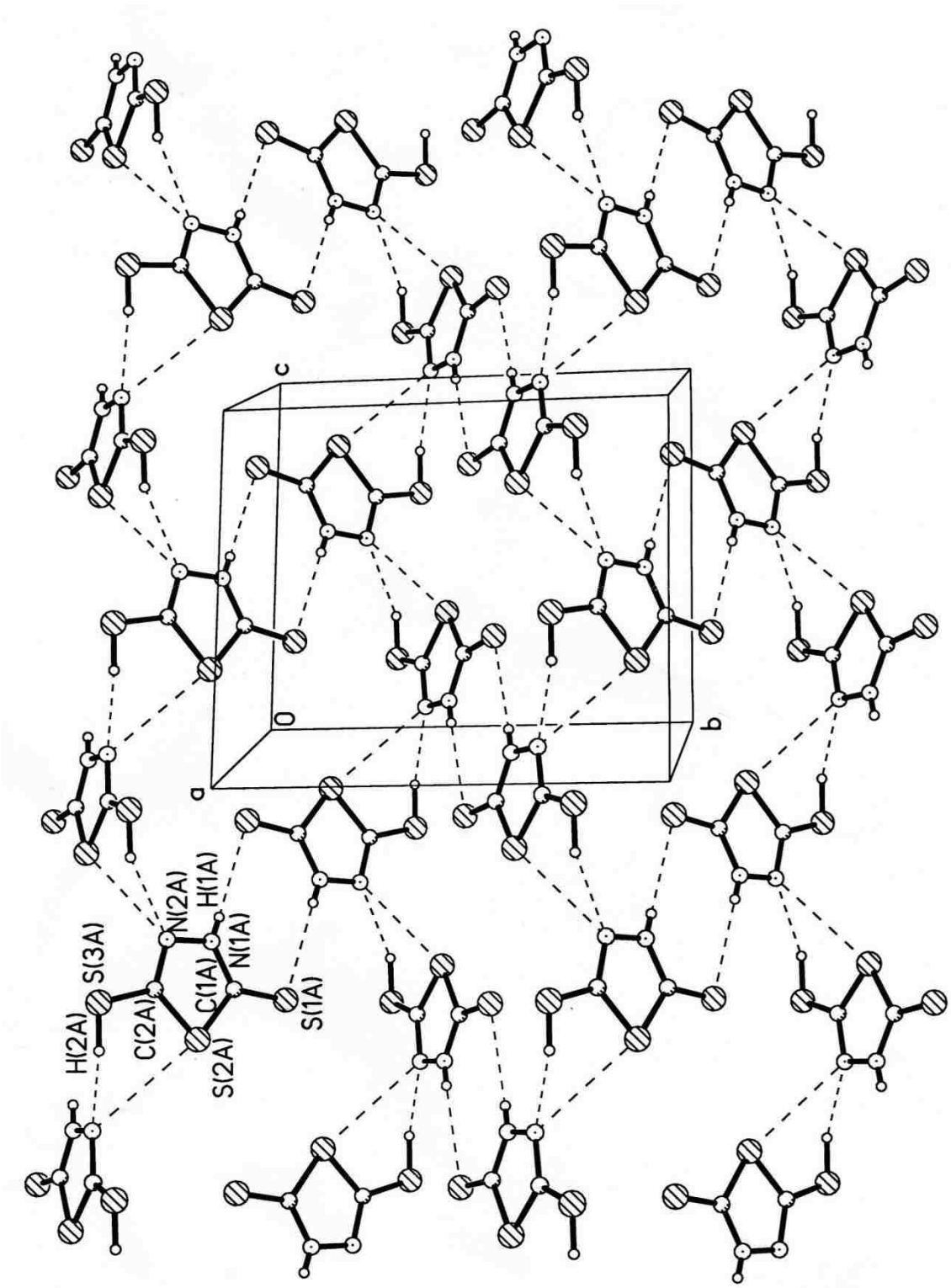


**Figure S.9** Lattice arrangement of MTT crystals depicting the S-N intramolecular interaction, as portrayed from the results of X-ray crystallography

# III. AZIRIDINE CURE OF COLLOIDAL UNIMOLECULAR POLYMERS (CUPs)

**Jigar K. Mistry and Michael R. Van De Mark***

*Missouri S&T Coatings Institute & Department of Chemistry,*
*Missouri University of Science & Technology, Rolla, MO-65409, USA.*

**(Submitted for publication as an Article in the *Journal of Coatings Technology: Research)***

## 1. ABSTRACT

Polymers were synthesized with a 1:7 or 1:8 ratio of acrylic acid to acrylate monomers to produce an acid rich resin. The polymers were water-reduced and solvent stripped to produce Colloidal Unimolecular Polymers (CUPs). These particles are typically 3-9 nanometers in diameter depending upon the molecular weight and have different rheological behavior from micelles, polyeletrolytes, $C_{60}$ and latex due to their charged surface and large surface areas. They were then formulated into an ambient cure clear coating with aziridine crosslinking. These aziridine cured acrylic CUPs were either solvent free or very low VOC. The coatings were evaluated for their MEK resistance, adhesion, hardness, gloss, flexibility, wet adhesion, abrasion and impact resistance properties.

**Keywords:** Colloidal Unimolecular Polymer, CUP, Aziridine, Water-reduction, Zero VOC, Acrylic polymer.

## 2. INTRODUCTION

The promise of nanotechnology to deliver breakthrough coating performance in areas such as scratch resistance, hardness, barrier properties, mechanical properties, etc. has been the main reason for the high level of interest in the scientific community. Researchers of nanotechnology have promoted the idea that "smaller is better"[1]. Although early work on applications of nanomaterials in coating has been scattered, there are many coatings scientists, formulators and researchers around the world today who are investigating different aspects of nano-dispersions in coatings[2,3,4]. As a result, the conditions are set for breakthroughs in this area over the next several years.

Numerous methods have been developed for the water-reduction of polymers to give resins for coatings. One such method describes that when multiple chain polymers containing blocks of both hydrophilic and hydrophobic regions are placed in an aqueous environment at an appropriate pH, the hydrophilic polyether ester portions of the chains orient into the water phase such that they leave the hydrophobic region in the interior domain, forming macromolecular polymeric micelles with an average diameter of 50-120 nm; larger than typical micelles of 2-10 nanometers or roughly twice the diameter of the hydrocarbon chain[5]. In another water-reduction study by Morishima, the micelle behavior of a single polyelectrolyte chain was observed to be "self-assembled" in a poor solvent when the chains collapsed into unimolecular micelles of a diameter of approximately 5.5 nm[6]. Multiple chain polymer collapse has also been observed in waterborne urethane resins synthesized by reaction of iso-cyanate by Reichhold with subsequent removal of the acetone solvent from the resin water blend, causing the chains to collapse into aggregates with a diameter of approximately 25 nm[7,8]. Water-reducible

resins containing ionizable carboxylic acid groups neutralized with amines were synthesized in another study and dissolved in high boiling, water miscible solvents after which water was introduced into the system, until the solvent blend became a less-than theta solvent condition which caused the entangled polymer chains to collapse[9].

The term Colloidal Unimolecular Polymer[10] (CUP) has been introduced to describe the solid spherical single molecule polymer particles suspended in the continuous aqueous phase. CUPs contain a hydrophobic backbone and hydrophilic groups such as carboxylic acid salts. The process by which these are formed is basically water reduction with subsequent removal of a volatile water loving solvent. Therefore, the CUP solution can be VOC free. This research paper explores the synthesis of acrylic Colloidal Unimolecular Polymers in the true nano-scale range (less than 10nm) with particular emphasis on coating performance enhancements offered by the aziridine curing of the polymeric films.

In this study, polymers of Colloidal Unimolecular Polymers (CUPs) were synthesized in THF using acrylic monomers by free radical polymerization. Four polymers were investigated: two of low Tg, below room temperature, and two of high Tg, above room temperature. For both the polymers, two molecular weights were chosen: one high ~50,000 and the other a lower molecular weight ~20,000. The low molecular weight would require crosslinking to obtain any respectable physical properties whereas the higher molecular weight would have marginal lacquer performance. THF was selected as the primary solvent due to its good solvency for acrylics, its miscibility with water and low boiling point allowing it to be easily stripped off after water reduction without loss of a significant amount of water. The hydrophilic/lipophilic balance requires that the acid

monomer to the acrylate used have a ratio between 1:7 and 1:8. This ratio yields a monomolecular reduction to the CUP particles. If less acid groups are incorporated, some aggregation was observed. Triethylamine was added to neutralize the carboxylic acid groups on the synthesized polymers during water reduction. Bases like NaOH and KOH cannot be used for neutralization as they form a salt that does not leave the film during drying and thus, will not crosslink with the aziridine. Ammonium hydroxide can be used for neutralization but triethylamine was chosen in this study. Water is added slowly during water reduction to avoid a large regional solvent composition change which causes the formation of more coagulum and leads to visible cloudiness indicating large aggregates. A modest stirring rate is essential for avoiding any regional solvent composition change. The synthesized acrylic CUP resins will give the performance of a lacquer without a crosslinker and therefore to enhance the performance, a commercially available aziridine (CX-100 from DSM Neoresins Inc.) with a functionality of 3 was chosen. The low Tg CUP resin developed is a zero VOC system, except for the base. For high Tg polymers cured by means of aziridine, Texanol (Eastman Chemical Co.) was used as a coalescing aid to ease the process of film formation. The coalescent aid was the only VOC in the system, other than the base, making the high Tg resin a low VOC system.

*Figure* 1 illustrates the size comparison of two conventional small coating resin particles represented by a latex and a typical waterborne urethane resin. The third particle in the series is the Colloidal Unimolecular Polymer[10] particle which is the topic of this report. The CUPs are single polymer chain particles which are collapsed and

suspended in water. Their small size and high charge density coupled with the Brownian motion of the solvent molecules allows them to be thermodynamically stable in water [11].

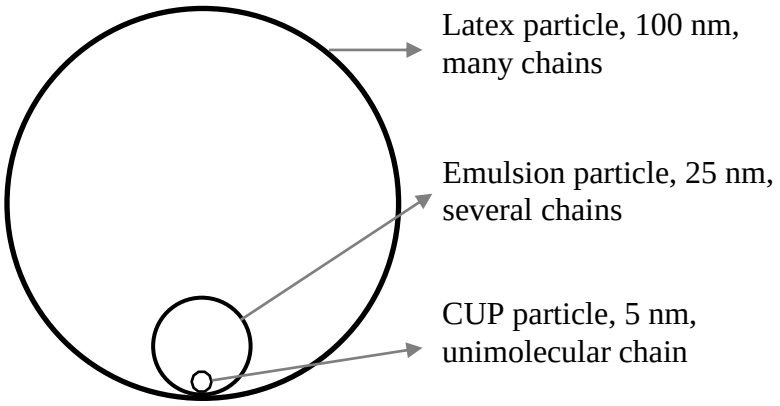


**Figure 1.** Particle size comparison for water borne particulate coating resins

## 3. EXPERIMENTAL

### 3.1 Materials

Methacrylic acid (MAA), butyl methacrylate (BMA), ethyl acrylate (EA), ethyl methacrylate (EMA), 2-ethylhexyl methacrylate (2-EHMA), 2,2′-azobis(2-methylpropionitrile) (AIBN) and 1-dodecanethiol were obtained from Aldrich. MAA was purified by distillation with copper (I) bromide under vacuum. All other monomers were purified by washing with a 10% (w/w) aqueous solution of sodium bicarbonate, followed by rinsing with de-ionized water, and brine after which the solution was filtered after drying over sodium sulfate and purified by distillation under nitrogen with Copper (I) bromide as an inhibitor. The solvent THF was dried and distilled before use. The

initiator AIBN was recrystallized before use from methanol while 1-dodecanethiol was used as received.

**3.2 Polymer syntheses**

All polymers were synthesized by free radical polymerization in tetrahydrofuran (THF). The monomer composition of polymers J-31 & J-32 was in molar ratios - MAA : EMA : BMA = 1 : 2.5 : 5.5 with the acid: acrylate ratio 1:8 while the monomer composition of polymers J-51 & J-52 was in molar ratios – MAA : EA : 2-EHMA : BMA = 1 : 1.5 : 1.5 : 4 with the acid: acrylate ratio 1:7. The monomer ratios were chosen such that the glass transition temperature of two of those polymers would be above and two below room temperature for adequate evaluation of the polyacrylic resins synthesized. The molar ratio of dodecanethiol was varied to produce a low and a high range of molecular weight. The solvent THF was added in the amount of 2.5 times the total weight of monomers. It should be noted that all the polymers were insoluble in water as well as at an alkaline pH.

*Synthesis for polymer J-31*: The monomers, BMA (0.477 moles, 67.79 g), EMA (0.217 moles, 24.74 g) and MAA (0.0865 moles, 7.47 g) in a 1000 ml 3-neck round bottom flask with the initiator AIBN (0.781 moles, 0.094 g) along with chain transfer agent dodecanethiol (0.0033 moles, 0.658 g) and THF (250 g) were stirred. The flask was fitted with a nitrogen line, condenser, and a gas outlet adapter connected to an oil bubbler to allow a positive pressure of nitrogen throughout the polymerization process. The flask was heated slowly to reflux and allowed to react for 24 hours. The polymer solution was then cooled to room temperature, and precipitated in cold de-ionized water under high

shear, then dried in vacuo. Polymers J-32, J-51 and J-52 were also synthesized as per the above mentioned protocol.

### 3.3 Characterization of polymers synthesized

The $^{1}H$ NMRs were recorded on the synthesized polymers using a Varian 400 MHz FT/NMR spectrometer in a 5 mm outer diameter thin-walled glass tube with sample concentrations around 30 mg/ml in $CDCl_3$. All spectra were consistent with proposed polymer structures and no THF peak was detected. Absolute number average molecular weights (Mn) were measured by gel permeation chromatography (GPC) in THF at 25 $^{o}C$ on a Viscotek GPCmax from Malvern instruments coupled with a triple detector array TDA305 (static light scattering, differential refractometer and intrinsic viscosity). Acid value (AV - reported in mg of KOH/ g of polymer sample) for all polymers were measured by titration method ASTM D-974 which was modified by using potassium hydrogen phthalate (KHP) in place of hydrochloric acid, and phenolphthalein as indicator in place of methyl orange**.** Glass transition temperature (Tg) was measured on TA Instruments Q2000 by means of Modulated-Differential Scanning Calorimeter (DSC) method at a scan rate of 10 $^{o}C$/min.

### 3.4 Water-reduction of polymers to form CUPs

Polymers were dissolved in a low boiling water miscible solvent, THF (20% w/w) and stirred overnight. The acid groups were neutralized with triethyl amine; de-ionized water was added by a peristaltic pump at the rate of 1.24g/minute and the pH of solution was maintained between 8.3-8.7 using triethylamine. After the water was added, the THF was stripped off under vacuum, giving CUPs in VOC free aqueous solution, except for

the added base, at the desired concentration. It should be noted that ammonium hydroxide works equally well and further reduces the VOC.

*Water-reduction process for the polymer J-31*: Polymer J-31 (0.0174 moles, 20 g) was dissolved in THF (80 g) to make a 20% w/w solution; the acid groups were neutralized with triethylamine (0.006 moles, 0.61 g); and de-ionized water (80 g) was added by means of a peristaltic pump after which the THF was stripped off under vacuum to give a 20% solution of CUPs in water. The CUP solutions were then filtered through a 0.45μm Millipore membrane to remove any foreign materials that were typically measured to be less than 0.05% by weight. *Figure* 2 depicts the process of CUP particles formation. It was found that the ratio of water to THF used was critical since the collapse from a random coil into a hard sphere can create a poly-chain particle instead of a CUP particle due to chain-chain entanglement if the collapse occurs at a high concentration.

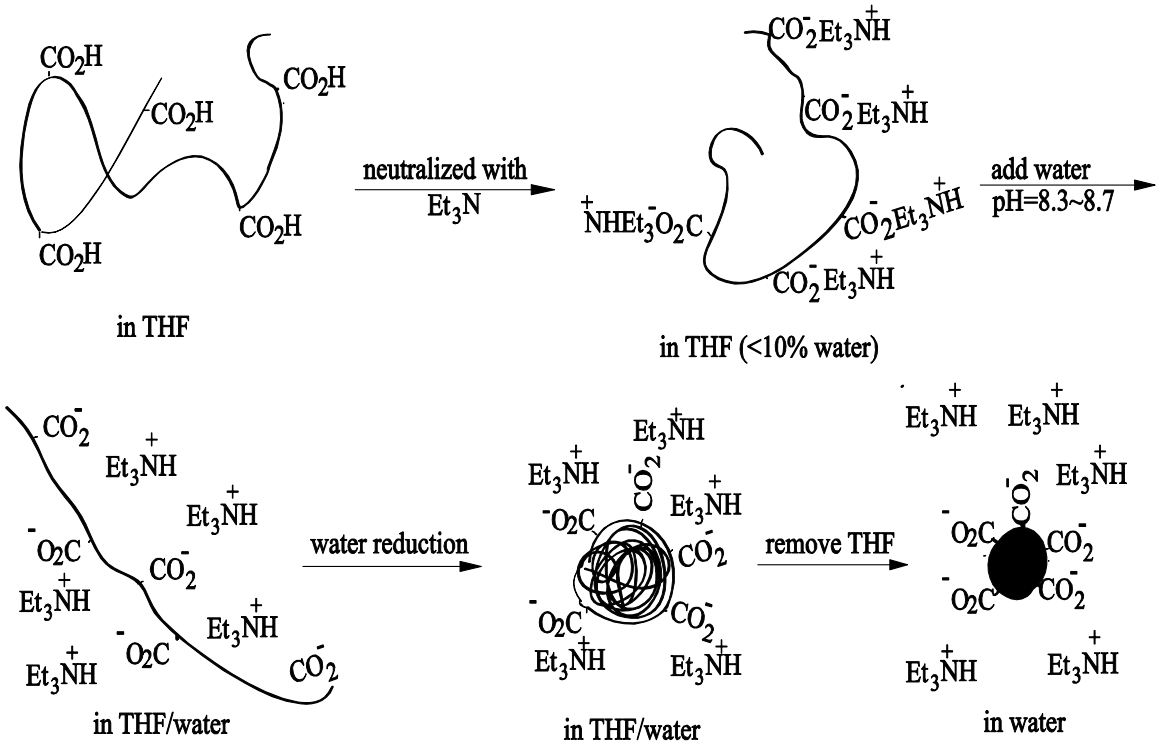


**Figure 2.** Process of formation of CUP particles

### 3.5 Characterization of CUPs

After the water reduction process, viscosity measurements were done by Ubbelohde viscometer method at 25 $^{o}$C and 30 $^{o}$C for use in measuring the particle size and reported in the units of centiStokes. The viscosity of 10% CUP solution in water was done at 25 $^{o}$C on a Brookfield Rheometer model DV-III at a shear rate of 112.5 $sec^{-1}$ and reported in centipoise. Particle sizes were measured by dynamic light scattering on a Nanotrac 250 particle size analyzer from Microtrac with a laser diode of 780 nm wavelength, and 180° measuring angle. The principle for the particle size measurement was that the particles in solution were constantly moving due to collisions by the solvent molecules, which is called Brownian motion. If the particles or molecules are illuminated with a laser, the intensity of the back scattered light that strikes the detector is Doppler shifted, and is dependent upon the size of the particles. The $^{1}$H NMRs were recorded on a Varian 400 MHz FT/NMR spectrometer in a 5 mm outer diameter thin-walled glass tube with sample concentrations around 10 mg/ml in $D_2O$ and no THF peak was observed. Minimum Film Formation Temperature (MFFT) was measured on a Rhopoint WP-Bar90 as per the method described in ASTM D-2354.

### 3.6 CUP coatings

The CUPs were prepared at 20% solids in water and cured by means of an aziridine for evaluating the coating characteristics of the clear coat CUPs. The cross-linker was used in a 1:1 ratio of the acid equivalent of the resin. The aziridine used to cure CUP clear coats was CX-100, obtained from DSM Resins with a functionality of 3, *Figure 3*. The aziridine was added just prior to application and used after 30 minutes to simulate use conditions. The coated samples were dried for 24 hours at ambient

conditions. As the MFFT of J-31 and J-32 was higher than room temperature, Texanol obtained from Eastman chemicals was used as a coalescing aid to lower the MFFT for the aziridine cure. After addition of Texanol at 3% w/w of the total formulation, the MFFT of J-31 and J-32 was found to be lowered to 18.6 $^{o}$C.

*CUP coatings from J-31*: For 100 g of water reduced resin, 2.80 g (0.006 moles) of CX-100 was added along with 3 g of Texanol (3% w/w on total formulation).

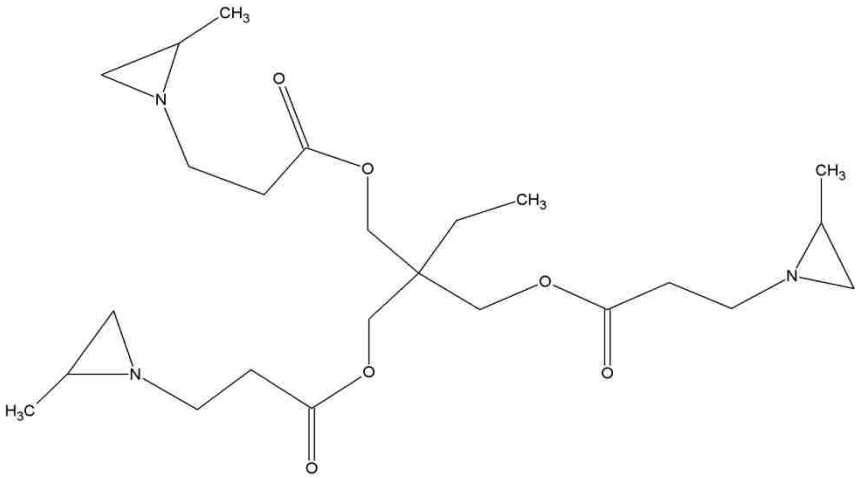


**Figure 3.** Trimethylolpropane tris(2-methyl-1-aziridinepropionate)

### 3.7 Testing of the CUP clear coats

Aluminum panels A-36 mill finish and iron phosphated steel panels R-36 dull matte finish from Q-panel were used to test CUP clear coats. The aziridine cured coatings were ambient cured for 24 hours and aged at 50 $^{o}$C for 24 hours to accelerate aging. The CUP clear coats were tested for their mechanical dry time, appropriate ratio of aziridine to acid for effective curing of CUPs, pot-life at constant temperature, MEK resistance, adhesion, hardness, gloss, flexibility, abrasion and impact resistance properties. The controls used for the testing protocol were the CUP clear coats cast on panels without any crosslinker. Mechanical dry time was measured as per ASTM D-5895 by means of a

Gardener dry time recorder. The ratio of aziridine: acid, based on the equivalent weight, was varied from 0.5:1, 0.75:1, 1:1, 1.25:1 and 1.5:1 to find out the appropriate ratio required for effective cure of CUPs. To determine the pot-life, samples were stirred for 30 min. and kept in a constant temperature water bath at 25 $^{o}$C after which drawdowns were casted every 15 minutes for the next 2 hours. The results of MEK double-rubs and pencil hardness were evaluated to determine the pot-life and the effective ratio of aziridine: acid for total cure of CUPs. All other CUP coatings were formulated at aziridine: acid ratio of 1:1. Gloss was measured on aluminum panels by a Byk-Gardener micro-gloss meter and an average of 3 readings with std. deviation less than 1 were recorded at 3 angles: 20$^{o}$, 60$^{o}$ and 85$^{o}$. MEK double rub test were performed on aluminum panels by employing a lint-free cloth as per ASTM method D-4752 and an average of 2 readings was reported. Pencil hardness test were performed on aluminum panels as per the ASTM method D-3363 by using pencils of varying hardness in the range of 9B-9H and an average of 3 readings was reported. Film thickness was measured on aluminum panels by a coating thickness gauge by Elcometer-6000 Positector and an average of 3 readings was reported in mil. Impact testing was done on iron phosphate steel Q-panels as per ASTM D-2794 using Gardner Impact Tester with a 5/8 inch ball indenter of 4-lb weight and results were reported in units of inch-lbs. Flexibility was tested on aluminum Q-panels by mandrel test method as per ASTM D-522. Adhesion testing was done as per the ASTM D-4541 on iron phosphate steel Q-panels by prepping the coatings with sandpaper # 320, wiping with iso-propanol, air-drying for 1 hour and gluing the grit-blasted and MEK-cleaned pucks onto the coating with a Locktite Quick Set 2-ton epoxy, and allowed to cure for 48 hours after which a torque wrench

ComputorQ-II was used instead of a pull-off tester to record the failure type and the torque value. The torque displayed in inch-pound units was recorded in PSI units by appropriate conversion and an average of 4 readings was reported. Wet adhesion testing was done by immersing 1/3$^{rd}$ part of the aluminum panels in deionized water for 1 hour and then inspecting the panels for delamination, change in clarity/transparency, etc. Pencil hardness was also done after exposure on those panels. Abrasion resistance testing was performed on 4" x 4" iron phosphate steel panels R-44 dull matte finish from Q-panel by using a Taber Abraser 5150 with a load weight of 1000g for 100 cycles utilizing H-10 wheels as per the ASTM D-4060.

# 4. RESULTS AND DISCUSSION

## 4.1 Polymer syntheses & characterization

The initial study investigated four polymers, two of low Tg, below room temperature, and two of high Tg, above room temperature. For both the polymers, two molecular weights were chosen: one high ~50,000 and the other a lower molecular weight ~20,000. The molecular weights chosen here are only examples. The monomer composition can also be varied. Polymers with molecular weights ranging from 6000 to 130,000 have been successfully reduced to form CUPs.

The monomers methacrylic acid (MAA), butyl methacrylate (BMA), ethyl acrylate (EA), ethyl methacrylate (EMA) and 2-ethylhexyl methacrylate (2-EHMA) were chosen in the particular composition specified to yield polymers with specified Tg. The actual acid value of the synthesized polymers was found to be slightly higher than the theoretical acid value as expected, because a part of the monomer MMA was lost with

nitrogen purging through evaporation with solvent during polymer synthesis, *Table* 2. Good yields are reported for all the polymers synthesized.

**Table 1: Monomer Composition, MAA: Acrylate Ratio, Tg and Mol. Wt. of the Synthesized Polymers**

| Polymer Synthesized | Monomer Composition | MAA: acrylate Ratio | Glass Transition Temp. (Tg/$^{o}$C) | Molecular Weight (Mn) |
|---|---|---|---|---|
| J-31 | MAA:BMA:EMA | 1:8 | 55.1 | 19,000 |
| J-32 | MAA:BMA:EMA | 1:8 | 54.9 | 50,000 |
| J-51 | MAA:BMA:EA:2-EHMA | 1:7 | 21.3 | 21,000 |
| J-52 | MAA:BMA:EA:2-EHMA | 1:7 | 20.9 | 51,000 |

**Table 2: Polymer Characterization: % Yield, Tg, Mol. Wt, Acid Value and Mark-Houwink Parameters in THF**

| Polymer Synthesized | % Yield | Acid Value | | Mark-Houwink "a" | Mark-Houwink “log K” |
|---|---|---|---|---|---|
| | | Theo. | Expt. | | |
| J-31 | 89 | 48.7 | 48.8 | 0.65 | -3.69 |
| J-32 | 93 | 48.7 | 48.7 | 0.68 | -3.88 |
| J-51 | 91 | 50.9 | 52.5 | 0.70 | -3.97 |
| J-52 | 93 | 50.9 | 51.7 | 0.64 | -4.37 |

The MFFT of the synthesized polymers were found to be lower than the Tg as is typical for waterborne resins, *Table* 3. The viscosity of water-reduced CUPs was water-like and the actual/measured particle sizes were close to the theoretical particle size indicating the true nano-scale characteristics of the synthesized CUPs. As seen from *Figure 4*, the viscosity profile of CUPs, as measured by a Brookfield rheometer, was

linear for the sq. rt. of shear rate vs sq. rt. of shear stress with a slope of 0.1456. Therefore, zero point viscosity at 25 $^{o}$C was 2.12 cP. This corroborates with the results of kinematic viscosity, measured by an Ubbelohde viscometer, that the viscosity of water-reduced CUPs were water-like.

**Table 3: Viscosity, Particle Size, Tg and MFFT of the Water-Reduced CUPs**

| Polymer Synthesized | Kinematic Viscosity (cSt) | Visc. at shear rate of 112.5 (cP) | Particle Size (nm) | | Avg. MFFT ($^{o}$C) |
|---|---|---|---|---|---|
| | | | Theo. | Expt. | |
| J-31 | 2.19 | 2.31 | 3.7 | 4.0 | 45.2 |
| J-32 | 2.51 | 3.96 | 5.1 | 4.5 | 45.5 |
| J-51 | 2.45 | 2.57 | 3.8 | 3.1 | 2.5 |
| J-52 | 3.13 | 3.82 | 5.1 | 4.7 | 2.4 |

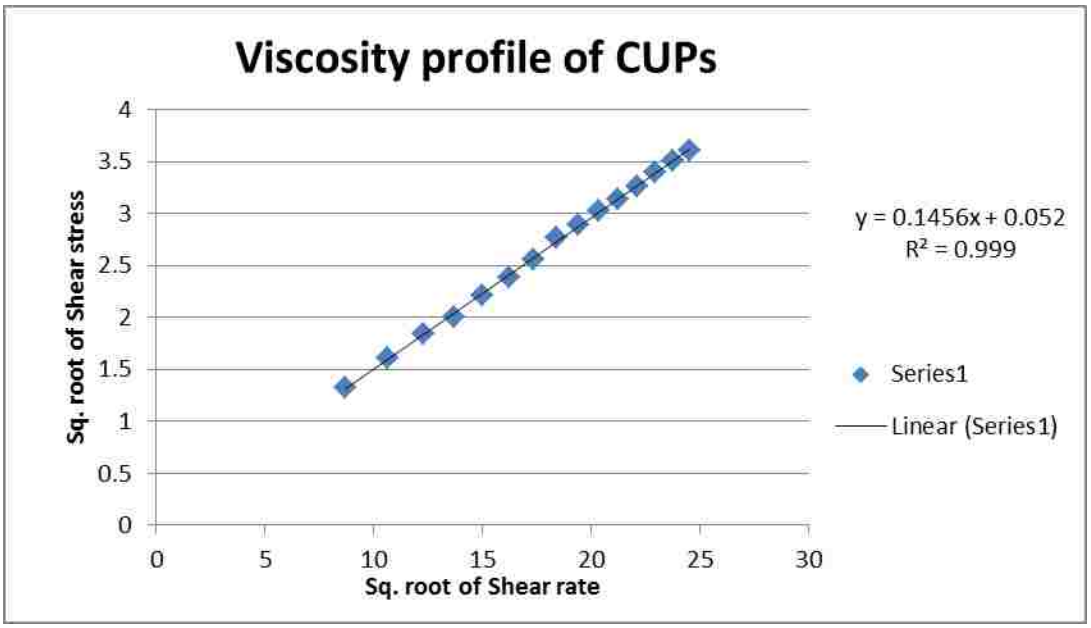


**Figure 4.** Viscosity of 10% solution of CUP J-32 in water at 25 $^{o}$C

The four synthesized polymers were analyzed for comparison between the theoretical particle size calculated from the GPC fractions at different molecular weights and the actual/experimental particle size as found via DLS. As seen from *Figure 5*, there

was a good agreement between the distribution calculated from the molecular weights of fractions from the GPC and the particle diameters from DLS, assuming the density of the bulk polymer were the same as that of CUPs. The presence of THF, if not stripped off completely, influences the measured diameter of the CUPs as it can migrate into the interior of the CUP particles and give a larger diameter than expected due to swelling. However, NMR was employed in this research to verify the removal of THF. It should be noted that water must be added in a slow gradient during reduction to avoid regional large solvent compositional changes. If they occur, coagulum may be formed resulting in a cloudy solution due to large aggregates. The water must also be free of polyvalent cations like calcium or magnesium which can bind to the carboxylates and cause gelling. If performed correctly, the solution appears water-clear as evident from *Figure 6*.

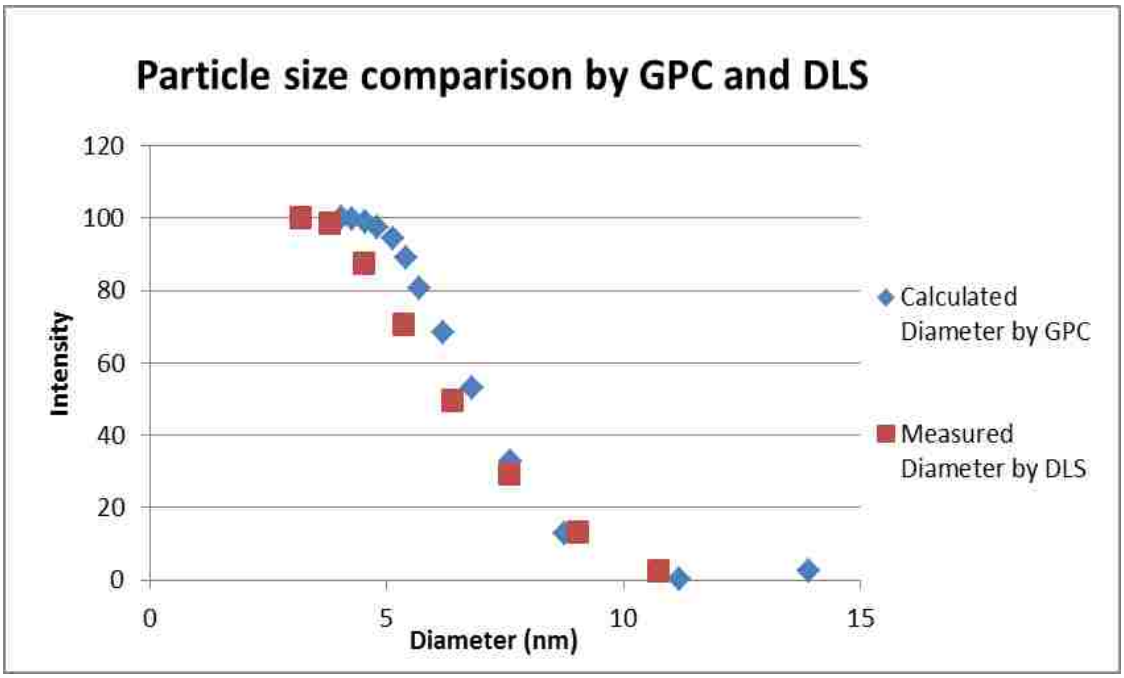


**Figure 5.** Particle size comparison by GPC and DLS for polymer J-32


**Figure 6**. Vial 1: improperly water-reduced CUPs; Vial 2: properly water-reduced CUPs

### 4.2 Aziridine cured CUPs

Mechanical dry time study was conducted to determine the drying stages of film formation for the CUP clear coats. As evident from *Table* 4, the process of drying of the CUPs was complete around 3 hours and gave an idea of when a freshly painted surface can be put back to use. The low molecular weight polymers are expected to have a slightly faster drying time as compared to the higher molecular weight polymers owing to their faster reptational motion but no such demarcation was observed due to the aziridine crosslinking of the CUP clear coats. It should be noted that full aziridine cure will require additional time past through dry.

**Table 4: Mechanical Dry Time (min.) of Aziridine Cured CUPs as per ASTM D-5895**

| Polymer Synthesized | Cure Type | Set-to-touch time | Tack-free time | Dry hard time | Dry through time |
|---|---|---|---|---|---|
| J-31 | Control | 53 | 105 | 145 | 190 |
| | Aziridine | 55 | 110 | 145 | 195 |
| J-32 | Control | 55 | 105 | 145 | 190 |
| | Aziridine | 57 | 110 | 145 | 195 |
| J-51 | Control | 53 | 100 | 150 | 195 |
| | Aziridine | 50 | 100 | 140 | 180 |
| J-52 | Control | 51 | 100 | 150 | 195 |
| | Aziridine | 51 | 100 | 140 | 180 |

The ratio of aziridine: acid based on the equivalent weight was varied from 0.5:1, 0.75:1, 1:1, 1.25:1 and 1.5:1 to find out the appropriate ratio required for effective cure of CUPs. The performances of the samples were evaluated on the basis of their pencil hardness and MEK double rubs. As seen from *Table* 5 and *Figure 7*, it was evident that the optimum ratio of aziridine: acid for the effective cure of acrylic colloidal unimolecular polymers was about 1.25:1. An aziridine with a functionality of 3 was used for the study, but some of the molecules might be bi-functional. If the aziridine: acid ratio is greater than 1.25:1, the excess aziridine will only be able to link one tri-aziridine with a carboxylate group on all polymer chains which decreases the crosslink density. Again, the excess aziridine reacts with water to form an aminoalcohol. These two factors can substantially lower the performance of the CUP clear coats. At the aziridine: acid ratio of 1.25:1, the slight excess of aziridine ensures that even if one of the three aziridine

functionality was hydrolyzed, the other two will be available for crosslinking, thus giving a highly crosslinked coating with excellent performance.

**Table 5: Effect of Aziridine: Acid Ratio on Pencil Hardness and MEK Double-Rubs**

| Polymer Synthesized | Aziridine: Acid Ratio | Pencil Hardness |
|---|---|---|
| J-31 | 0.5 : 1 | B |
| | 0.75: 1 | HB |
| | 1.00 : 1 | F |
| | 1.25 : 1 | H |
| | 1.5 : 1 | F |
| J-32 | 0.5 : 1 | B |
| | 0.75 : 1 | B |
| | 1.00 : 1 | B |
| | 1.25 : 1 | H |
| | 1.5 : 1 | H |
| J-51 | 0.5 : 1 | B |
| | 0.75 : 1 | F |
| | 1.00 : 1 | F |
| | 1.25 : 1 | H |
| | 1.5 : 1 | HB |
| J-52 | 0.5 : 1 | B |
| | 0.75 : 1 | HB |
| | 1.00 : 1 | F |
| | 1.25 : 1 | H |
| | 1.5 : 1 | F |

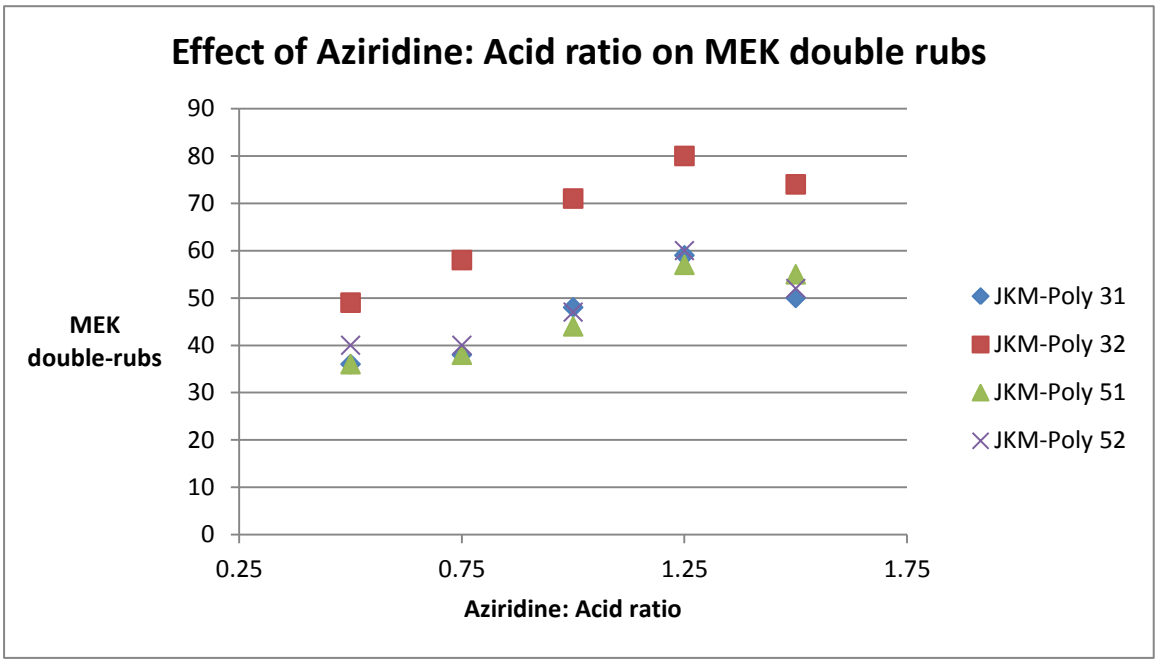


**Figure 7.** Graph depicting the effect of aziridine: acid ratio on MEK double-rubs

It is important to know the time frame in which the CUP coatings can be used after they are mixed with the aziridine crosslinker. The pot life study gives an estimate of the time after which the crosslinker becomes less effective. It is evident from *Table 6* that the pot-life of aziridine cured acrylic colloidal unimolecular polymers were at least 120 minutes, after which the samples start to have lower performance. Even though aziridines are reactive compounds, the conditions for the nucleophile to attack on the aziridine ring are not conducive until the water leaves and therefore it takes some time for the crosslink density to gain optimal strength which was reflected in the performance of the coatings during MEK double-rubs and pencil hardness. One possible rational for the increase in performance during the first 120 min. maybe a pre-equilibrium partitioning of the aziridines between the CUP interior and the water phase. Further investigations would be required to fully validate this possibility. The data clearly shows that the usable pot life was over 2 hours with only about a 20% loss of performance in 2.5 hours.

**Table 6: Pot-Life Study for Aziridine Cure of Acrylic CUPs**

| Polymer Synthesized | Pot-life time (min.) | Pencil Hardness | MEK double-rubs |
|---|---|---|---|
| J-31 | 30 | HB | 47 |
| | 45 | HB | 48 |
| | 60 | F | 46 |
| | 75 | F | 48 |
| | 90 | H | 56 |
| | 105 | H | 49 |
| | 120 | H | 47 |
| | 135 | H | 47 |
| | 150 | HB | 39 |
| J-32 | 30 | HB | 72 |
| | 45 | F | 70 |
| | 60 | F | 73 |
| | 75 | H | 71 |
| | 90 | H | 75 |
| | 105 | H | 69 |
| | 120 | H | 68 |
| | 135 | H | 65 |
| | 150 | HB | 60 |
| J-51 | 30 | HB | 42 |
| | 45 | HB | 44 |
| | 60 | F | 43 |
| | 75 | H | 44 |
| | 90 | H | 56 |
| | 105 | H | 50 |
| | 120 | H | 50 |
| | 135 | H | 40 |
| | 150 | F | 39 |

| | | | |
|---|---|---|---|
| J-52 | 30 | F | 37 |
| | 45 | F | 39 |
| | 60 | H | 47 |
| | 75 | H | 47 |
| | 90 | H | 56 |
| | 105 | H | 45 |
| | 120 | H | 46 |
| | 135 | H | 41 |
| | 150 | F | 38 |

Pencil hardness is a measure of the hardness of the coating while the MEK double rub test is a measure of the solvent resistance and an estimate of the crosslink density of a coating. It was observed that the CUP clear coat made from high Tg polymer (J-31 & J-32) gave good gloss while the CUP clear coat made from low Tg polymer (J-51 & J-52) gave high gloss, *Table 7*. Coalescing aid was required in the high Tg polymer to lower its Tg and ease the process of film formation, but its presence can be the reason for the lower gloss of the high Tg polymers as compared to the high gloss of low Tg polymers. The lack of any crosslinker would render the coating a lacquer, thus resulting in lower hardness and solvent resistance as seen from the results of the control. It was observed that the MEK double rubs were moderate for all of the aziridine cured CUP clear coats, but higher compared to the controls indicating that crosslinking with aziridine gave better performance.

**Table 7: Film Thickness, Gloss, MEK Double Rubs and Pencil Hardness Results of the CUP Clear Coats**

| Polymer Synthesized | Cure type | Film thickness(mil) | Gloss $20^o$ / $60^o$ / $85^o$ | MEK double rubs | Pencil Hardness |
|---|---|---|---|---|---|
| J-31 | Control | 0.5 | 81 / 83 / 90 | 5 | B |
| | Aziridine | 0.6 | 81 / 82 / 89 | 48 | H |
| J-32 | Control | 0.5 | 87 / 91 / 93 | 7 | B |
| | Aziridine | 0.5 | 86 / 90 / 92 | 71 | H |
| J-51 | Control | 0.7 | 90 / 93 / 97 | 5 | B |
| | Aziridine | 0.8 | 90 / 94 / 98 | 44 | H |
| J-52 | Control | 0.5 | 90 / 94 / 97 | 7 | B |
| | Aziridine | 0.5 | 89 / 91 / 95 | 47 | H |

As evident from *Table 7*, crosslinking the Colloidal Unimolecular Polymers gave a significant boost to the performance characteristics of the resin, as measured by the MEK double rubs and pencil hardness. In the CUP system, the carboxylates are on the surface of the particle and thus are all easily accessible to the aziridine for crosslinking. Thus, the CUP particles do not require extensive reptational motion to access the aziridine, nor to coalesce.

All formulated CUP clear coats had excellent flexibility and impact resistance, *Table 8*. CUP dispersions require less diffusion time since the distance of migration is only 3-5 nm and therefore, it can access the crosslinking agent without the need for penetration into a larger particle, thereby accelerating the film formation process.

**Table 8: Mandrel Flexibility and Impact Resistance Results of the Clear Coats Formulated from CUPs**

| Polymer Synthesized | Cure type | Mandrel [inch] | Impact (forward) [inch-Lbs.] | Impact (reverse) [inch-Lbs.] |
|---|---|---|---|---|
| J-31 | Control | 1/8” | 160+ | 160+ |
| | Aziridine | 1/8” | 160+ | 160+ |
| J-32 | Control | 1/8” | 160+ | 160+ |
| | Aziridine | 1/8” | 160+ | 160+ |
| J-51 | Control | 1/8” | 160+ | 160+ |
| | Aziridine | 1/8” | 160+ | 160+ |
| J-52 | Control | 1/8” | 160+ | 160+ |
| | Aziridine | 1/8” | 160+ | 160+ |


**Figure 8**. High impact resistance and flexibility of aziridine cured CUP clear coatings

*Table* 8 and *Figure 8* are evidence of the high flexibility and impact resistance of the resin developed. It was observed that the aziridine cured CUP clear coats had both

coating, as well as epoxy-amine, adhesive failure indicating good adhesion of the polymeric film to the substrate, *Table 9*.

**Table 9: Adhesion Testing Results of the Clear Coats Formulated from CUPs**

| Polymer | Cure type | Avg. Torque (PSI) | Failure of | Failure type | % Failure |
|---|---|---|---|---|---|
| J-31 | Control | 810 | Coating to substrate | Adhesive | 100% |
| | Aziridine | 1055 | Coating+Epoxy | Adhesive | 90: 10% |
| J-32 | Control | 1021 | Coating to substrate | Adhesive | 100% |
| | Aziridine | 984 | Coating+Epoxy | Adhesive | 90 : 10% |
| J-51 | Control | 838 | Coating to substrate | Adhesive | 100% |
| | Aziridine | 859 | Coating+Epoxy | Adhesive | 90: 10% |
| J-52 | Control | 1065 | Coating to substrate | Adhesive | 100% |
| | Aziridine | 927 | Coating+Epoxy | Adhesive | 90: 10% |

No significant change was observed on any of the polymeric films after a 1 hour water immersion. The aziridine crosslinked CUP clear coats showed no hazing and no change in pencil hardness, *Table 10*. It was observed that the wear index of control was usually high indicating low abrasion resistance while no trend was observed in the wear index of aziridine cured CUPs indicating moderate abrasion resistance of the clear coats formulated from CUPs, *Table 11*. This corroborates that crosslinking the CUPs with aziridine enhances its performance as a coating.

**Table 10: Wet Adhesion Test Results of the CUP Clear Coats**

| Polymer Synthesized | Cure type | Appearance/ Observations | Pencil Hardness |
|---|---|---|---|
| J-31 | Control | No change | B |
| | Aziridine | No change | H |
| J-32 | Control | No change | B |
| | Aziridine | No change | H |
| J-51 | Control | No change | B |
| | Aziridine | No change | H |
| J-52 | Control | No change | B |
| | Aziridine | No change | H |

**Table 11: Abrasion Resistance Test Results of the CUP Clear Coats**

| Polymer Synthesized | Cure type | mg lost/100 cycles | Wear Index |
|---|---|---|---|
| J-31 | Control | 39 | 390 |
| | Aziridine | 17 | 170 |
| J-32 | Control | 27 | 270 |
| | Aziridine | 10 | 100 |
| J-51 | Control | 22 | 220 |
| | Aziridine | 14 | 140 |
| J-52 | Control | 23 | 230 |
| | Aziridine | 13 | 130 |

## 5. CONCLUSION

The true nano-scale nature of CUPs can result in a well crosslinked acrylic clear coat. The coalescing mechanism for CUPs was similar to latex and the effect of

coalescent aid was found to be analogous. Aziridine cured CUP coatings produced well cross-linked films. This work illustrates the true nano-unimolecular nature of CUPs and its low viscosity. These near zero VOC systems (if ammonia is used) offer a potentially high performance technology option for future coatings for both OEM and architectural applications.

Over the past few years, the development of acrylic Colloidal Unimolecular Polymers (CUPs) has moved from the realm of laboratory investigation to the point today at which they can be tested and developed commercially in numerous applications. Thus, the utilization of aziridine curing agents for water-reduced acrylic CUPs have illustrated their usefulness and potential in such applications as clear floor finishes or clear topcoats.

## 6. ACKNOWLEDGEMENT

The authors would like to acknowledge the Missouri S&T Coatings Institute for the financial support and the following for CUP allied work: Cynthia Riddles, Minghang Chen, Sagar Gade, Ameya Natu and Catherine Hancock.

## 7. REFERENCES

1) Fernando, R., "Nanomaterial technology applications in coatings." *JCT Coatings Tech.*, **1** (5) 32-38 (2004).

2) Schaller, E. J., "Critical pigment volume concentration of emulsion based paints." *Journal of Paint Technology*, **40** (525) 433-438 (1968).

3) Craver, J. K., Tess, R. W., "*Applied Polymer Science*", Organic Coatings and Plastics division, American Chemical Society: Washington D. C. (1975).

4) Repenning, D., "Nanodispersed hardened chrome coatings. Variable properties for a wide range of applications." *Galvanotechnik* **91** (10) 2878-2883 (2000).

5) Myers, D., *Surfactant Science and Technology*, 3rd ed.; John Wiley and Sons: New Jersey (2006).

6) Morishima, Y., Nomura, S., Ikeda, T., Seki, M., Kamachi, M., "Characterization of unimolecular micelles of random copolymers of Sodium 2-(acryamido)-2-methylpropanesulfonate and methacrylamides bearing bulky hydrophobic subtituents." *Macromolecules* **28** (8) 2874-2881 (1995).

7) United States Patent No. 5,369,152 assigned to Reichhold Chemicals, Inc.

8) Klempner, D., Frisch, K., *Advances in Urethane Science and Technology;* Smithers Rapra Press (2001).

9) Saravari, O., Phaphant, P., Pimpan, V., "Synthesis of water reducible acrylic-alkyd resins based on modified palm oil." *Journal of Applied Polymer Science*, **96** (4) 1170-1175 (2005).

10) Riddles, C. J., Hua-Jung Hu, W. Z., Van De Mark, M. R., **"**Colloid unimolecular polymers (CUPs) synthesized by random copolymerization of MMA/MAA"; *Polymer Preprints,* **52** (2) 232-233 (2011).

11) Chen, M., Van De Mark, M. R., "Rheology studies on colloidal unimolecular polymer (CUP) particles in absence and presence of NaCl"; *Polymer Preprints*, **52** (2) 336-337 (2011).

# IV. MELAMINE CURE OF COLLOIDAL UNIMOLECULAR POLYMERS (CUPs)

**Jigar K. Mistry and Michael R. Van De Mark***

*Missouri S&T Coatings Institute & Department of Chemistry,*
*Missouri University of Science & Technology, Rolla, MO-65409, USA.*

**(Submitted for publication as an Article in the *Journal of Applied Polymer Science)***

## 1. GRAPHICAL ABSTRACT

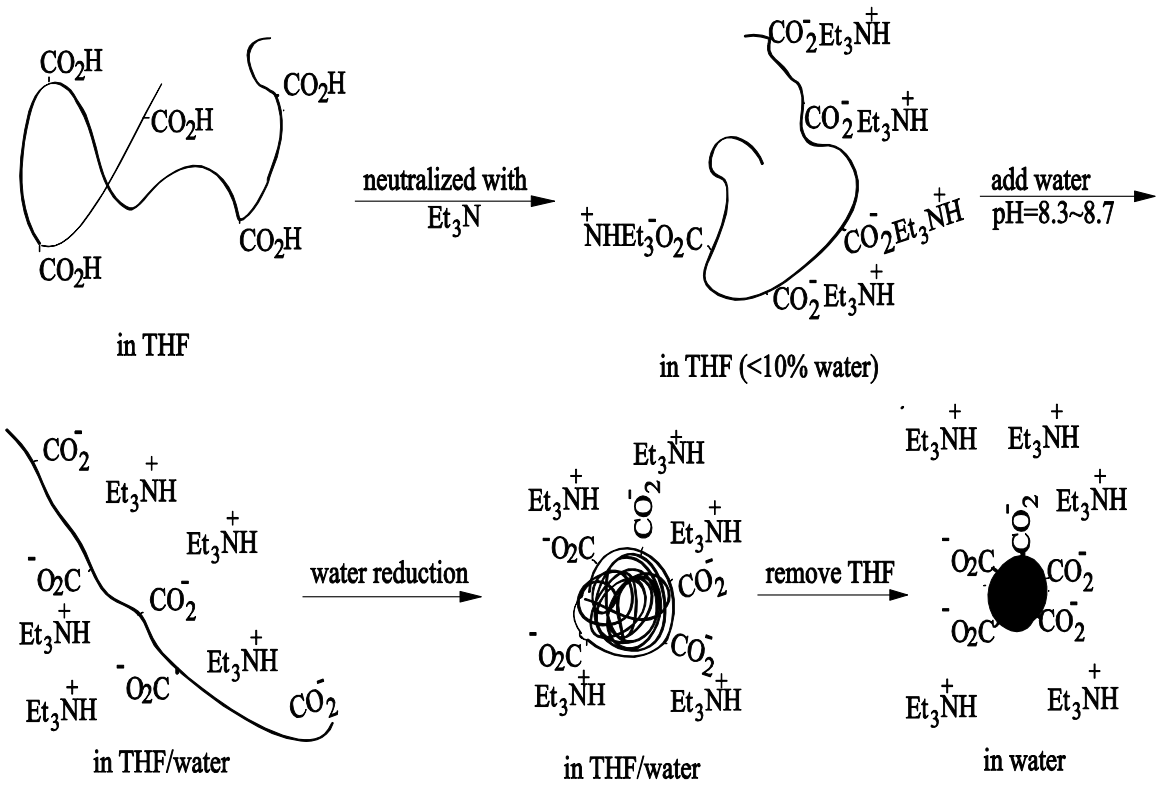


**Process of forming CUPs**

*Corresponding author: *mvandema@mst.edu*

## 2. ABSTRACT

Polymers were synthesized with a 1:7 or 1:8 ratio of acrylic acid to acrylic ester monomers to produce an acid rich resin. The polymers were water-reduced and solvent stripped to produce Colloidal Unimolecular Polymers (CUPs). These particles are typically 3-9 nanometers in diameter depending upon the molecular weight and have different rheological behavior from micelles, polyeletrolytes, $C_{60}$ or latex due to their charged surface and large surface areas. They were then formulated into a clear coating with melamine as the cross linker with thermal curing. These melamine cured acrylic CUPs were solvent free and near zero VOC. The coatings were evaluated for their MEK resistance, adhesion, hardness, gloss, flexibility, abrasion and impact resistance properties.

**Keywords:** Colloidal Unimolecular Polyer, CUP, Melamine, Water-reduction, Zero VOC, Acrylic polymer.

## 3. INTRODUCTION

Water-reducible resins typically used in the coatings industry are composed of particles containing multiple chains entangled onto each other due to the high concentration of polymer when it. This research article uses a water reduction process which is conceptually similar except that the collapse of the chains is unimolecular due to the low concentration of polymer at reduction point and that the solvent is stripped off

leaving the particles suspended in water to give the final resin as a product which can be crosslinked to give films with superior properties.

When multiple chain polymers containing blocks of both hydrophilic and hydrophobic regions are placed in an aqueous environment at an adjusted pH, the hydrophilic polyether ester portions of the chains orient into the water phase such that they leave the hydrophobic region in the interior domain, forming macromolecular polymeric micelles with an average diameter of 50-120 nm; larger than typical micelles of 2-10 nanometers or roughly twice the diameter of the hydrocarbon chain[1]. In a study by Morishima, the micelle behavior of a single polyelectrolyte chain was observed to be "self-assembled" in a poor solvent when the chain collapsed and the chains collapsed into unimolecular micelles of a diameter of approximately 5.5 nm[2]. Multiple chain polymer collapse has also been observed in waterborne urethane resins synthesized by reaction of iso-cyanate by Reichhold when acetone was removed from the resin water blend, causing the chains to collapse into aggregates with a diameter of approximately 25 nm[3,4]. Water-reducible resins containing ionizable carboxylic acid groups neutralized with amines were synthesized in another study and dissolved in high boiling, water miscible solvents after which water was introduced into the system, until the solvent blend became a less-than theta solvent condition which caused the entangled polymer chains to collapse[5].

The term Colloidal Unimolecular Polymer[6] (CUP) has been introduced to describe the solid spherical unimolecular particles suspended in the continuous aqueous phase. CUPs contain a hydrophobic backbone and hydrophilic group such as carboxylic acid salts. The process by which these are formed is basically water reduction with subsequent removal of a volatile water loving solvent. Therefore, the CUP solution can

be VOC free. The collapsed CUP particles resemble a sphere due to the repulsive nature of the carboxylate groups towards each other. Unlike the larger latex particles which settle with time, CUP particles are thermodynamically stable due to the nano-scale particle size as Brownian motion keeps the CUP particles. No change in particle size and aggregation/settling is observed in the samples of the reduced cup particle suspensions retained for over three years. This research paper explores the synthesis of acrylic colloidal unimolecular polymers in true nano-scale range (less than 10nm) with particular emphasis on coating performance enhancements offered by the melamine cure of the polymeric films.

In this study, colloidal unimolecular polymers (CUPs) were synthesized in THF using acrylic monomers by free radical polymerization. Four polymers were investigated: two of low Tg, below room temperature, and two of high Tg, above room temperature. For both the polymers, two molecular weights were chosen: one high ~50,000 and the other a lower molecular weight ~20,000. The low molecular weight would require crosslinking to obtain any respectable physical properties whereas the higher molecular weight would have marginal lacquer performance. THF was selected as the primary solvent due to its good solvency for acrylics, its miscibility with water and low boiling point allowing it to be easily stripped off after water reduction without loss of significant amount of water. The hydrophobic/lipophilic balance requires that the acid monomer to ester ratio be between 1:7 and 1:8. This ratio yields a monomolecular reduction to the CUP particles. If less acid groups are incorporated, aggregation was observed. Triethylamine was added to neutralize the carboxylic acid groups on the synthesized polymers during water reduction. Bases like NaOH and KOH cannot be used for

neutralization as they do not leave any free acid groups on the polymer and tend to leave the cations behind during the process of drying. Ammonium hydroxide can be used for neutralization as it can react with the free formaldehyde content of the melamine during the cross-linking process. Thus, triethylamine was chosen for this study. Water is added slowly during water reduction to avoid a large regional solvent composition change which causes the formation of more coagulum which leads to visible cloudiness indicating large aggregates. A modest stirring rate is essential for avoiding any regional solvent composition change. The synthesized acrylic CUP resins will give the performance of a lacquer without a crosslinker and therefore to enhance the performance, a commercially available melamine (Cymel 373 from Cytec Industries Inc.) with an assumed functionality of 4.5 is chosen. The aforementioned acrylic CUP resin crosslinked with melamine is a zero VOC coating system, excluding the amine.

*Figure 1* illustrates the two conventional small coatings resin particles represented by a latex and a typical waterborne urethane resin. The third particle in the series is the Colloidal Unimolecular Polymer[6] particle which is the topic of this report. These are single polymer chains which are collapsed and suspended in water. Their size allows them to be a thermodynamically stable in water[7].

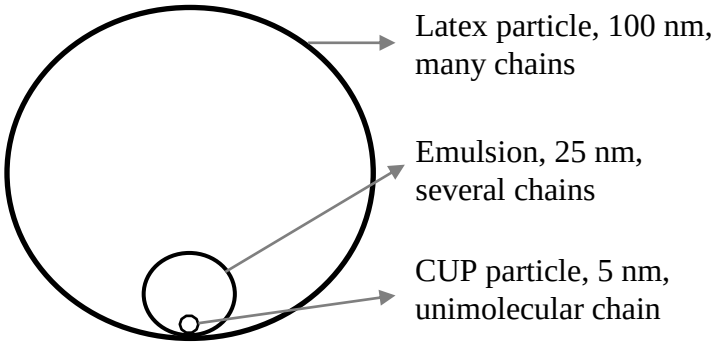


**Figure 1.** Particle size comparison for water borne particulate coating resins.

# 4. EXPERIMENTAL

## 4.1 Materials

Methacrylic acid (MAA), butyl methacrylate (BMA), ethyl acrylate (EA), ethyl methacrylate (EMA), 2-ethylhexyl methacrylate (2-EHMA), 2,2′-azobis(2-methylpropionitrile) (AIBN) and 1-dodecanethiol were obtained from Aldrich. MAA was purified by distillation with copper (I) bromide under vacuum. All other monomers were purified by washing with a 10% (w/w) solution of sodium bicarbonate, followed by rinsing with de-ionized water, and brine after which the solution was filtered after drying over sodium sulfate and purified by distillation under nitrogen with Copper (I) bromide as an inhibitor. The initiator AIBN was recrystallized before use from methanol while 1-dodecanethiol was used as received.

## 4.2 Polymer syntheses

All polymers were synthesized by free radical polymerization in tetrahydrofuran (THF). The monomer composition of polymers J-31 & J-32 was in molar ratios - MAA : EMA : BMA = 1 : 2.5 : 5.5 with the acid: acrylate ratio 1:8 while the monomer composition of polymers J-51 & J-52 was in molar ratios – MAA : EA : 2-EHMA : BMA = 1 : 1.5 : 1.5 : 4 with the acid: acrylate ratio 1:7. The monomer ratios were chosen such that two of those polymers would be above and two below room temperature for adequate evaluation of the polyacrylic resins synthesized. The molar ratio of dodecanethiol was varied to produce a low and a high range of molecular weight. The solvent THF was added in the amount of 2.5 times the total weight of monomers.

*Synthesis for polymer J-32*: The monomers, BMA (0.477 moles, 67.79 g), EMA (0.217 moles, 24.74 g) and MAA (0.0865 moles, 7.47 g) in a 1000 ml 3-neck round bottom flask with the initiator AIBN (0.781 moles, 0.094 g) along with chain transfer agent dodecanethiol (0.0011 moles, 0.257 g) and THF (250 g) were stirred. The flask was fitted with a nitrogen line, condenser, and a gas outlet adapter connected to an oil bubbler to allow a positive pressure of nitrogen throughout the polymerization process. The flask was heated slowly to reflux and allowed to react for 24 hours. The polymer solution was then cooled to room temperature, and precipitated in cold de-ionized water under high shear, then dried under vacuum. Polymers J-31, J-51 and J-52 were also synthesized as per the above mentioned protocol.

**4.3 Characterization of polymers synthesized**

The $^{1}H$ NMRs were carried out on synthesized polymers using a Varian 400 MHz FT/NMR spectrometer in a 5 mm outer diameter thin-walled glass tube with sample concentrations around 30 mg/ml in $CDCl_3$. All spectra were consistent with proposed polymer structures and no THF peak was observed. Absolute number average molecular weights (Mn) were measured by gel permeation chromatography (GPC) on a Viscotek GPCmax from Malvern instruments coupled with a triple detector array TDA305 (static light scattering, differential refractometer and intrinsic viscosity). Acid value (AV - reported in mg of KOH/ g of polymer sample) for all polymers were measured by titration method ASTM D-974 which was modified by using potassium hydrogen phthalate (KHP) in place of hydrochloric acid, and phenolphthalein as indicator in place

of methyl orange**.** Glass transition temperature (Tg) was measured on TA Instruments Q2000 by means of Modulated-Differential Scanning Calorimeter (DSC) method.

**4.4 Water-reduction of polymers to form CUPs**

Polymers were dissolved in a low boiling water miscible solvent, THF (20% w/w) and stirred overnight. De-ionized water was added by a peristaltic pump in the rate of 1.24g/minute and the pH of solution was maintained between 8.3-8.7. After the water was added, the THF was stripped off under vacuum, giving CUPs in VOC free aqueous solution, except for the added base, at the desired concentration. Ammonium hydroxide works equally well and makes this system even lower in VOC.

*Water-reduction process for the polymer J-32*: Polymer J-32 (0.0174 moles, 20 g) was dissolved in THF (80 g) to make a 20% w/w solution; the acid groups were neutralized with triethylamine (0.006 moles, 0.61 g); and de-ionized water (80 g) was added by means of a peristaltic pump after which the THF was stripped off under vacuum to give a 20% solution of CUPs. The CUP solutions were then filtered through 0.45μm Millipore membrane to remove any foreign materials which were typically measured to be less than 0.05% by weight. Polymers J-31, J-51 and J-52 were also water-reduced as per the above mentioned protocol. *Figure 2* depicts the process of forming CUPs. It was found that the amount of water used as well as the amount of THF was critical since if the collapse from a random coil into a hard sphere occurs at too high a concentration the particle becomes a poly-chain particle instead of a CUP due to the chain-chain entanglement.

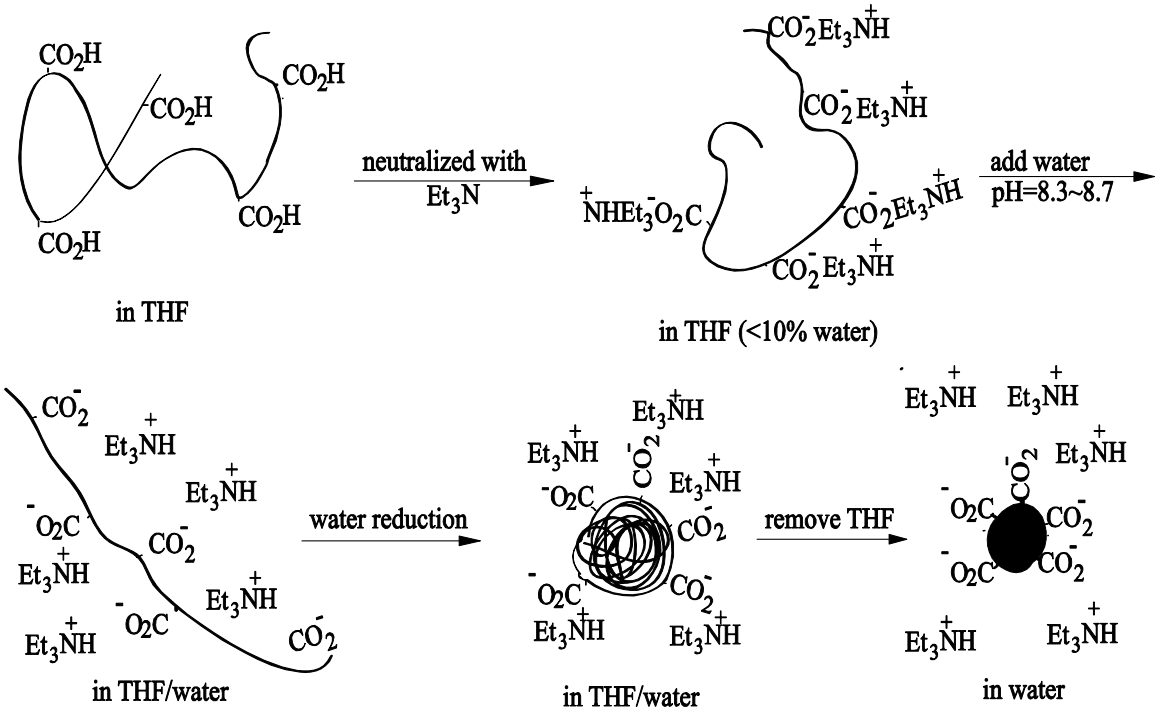


**Figure 2.** Process of forming CUP particles.

### 4.5 Characterization of CUPs

After the water reduction process, viscosity measurements were done by Ubbelohde viscometer method at 25 $^{o}$C and 30 $^{o}$C for use in measuring the particle size and reported in the units of centiStokes. The viscosity of 10% CUP solution in water was done at 25 $^{o}$C on a Brookfield Rheometer model DV-III at a shear rate of 112.5 and reported in centipoise. Particle sizes were measured by dynamic light scattering on a Nanotrac 250 particle size analyzer from Microtrac with a laser diode of 780 nm wavelength, and 180° measuring angle. The principle for the particle size measurement was that the particles in solution were constantly moving due to collisions by the solvent molecules, which is called Brownian motion. If the particles or molecules are illuminated with a laser, the intensity of the back scattered light that strikes the detector is Doppler shifted, and is dependent upon the size of the particles. The $^{1}$H NMRs were recorded on a

Varian 400 MHz FT/NMR spectrometer in a 5 mm outer diameter thin-walled glass tube with sample concentrations around 10 mg/ml in $D_2O$ and no THF peak was observed. Minimum Film Formation Temperature (MFFT) was measured on Rhopoint WP-Bar90 as per the method described in ASTM D-2354.

**4.6 CUP coatings**

The CUPs were prepared at 20% solids and cured by means of a melamine for evaluating the coating characteristics of the clear coat CUPs. The cross-linker was used in 1:1 ratio of the acid equivalent of the resin. The melamine used to cure CUP clear coats was Cymel-373 obtained from Cytec Industries Inc. and used as is. The functionality was assumed to be 4.5. The p-TSA catalyst used was Na-Cure 2547 which was obtained from King Industries Inc. and used as is.

*CUP coatings from J-32*: For 100 g of water reduced resin, 1.39 g (0.004 moles) of Cymel 373 was used along with 0.21 g (1% w/w of total solids of the formulation) of Na-Cure catalyst. The coated samples were cured at 300 F (~150 $^{o}$C) for 30 min.

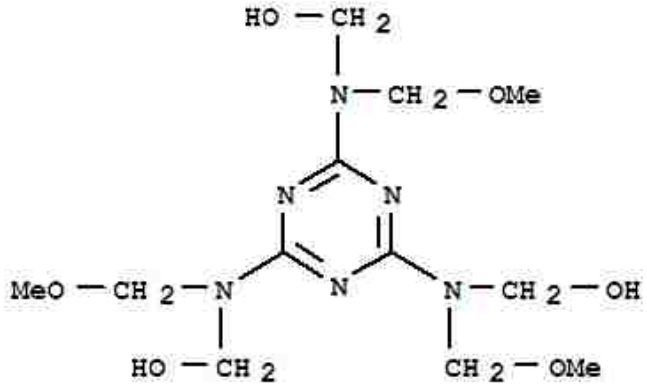


**Figure 3.** Modified melamine crosslinker.

**4.7 Testing of the CUP clear coats**

Aluminum panels A-36 mill finish and iron phosphate steel panels R-36 dull matte finish from Q-panel were used for the testing of CUP clear coats. The melamine cured CUP clear coats were baked at 300 $^{o}$F (150 $^{o}$C) for 30 min. and tested for the % active catalyst required for effective curing, optimum curing time and temperature, appropriate functionality of melamine required for effective curing, MEK resistance, adhesion, hardness, gloss, flexibility, abrasion and impact resistance properties. The controls used for the testing protocol were the CUP clear coats cast on panels without any crosslinker. The amount of catalyst was varied and the samples were cured at a fixed temperature (150 $^{o}$C) and time (30 min.) to find out the optimum % active catalyst required for effective curing. The curing time was varied as 10, 20, 30 and 40 min. at a fixed curing temperature (150 $^{o}$C) and % active catalyst (0.25% on resin solids) to find out the optimum time required for effective cure. The curing temperature was varied as 100, 125, 150 and 175 $^{o}$C at a fixed curing time (30 min.) and at 200 $^{o}$C for a curing time of 20 min. with fixed % active catalyst (0.25%) to find out the optimum temperature required for effective cure. The amount of melamine content required to cure the CUPs was changed by estimating a different functionality of melamine as 3.0, 3.5, 4.0, 4.5 and 5 to find out the appropriate amount of melamine (estimated functionality of melamine) required for effective curing of acrylic CUPs. Gloss was measured on aluminum panels by a Byk-Gardener micro-gloss meter and an average of 3 readings with std. deviation less than 1 were recorded at 3 angles: 20$^{o}$, 60$^{o}$ and 85$^{o}$. MEK double rub test was performed on aluminum panels by employing a lint-free cloth as per ASTM method D-4752 and an average of 2 readings was reported. Pencil hardness test were performed on

aluminum panels as per the ASTM method D-3363 by using pencils of varying hardness in the range of 9B-9H and an average of 3 readings was reported. Film thickness was measured on aluminum panels by a coating thickness gage by Elcometer-6000 Positector and an average of 3 readings was reported in mil. Impact testing was done on iron phosphate steel Q-panels as per ASTM D-2794 using Gardner Impact Tester with a 5/8 inch ball indenter of 4-lb weight and results were reported in units of inch-Lbs. Flexibility was tested on aluminum Q-panels by mandrel test method as per ASTM D-522 and results were recorded in inches. Adhesion testing was done as per the ASTM D-4541 on iron phosphate steel Q-panels by prepping the coatings with a sandpaper # 320, cleansing with iso-propyl alcohol and gluing the grit-blasted and MEK-cleaned pucks onto the coating with either a Locktite Quick Set 2-ton epoxy or a 3M Scoth Weld DP-460 epoxy and allowed to cure for 48 hours after which a torque wrench ComputorQ-II was used to record the failure type and the torque value. The torque displayed in inch-pound units was recorded in PSI units by appropriate conversion and an average of 4 readings was reported. Wet adhesion testing was done by immersing 1/3$^{rd}$ part of the aluminum panels in deionized water for 1 hour and then inspecting the panels for delamination, change in clarity/transparency, etc. Pencil hardness was also done on those panels. Abrasion resistance testing was performed on 4” x 4” iron phosphate steel Q-panels R-44 dull matte finish from Q-panel by using a Taber Abraser 5150 with a load weight of 1000g for 100 cycles utilizing H-10 wheels as per the ASTM D-4060.

# 5. RESULTS AND DISCUSSION

## 5.1 Polymer synthesis & characterization

The initial study investigated four polymers, two of low Tg, below room temperature, and two of high Tg, above room temperature. For both the polymers, two molecular weights were chosen: one high ~50,000 and the other a lower molecular weight ~20,000. The molecular weights chosen here are only examples. The monomer composition can also be varied. Polymers with molecular weights ranging from 6000 to 130,000 have been successfully reduced to form CUPs.

The monomers methacrylic acid (MAA), butyl methacrylate (BMA), ethyl acrylate (EA), ethyl methacrylate (EMA) and 2-ethylhexyl methacrylate (2-EHMA) were chosen in the particular composition specified to yield polymers with specified Tg. The actual acid value of the synthesized polymers was found to be slightly higher than the theoretical acid value as expected, because a part of the monomer MMA was lost with nitrogen purging through evaporation with solvent during polymer synthesis, *Table 2*. Good yields are reported for all the polymers synthesized. The MFFT of the synthesized polymers were found to be lower than the Tg as is typical for waterborne resins.

The viscosity of water-reduced CUPs was water-like and the actual/measured particle sizes were close to the theoretical particle size indicating the true nano-scale characteristics of the synthesized CUPs, *Table 2*. As seen from *Figure 4*, the viscosity profile of CUPs, as measured by a Brookfield rheometer, is linear for the graph of sq. rt. of shear rate vs sq. rt. of shear stress with a slope of 0.1456. Therefore, zero point viscosity at 25 $^{o}$C will be 2.02 cP. This corroborates with the results of kinematic

viscosity, measured by an Ubbelohde viscometer, that the viscosity of water-reduced CUPs is water-like.

**Table 1. Monomer composition, MAA: acrylate ratio, % yield, glass transition temperature and molecular weight of the synthesized polymers**

| Polymer | Monomer Composition | MAA: acrylic Ratio | % Yield | Glass Transition Temp. (Tg/$^{o}$C) | Molecular Weight (Mn) |
|---|---|---|---|---|---|
| J-31 | MAA:BMA:EMA | 1:5.5:2.5 | 89 | 55.1 | 19,000 |
| J-32 | MAA:BMA:EMA | 1:5.5:2.5 | 93 | 54.9 | 50,000 |
| J-51 | MAA:BMA:EA:2-EHMA | 1:4:1.5:1.5 | 91 | 21.3 | 21,000 |
| J-52 | MAA:BMA:EA:2-EHMA | 1:4:1.5:1.5 | 93 | 20.9 | 51,000 |

**Table 2. Characterization: Acid value of the synthesized polymers; Particle Size, MFFT and viscosity of CUPs**

| Polymer | Acid Value Theo./Exp. | Particle Size (nm) Theo./Exp. | Kinematic Viscosity (cSt) | Visc. at shear rate of 112.5 (cP) | MFFT ($^{o}$C) |
|---|---|---|---|---|---|
| J-31 | 48.7 / 48.8 | 3.7 / 4.0 | 2.19 | 3.96 | 45.2 |
| J-32 | 48.7 / 48.7 | 5.1 / 4.5 | 2.51 | 2.31 | 45.5 |
| J-51 | 50.9 / 52.5 | 3.8 / 3.1 | 2.45 | 2.57 | 2.5 |
| J-52 | 50.9 / 51.7 | 5.1 / 4.7 | 3.13 | 3.82 | 2.4 |

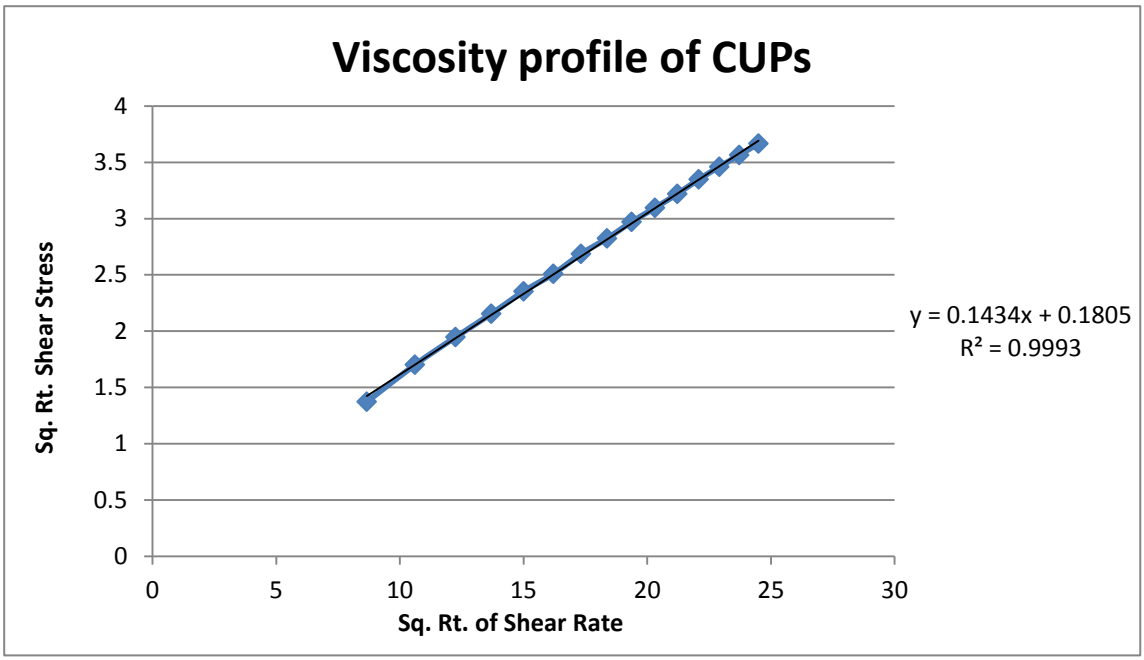


**Figure 4.** Viscosity of 10% solution of CUP J-51 in water at 25 $^{o}$C

The four synthesized polymers were analyzed for comparison between the theoretical particle size calculated from the GPC fractions at different molecular weights and the actual/experimental particle size as found out from DLS. *Figure 5* validates a good agreement between the distribution and the particle diameters, assuming the density of the bulk polymer were the same as that of CUPs. The presence of THF, if not stripped off completely, influences the measured diameter of the CUPs as it can migrate into the interior of the CUP particles and give a larger diameter than expected due to swelling. However, NMR was employed in this research to verify the removal of THF. It should be noted that water must be added in a slow gradient during reduction to avoid regional large solvent compositional changes. If they occur, coagulum may be formed resulting in a cloudy solution due to large aggregates. The water must also be free of polyvalent cations like calcium or magnesium which can bind to the carboxylates and cause gelling. If performed correctly, the solution appears water-clear as evident from *Figure 6*.

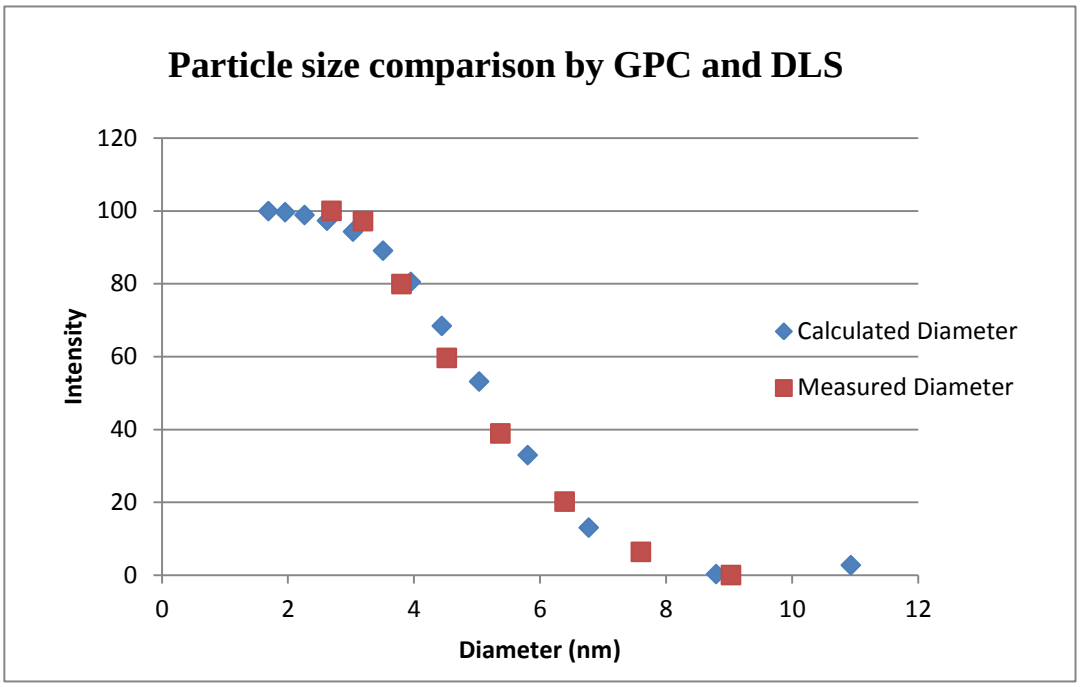


**Figure 5.** Particle size comparison by GPC and DLS for polymer J-51.

**Figure 6**. Jar 1: improperly water-reduced CUPs; Jar 2: properly water-reduced CUPs.

### 5.2 Melamine cured CUPs

Catalysts being an acid, can cause corrosion or degrade the polymer with time. Therefore, the optimum % active catalyst level required for effective curing of CUPs by melamine constituted an important study.

**Table 3. % Active catalyst required for effective curing of CUPs**

| Polymer | % Active Catalyst | Pencil Hardness |
|---|---|---|
| J-31 | 0.125 | HB |
| | 0.25 | F |
| | 0.375 | F |
| | 0.5 | HB |
| J-32 | 0.125 | HB |
| | 0.25 | H |
| | 0.375 | H |
| | 0.5 | F |
| J-51 | 0.125 | HB |
| | 0.25 | H |
| | 0.375 | H |
| | 0.5 | H |
| J-52 | 0.125 | F |
| | 0.25 | H |
| | 0.375 | H |
| | 0.5 | H |

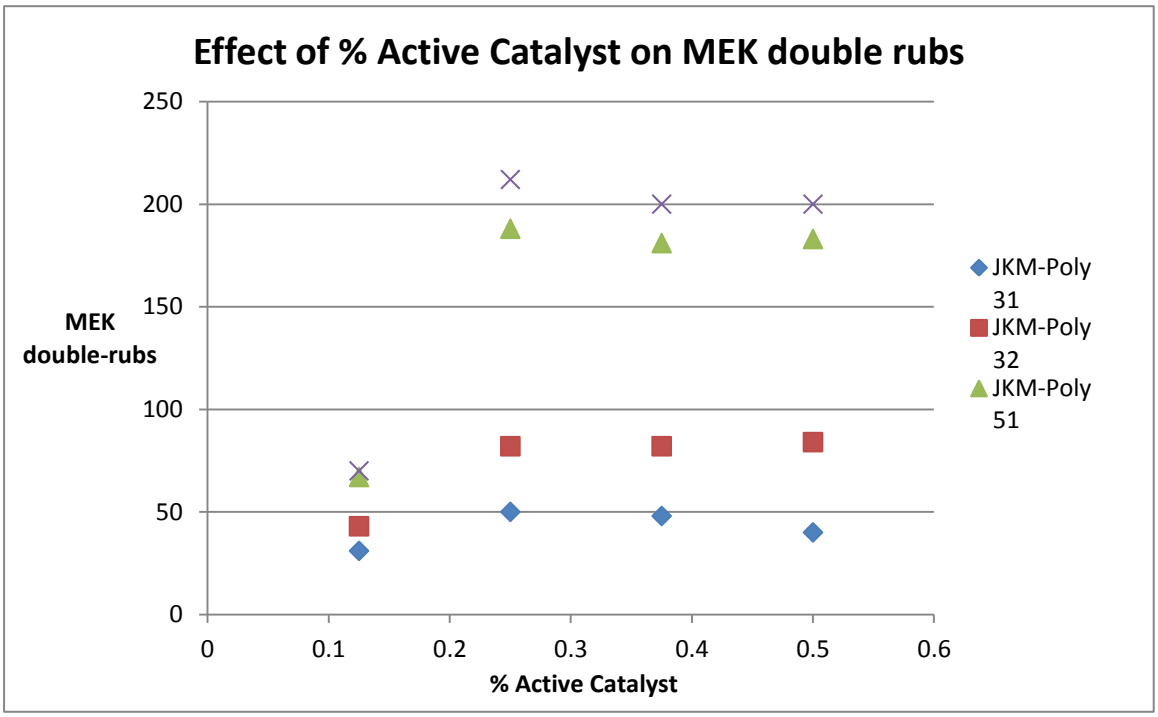


**Figure 7.** Effect of % active catalyst on MEK double rubs of melamine cured acrylic CUPs.

As evident from *Table 4* and *Figure 7, 0.2*5% active catalyst (as supplied; based on resin solids) gave the optimum performance for melamine cure of acrylic CUPs.

The curing time study was executed by varying the baking time of the panels as 10, 20, 30 and 40 min. at a fixed curing temperature (150 $^{o}$C) and 0.25% active catalyst to find out the optimum time required for effective cure.

The performance of the coating reaches its peak value after 20 min. of curing and plateaus after 30 min, *Figure 8*. To ensure thorough cure, a 30 min. curing time for melamine cured acrylic CUPs was chosen as optimum at 150 $^{o}$C.

**Table 4. Curing time study for melamine cured acrylic CUPs**

| Polymer | Curing time (min.) | Pencil Hardness |
|---|---|---|
| J-31 | 10 | HB |
| | 20 | F |
| | 30 | F |
| | 40 | F |
| J-32 | 10 | HB |
| | 20 | H |
| | 30 | H |
| | 40 | H |
| J-51 | 10 | HB |
| | 20 | H |
| | 30 | H |
| | 40 | H |
| J-52 | 10 | HB |
| | 20 | H |
| | 30 | H |
| | 40 | H |

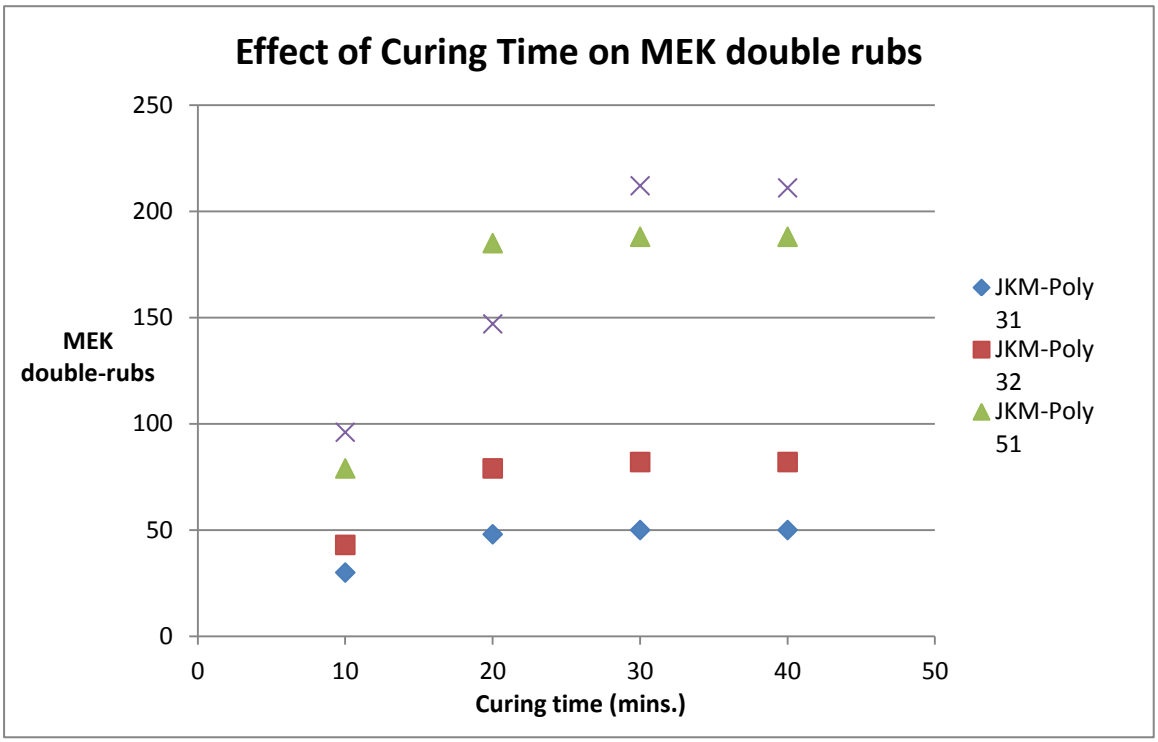


**Figure 8.** Effect of curing time on MEK double rubs of melamine cured acrylic CUPs.

A curing temperature study was executed by varying the oven temperature as 100, 125, 150 and 175 $^{o}$C at a fixed curing time (30 min.) and at 200 $^{o}$C for a curing time of 20 min. with fixed % active catalyst (0.25%) to find out the optimum temperature required for effective cure.

A curing temperature study was executed by varying the oven temperature as 100, 125, 150 and 175 $^{o}$C at a fixed curing time (30 min.) and at 200 $^{o}$C for a curing time of 20 min. with fixed % active catalyst (0.25%) to find out the optimum temperature required for effective cure. The best performance was observed in the coatings cured at 150 $^{o}$C for 30 min, *Figure 9*. For the polymers J-51 and J-52, over baking of the resin (over 175 $^{o}$C) leads to their degradation, most likely via cis-elimination, producing the carboxylic acid and alkene as degradation products. Another possible explanation for the degradation of

CUP resins might be the rapid flash-off of water at temperatures over 150 $^{o}$C. However, optimum performance was recorded at a curing temperature of 150 $^{o}$C, *Table 5*.

**Table 5. Curing temperature study for melamine cured acrylic CUPs**

| Polymer | Curing Temp. (C) | Pencil Hardness |
|---|---|---|
| J-31 | 100 | HB |
| | 125 | HB |
| | 150 | F |
| | 175 | HB |
| | 200 | HB |
| J-32 | 100 | HB |
| | 125 | F |
| | 150 | H |
| | 175 | H |
| | 200 | F |
| J-51 | 100 | HB |
| | 125 | HB |
| | 150 | H |
| | 175 | B* |
| | 200 | B* |
| J-52 | 100 | HB |
| | 125 | HB |
| | 150 | H |
| | 175 | B* |
| | 200 | B* |

*Overbake resulted in the color change of the CUP clear coats

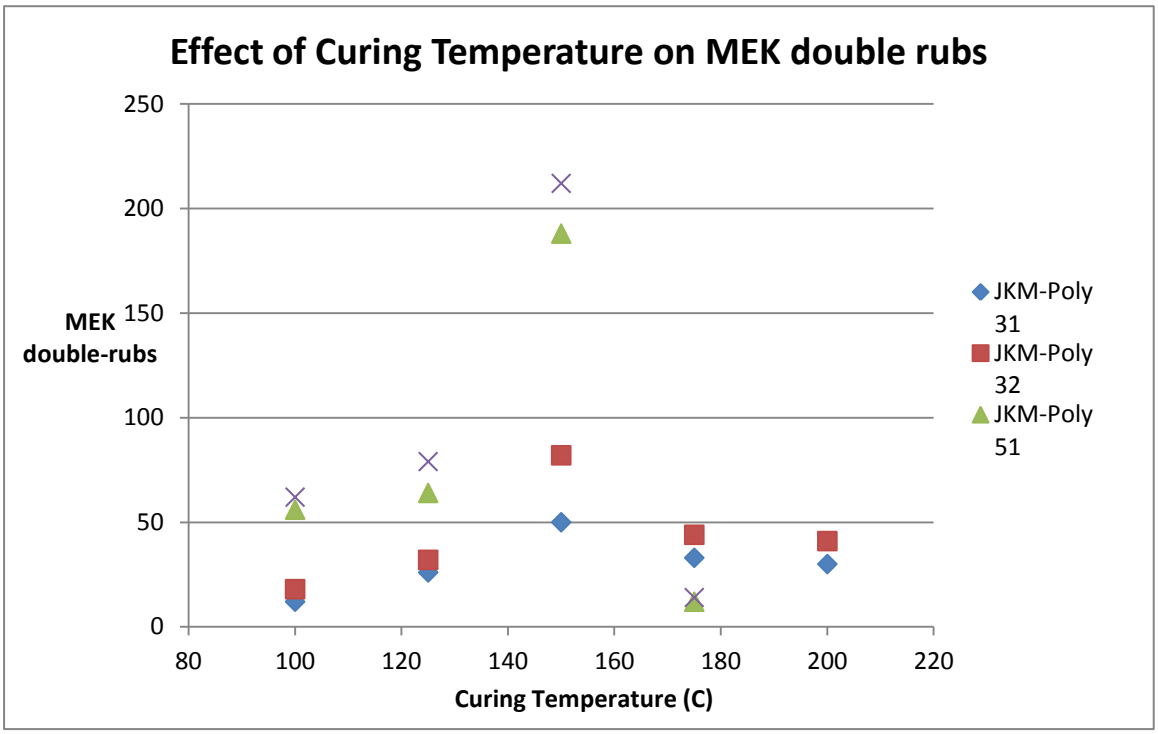


**Figure 9.** Effect of curing temperature on MEK double rubs of melamine cured acrylic CUPs.

To find out the appropriate amount of melamine (estimated functionality of melamine) required for effective curing of acrylic CUPs, the amount of melamine content required to cure the CUPs was changed by estimating a different functionality of melamine as 3.0, 3.5, 4.0, 4.5 and 5.

Optimum performance is observed as the assumed functionality of melamine as 4.5 as observed from *Table 6 and Figure 10*. However, if flexibility is desired, a lower value may be targeted.

**Table 6. Optimum melamine functionality assumed for effective curing of CUPs**

| Polymer | *f* of Melamine | Pencil Hardness |
|---|---|---|
| J-31 | 3 | HB |
| | 3.5 | HB |
| | 4 | HB |
| | 4.5 | F |
| | 5 | F |
| J-32 | 3 | HB |
| | 3.5 | F |
| | 4 | F |
| | 4.5 | H |
| | 5 | H |
| J-51 | 3 | HB |
| | 3.5 | F |
| | 4 | F |
| | 4.5 | H |
| | 5 | H |
| J-52 | 3 | F |
| | 3.5 | F |
| | 4 | F |
| | 4.5 | H |
| | 5 | H |

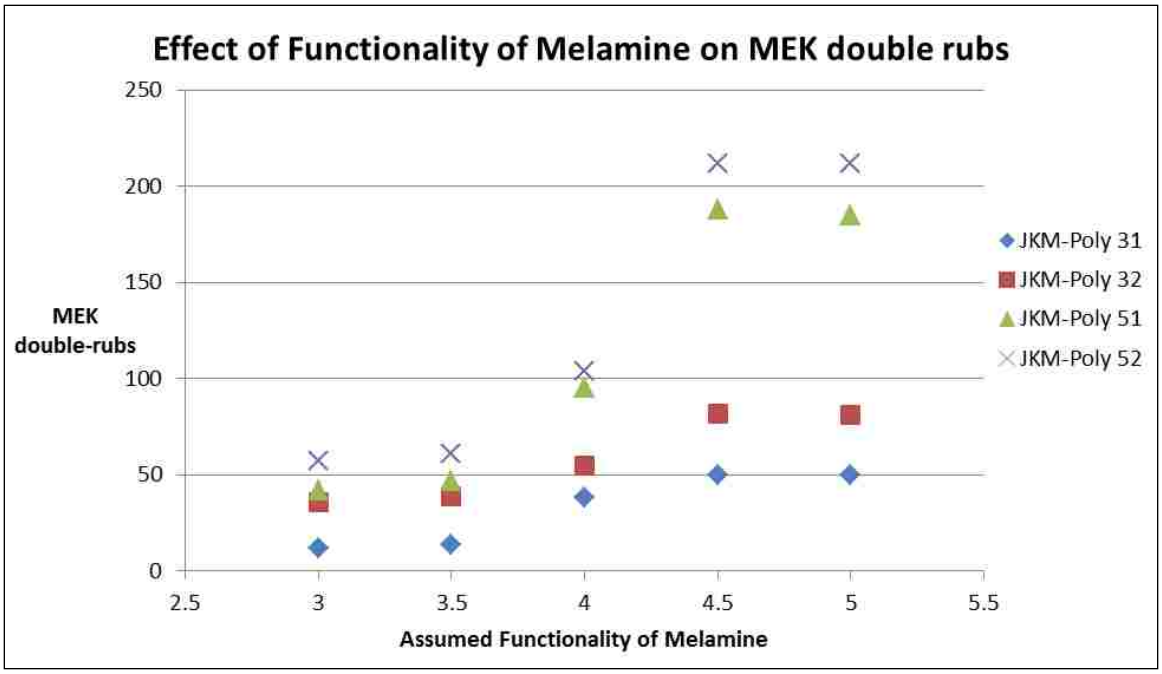


**Figure 10**. Effect of melamine functionality on MEK double rubs of melamine cured CUPs.

Pencil hardness is a measure of the hardness of the coating while MEK double rub test, a measure of the solvent resistance and an estimate of the crosslink density of a coating. It was observed that the MEK double rubs were high for all of the melamine cured CUP clear coats, *Table 7*. The low Tg high molecular weight CUPs (J-51 and J-52) cured by melamine showed excellent curability/crosslinkability and solvent resistance. The lack of any crosslinker would render the coating a lacquer, thus resulting in lower hardness and solvent resistance as seen from the results of the control. It was observed that melamine cured CUP clear coats had good hardness characteristics. It was also noted that the CUP clear coat made from high Tg polymer (J-31 & J-32) gave good gloss while the CUP clear coat made from low Tg polymer (J-51 & J-52) gave high gloss. As evident from *Table 7*, crosslinking the colloidal unimolecular polymers gives significant boost to

the performance characteristics of the resin, as measured by the MEK double rubs and pencil hardness.

**Table 7. Film thickness, gloss, MEK double rubs and pencil hardness results of the CUP clear coats**

| Polymer | Cure type | Film thickness(mil) | Gloss $20^o$ / $60^o$ / $85^o$ | MEK double rubs | Pencil Hardness |
|---|---|---|---|---|---|
| J-31 | Control | 0.5 | 81 / 83 / 90 | 5 | B |
| | Melamine | 0.5 | 85 / 89 / 93 | 50 | F |
| J-32 | Control | 0.5 | 87 / 91 / 93 | 7 | B |
| | Melamine | 0.5 | 84 / 90 / 93 | 82 | H |
| J-51 | Control | 0.7 | 90 / 93 / 97 | 5 | B |
| | Melamine | 0.7 | 90 / 91 / 95 | 188 | H |
| J-52 | Control | 0.5 | 90 / 94 / 97 | 7 | B |
| | Melamine | 0.5 | 91 / 94 / 98 | 212 | H |

It was observed that all the formulated CUP clear coats had excellent flexibility and impact resistance, *Table 8*. These properties can be attributed to the true nano-scale of CUP dispersions to form clear coats with ready access to the crosslinking agent without having to penetrate into a large particle which requires diffusion time.

*Table 8* and *Figure 11* are evidence of the high flexibility and impact resistance of the resin developed.

**Table 8. Mandrel flexibility and impact resistance results of the CUP clear coats**

| Polymer | Cure type | Mandrel [inch] | Impact (forward) [inch-Lbs.] | Impact (reverse) [inch-Lbs.] |
|---|---|---|---|---|
| J-31 | Control | 1/8” | 160+ | 160+ |
| | Melamine | 1/8” | 160+ | 160+ |
| J-32 | Control | 1/8” | 160+ | 160+ |
| | Melamine | 1/8” | 160+ | 160+ |
| J-51 | Control | 1/8” | 160+ | 160+ |
| | Melamine | 1/8” | 160+ | 160+ |
| J-52 | Control | 1/8” | 160+ | 160+ |
| | Melamine | 1/8” | 160+ | 160+ |


**Figure 11**. High impact resistance and flexibility of melamine cured CUP clear coatings.

It was observed that the melamine cured CUP clear coats had epoxy adhesive failure for the Locktite quickset 2-ton epoxy adhesive which implies that the polymeric

films are adhered strongly to the substrate, indicating excellent adhesion, *Table 9*. Therefore, to evaluate the actual adhesion potential of melamine cured acrylic CUPs, a higher strength adhesive, DP-460 by 3M was used. It is noted that the melamine cured CUPs depicted phenomenal adhesive strength to the substrate.

**Table 9. Adhesion testing results of the CUP clear coats**

| Polymer | Cure type | Epoxy Adhesive Used | Torque (PSI) | Failure of | Failure type | % Failure |
|---|---|---|---|---|---|---|
| J-31 | Control | Locktite | 810 | C/s | Adhesive | 100% |
| | Melamine | Locktite | 1175 | E/c | Adhesive | 100% |
| | Melamine | 3M | 4025 | C/s | Adhesive | 100% |
| J-32 | Control | Locktite | 1021 | C/s | Adhesive | 100% |
| | Melamine | Locktite | 1387 | E/c | Adhesive | 100% |
| | Melamine | 3M | 4655 | C/s | Adhesive | 100% |
| J-51 | Control | Locktite | 838 | C/s | Adhesive | 100% |
| | Melamine | Locktite | 969 | E/c | Adhesive | 100% |
| | Melamine | 3M | 4133 | C/s | Adhesive | 100% |
| J-52 | Control | Locktite | 1065 | C/s | Adhesive | 100% |
| | Melamine | Locktite | 1083 | E/c | Adhesive | 100% |
| | Melamine | 3M | 5070 | C/s | Adhesive | 100% |

* C/s = coating to substrate; E/c = epoxy to coating

No significant change was observed on any of the polymeric films as there was no hazing and no change in pencil hardness after a 1 hour water immersion, indicating very low water permeability of the clear coatings formulated from CUPs, *Table 10*.

**Table 10. Wet adhesion test results of the CUP clear coats**

| Polymer | Cure type | Appearance/ Observations | Pencil Hardness |
|---|---|---|---|
| J-31 | Control | No change | B |
| | Melamine | No change | F |
| J-32 | Control | No change | B |
| | Melamine | No change | H |
| J-51 | Control | No change | B |
| | Melamine | No change | H |
| J-52 | Control | No change | B |
| | Melamine | No change | H |

It was observed that the wear index of control was usually high indicating low abrasion resistance while no trend was observed in the wear index of melamine cured CUPs indicating moderate abrasion resistance of the clear coats formulated from CUPs, *Table 11*. This corroborates that crosslinking the CUPs with melamine enhances its performance as a coating.

**Table 11. Abrasion resistance test results of the clear coats formulated from CUPs**

| Polymer | Cure type | mg lost/100 cycles | Wear Index |
|---|---|---|---|
| J-31 | Control | 39 | 390 |
| | Melamine | 14 | 140 |
| J-32 | Control | 27 | 270 |
| | Melamine | 13 | 130 |
| J-51 | Control | 22 | 220 |
| | Melamine | 10 | 100 |
| J-52 | Control | 23 | 230 |
| | Melamine | 12 | 120 |

## 6. CONCLUSION

The true nano-scale nature of CUPs can result in a well crosslinked acrylic clear coat. The coalescing mechanism for CUPs was similar to latex and the effect of coalescent aid was found to be analogous. Melamine cured CUP coatings produced well cross-linked films, were found to be harder and likely more effectively cross-linked. Further studies should verify this. This work illustrates the true nano-unimolecular nature of CUPs and its low viscosity. These zero VOC systems (if ammonia is used) offer a potentially high performance technology option for future coatings for both OEM and architectural applications.

Over the past few years, the development of acrylic Colloidal Unimolecular Polymers (CUPs) has moved from the realm of laboratory investigation to the point today at which they can be tested and developed commercially in numerous applications. Thus,

the utilization of melamine curing agents for water-reduced acrylic CUPs have illustrated their usefulness and potential is such applications as clear floor finishes or clear topcoats.

## 7. ACKNOWLEDGEMENT

The authors would like to acknowledge the Missouri S&T Coatings Institute for the financial support and the following for CUP allied work: Cynthia Riddles, Minghang Chen, Sagar Gade, Ameya Natu and Catherine Hancock.

## 8. REFERENCES

1.) Myers, D.; Surfactant Science and Technology; John Wiley and Sons: New Jersey, **2006**.

2.) Morishima, Y.; Nomura, S.; Ikeda, T.; Seki, M.; Kamachi, M.; Macromolecules **1995**, 28 (8) 2874.

3.) United States Patent No. 5,369,152 assigned to Reichhold Chemicals, Inc.

4.) Klempner, D; Frisch, K.; Advances in Urethane Science and Technology; Smithers Rapra Press: Mercy, **2001**.

5.) Saravari, O.; Phaphant, P.; Pimpan, V.; Journal of Applied Polymer Science **2005**, 96 (4) 1170.

6.) Riddles, C. J.; Hua-Jung Hu, W. Z.; Van De Mark, M. R.; Polymer Preprints **2011**, 52, (2) 232.

7.) Chen, M; Van De Mark, M. R.; Polymer Preprints **2011**, 52, (2), 336.

# SECTION

# 2. SUMMARY

The structure of 5-mercapto-1,3,4-thiadiazole-2(3H)-thione and its alkylated derivatives was determined conclusively and the chemistry of its reaction mechanisms was explained by a corroborative study of X-ray crystallography. Yet, the structure of MTT in DMSO solution as well as the product of MTT-DMSO reaction remains unsolved. Further investigation, supported by the theoretical calculations should yield conclusive results. The use of sulfur containing ligating groups shows potential as effective flash rust inhibitors. Research work by Yousef Dawib and Dr. Aysel Buyuksagis on active corrosion inhibition studies should address the corrosion inhibition ability of the derivatives of MTT.

The development of acrylic Colloidal Unimolecular Polymers (CUPs) has moved from the realm of laboratory investigation to the point today at which they can be tested and developed commercially in numerous applications. The nano-scale size of CUPs allows them to be thermodynamically stable in water, provide excellent film forming characteristics and can potentially provide good pigment binding ability in architectural paints. The utilization of aziridine and melamine curing agents for water-reduced acrylic CUPs have illustrated their usefulness and potential in enhancing the coating performance for such applications as clear floor finishes, clear topcoats, etc.

# VITA

Jigar Kishorkumar Mistry was born in Surat, India. He obtained his primary and secondary education in Surat, India and received his Bachelor's degree in Paints Technology, First Class with Distinction in May 2007 from University Institute of Chemical Technology (UICT, formerly known as UDCT) in Mumbai, India. In 2007, Jigar joined the Missouri University of Science and Technology to pursue a Ph.D. degree in Chemistry. During the course of his Ph.D. work, Jigar has worked as a Teaching Assistant for the Department of Chemistry at MST, published 2 journal articles, submitted 2 articles for publication and presented his research work at 2 American Coatings Conferences (2008 & 2012), 1 ACS annual meeting (2011) and 1 MST Graduate Science Fair (2008). He has received several awards for his research presentations as well as an Outstanding Graduate Teaching Award 2010 by the Department of Chemistry at MST. A yearly scholarship in the name of "Jigar Mistry" is created by his alma-mater UICT, India (worth INR 10,000) for the Polymer Sci. & Coatings Division, to honor his contributions in successfully creating & organizing "RANGOTSAV"- The 1$^{st}$ Paper & Poster presentation competition cum Symposium for the Academia & the Coatings industry in India. Jigar joined The Valspar Corporation in Kansas City, Missouri at a Chemist-II position, following the completion of his Ph.D. degree in December 2012.